Università Ca'Foscari Venezia

Master's Degree program – Second Cycle (*D.M. 270/2004*)
in Science and Technologies of Bio and Nanomaterials

Final Thesis

Ca' Foscari
Dorsoduro 3246
30123 Venezia

Title:

Biogenic selenium nanoparticles from *Bacillus mycoides* SeITE01 and their potential as antimicrobial agents

Supervisor

Prof.ssa Silvia Lampis

Co-supervisors:

Prof. Raymond Joseph Turner

Dott. Emanuele Zonaro

Graduand

Elena Piacenza

Matriculation Number 850586

Academic Year

2014 / 2015

TABLE OF CONTENTS

ABSTRACT

Selenium is a nonmetallic, natural occurring element, essential in trace for humans and animals but toxic at concentrations higher than the dietary doses, with a narrow concentration margin between essentiality and toxicity. In natural environments, selenium occurs in four valence states: selenate (Se^{6+}), selenite (Se^{4+}), selenide (Se^{2-}), and elemental selenium (Se^0). Microorganisms play a major role in the biogeochemical cycle of this element: some of them, that are resistant to selenium oxyanions, are capable of reducing selenite and/or selenate to elemental selenium as Se nanoparticles (SeNPs). Interestingly, it has recently been shown that SeNPs can exert high antibacterial activity against human pathogenic bacteria, such as *Staphilococcus aureus*.

My thesis project is focused on synthesis and characterization of SeNPs biosynthesized by *Bacillus mycoides* SeITE01 bacterial strain, evaluating also their properties as antimicrobial agents. In so doing, a comparison between biogenically (synthetized using *B. mycoides* SeITE01) and chemically synthetized SeNPs (normally more used) was carried out, in order to analyze their differences in terms of size, stability, morphology, action mechanisms and efficacy.

I worked both in the Environmental Microbiology Laboratory at University of Verona and in Biofilm Research Group at University of Calgary (Canada). In the Environmental Microbiology Laboratory in Verona, SeNPs were synthetized using both biological and chemical protocols. In particular focus of the project was on biosynthesis of SeNPs from *Bacillus mycoides* SeITE01, grown in Nutrient Broth with Na_2SeO_3, compared to SeNPs chemically synthetized through several methods, using 3 different

reducing agents: L-cysteine, ascorbic acid or a reducing agent made with SDS and $Na_2S_2O_3$.

In the second part, SeNPs has been characterized using several tools such as Dynamic Light Scattering (DLS), Z potential measurement, Scanning Electron Microscopy (SEM) analysis and Energy Disperse Spectrometer (EDS) analysis. Thanks to these techniques, I was able to describe structures of both biogenic and chemical SeNPs, stressing differences and similarities.

Working in Biofilm Research Group in Calgary, the third part of the project was to evaluate SeNPs antimicrobial activity against biofilms formed by different bacterial pathogens. Biofilm is a complex structure consisting of bacteria immersed in an organic matrix, made of several kinds of macromolecules (proteins, carbohydrates, exopolysaccharides) and water. Biofilms can be present both in liquid or solid surfaces and, at the same time, in soft tissue of living organisms and are resistant to conventional methods of disinfection. Normally, they're also pathogenic in human and animal body. In order to use biogenic SeNPs as antimicrobial agents, it was important to investigate their ability to inhibit biofilm formation and to penetrate inside biofilm structures. In so doing, I've exposed several pathogenic biofilms to different concentrations of both biogenic and chemical SeNPs. To evaluate biofilm growth and SeNPs antimicrobial effect Calgary Biofilm Device (CBD) and Minimum Biofilm Eradication Concentration (MBEC) test have been used. MBEC test is a high throughput screening assay used to determine the efficacy of antimicrobials against biofilms of a variety of microorganisms. It's based on use of CBD: suitable methodology to test different concentrations of a biocide agent, in which one batch culture apparatus allows multiple species biofilms to be tested against a lot of variables. In particular, in this project CBDs coated of hydroxyapatite (HA) were used. HA is a calcium-posphate ceramic normally use as biomaterial, because it's the most important component of bones and teeth. Using MBEC assay, it was possible to verify that biogenically synthetized SeNPs have stronger antimicrobial activity than those chemically synthetized.

Finally, SeNPs mechanism of action against pathogenic biofilms has been verified using microscopy techniques, such as Confocal Laser Scanning Microscopy (CLSM) and Scanning Electron Microscopy (SEM) analysis. CLSM analysis were performed using specific dyes in order to evaluate SeNPs ability to inhibit pathogenic biofilm formation. At the same time, SEM analysis permitted to establish HA structure, possible interaction between HA and SeNPs and antimicrobial properties of SeNPs.

All data then were collected to make a rational comparison between chemical and biogenic SeNPs, in order to determine which were more competitive and stronger as antimicrobial agents.

INTRODUCTION

Se characteristics and properties

Selenium is a member of the chalcogen family. Chalcogens are elements in Group 16 of the periodic table. Selenium is belonging to the p block and its chemical configuration is: $[Ar]3d^{10}4s^{2}4p^{2}$. Since it has some characteristics of metals and other of non-metals, Selenium is considered a metalloid, or semi-metal element.

The element was discovered by Jöns Jacob Berzelius at Stockholm in 1817. He had shares in a sulfuric acid works and he was intrigued by a red-brown sediment which was collected at the bottom of the chambers in which the acid was made. Firstly, he thought it was the element Tellurium, because it gave off a strong smell of radishes when heated, but he also noted that it has some characteristic of the element Sulfur and he realized to have found a new chemical element: Selenium. He also supposed that its proprieties were intermediate between Sulfur and Tellurium. [1]

Selenium exists in several allotropic forms (forms of an element with differential physical and chemical properties). Selenium allotropes interconvert themselves on warming and chilling moved out at dissimilar degrees and rates. [1]

Selenium is normally amorphous (without crystalline shape) brick-red dust. When quickly melted, it forms the black vitreous shape, that is normally traded industrially as beads. Deep red-colored non-stable crystalline forms are created by the evaporation of black Selenium at different rates. They altogether have comparatively ring-based low, monoclinic crystal symmetries. [2]

Upon warming, amorphous form relaxes at 50°C and reorganizes to metallic crystalline silvery (or grey) selenium at 180°C. It has hexagonal crystal symmetry, in which Selenium atoms are placed in coiling polymeric chains. This represents the most stable Selenium allotrope. Whereas additional Selenium forms are insulators, grey Selenium is a semiconductor displaying considerable photoconduction. [2]

Different polymorphs are distinguished by correlation between neighboring dihedral angles and, depending on this correlation, Selenium can form either trans-chain like or cis-ring like configurations.

Selenium exhibits a combination of many interesting and useful properties: a relatively low melting point, a high photoconductivity, catalytic activity with respect to hydration and oxidation reactions and high piezoelectric, thermoelectric, and nonlinear optical responses. [3]

One of the most important physical characteristics of Selenium is its electrical property, and in particular, its semiconductivity. A semiconductor is a substance that conducts an electric current that exhibits intermediate conductivity between conductors and non-conductors. [4]

Other important properties of Selenium are both photovoltaic action, where light is converted directly into electricity, and photoconductive action, where the electrical resistance decreases with increased illumination. [5]

Selenium is a very reactive element and can react with: nitric acids, sulfuric acids, metals to form selenides, oxygen to form selenium dioxide (SeO_2), selenates such as $CaSeO_4$ and selenites such as Na_2SeO_3. [6]

Thanks to this proprieties, Selenium can be used in many different ways: electronics and glass industry, animal feeds and food supplements, photocopying, metal alloys for batteries, pigments, ceramics, plastics and lubricants. [7]

Presence and effect of Selenium in environment

Selenium is among rare elements on the surface of the planet. It generally occurs in relatively low amounts in geological raw, soils and sediments, but its contents in coals and crude oils can reach hundreds of mg/kg in certain cases. Concentrations in soils and sediments vary geographically, ranging from 0.01 mg/kg in deficient areas to 1200 mg/kg in organic rich soils in polluted areas. [7]

Selenium is also found associated with other elements in rare minerals, such as crooksite and clausthalite. [8]

Most of the world's Selenium is obtained from the anode muds produced during the electrolytic refining of copper. These muds are either roasted with sodium carbonate or sulfuric acid, or smelted with sodium carbonate to release the selenium. Furthermore, industrial activities such as oil refining, phosphate and metal ore mining and coal fire-based power production can all contribute to the dispersion of Selenium in the environment. [9]

Selenium settles from air and also tends to end up in the soils of disposal sites. Since Selenium in soils remains stable if it doesn't react with oxygen, it will not dissolve in water and it can became dangerous for organisms. Higher oxygen levels and increased in the acidity of the soil due to human activities will increase mobile forms of Selenium. When selenium is more mobile, the chances of exposure to its compounds will be greatly enhanced. Soil temperatures, moisture, concentrations of water-soluble

Selenium, the season of the year, organic matter content and microbial activity modify the mobility of selenium through soil. [9]
Since hydrogen selenide and other Selenium compounds are extremely toxic, Selenium contamination represents an important public health concern and requires remediation initiatives especially in those geographic locations where agricultural irrigation drainage waters transport significant amounts of Selenium by leaching seleniferous soils. [7]

Health effect

Humans may be exposed to Selenium in several different ways: food or water, soil or air that contains high concentrations of the element. The exposure to Selenium mainly takes place through food, because selenium is naturally present in grains, cereals and meat. Humans need to absorb certain amounts of this element daily, in order to maintain good health. Food usually contains enough Selenium to prevent disease caused by shortages. When the last occur, people may experience heart and muscle problems. [8]
Although Selenium can be considered an essential micronutrient for living systems at low concentrations, it becomes toxic at greater doses and the range between dietary deficiency (< 40 µg/day) and excess (> 400 µg/day) is fairly narrow. [7]
People that live near hazardous waste-sites will experience a higher exposure through soil and air. Selenium from hazardous waste-sites will end up in groundwater or surface water through irrigation and it causes contamination in local drinking water.

People that work in metal, Selenium-recovery and paint industries also tend to experience a higher exposure to the metalloid, mainly through breathing, since it's released to air through coal and oil combustion. As a consequence, exposure to Selenium through air is frequent only in working environment. It can cause dizziness, fatigue and irritations of the mucous membranes. When the exposure is extremely high, collection of fluid in the lungs and bronchitis may occur. [9]

When Selenium uptake is too high health effects will be likely to occur, such as brittle hair and deformed nails, rashes, heat, swelling of the skin and severe pains. When Selenium ends up in the eyes people experience burning, irritation and tearing. [9]

Selenium poisoning may become so severe in some cases that it can even cause death.

Overexposure of selenium fumes may produce accumulation of fluid in the lungs, garlic breath, bronchitis, pneumonitis, bronchial asthma, nausea, chills, fever, headache, sore throat, shortness of breath, conjunctivitis, vomiting, abdominal pain, diarrhea and enlarged liver. Selenium is an eye and upper respiratory irritant and a sensitizer. Overexposure may result in red staining of the nails, teeth and hair. [9]

Despite these toxic and non-desirable effects, Selenium is one of the key elements for maintaining the health of mammalians because it exerts anti-oxidative and pro-oxidative effects. Selenium has multiple beneficial effects for human health, through regulation of at least 25 selenoproteins, all containing selenocysteine. Among these selenoproteins, the most important are glutathione peroxidase and thioredoxin reductase. Glutathione peroxidases catalyze the reduction of hydrogen peroxide and a variety of organic hydroperoxides, including phospholipid

hydroperoxide, to water and corresponding alcohols, using glutathione as the hydrogen donor. Thioredoxin reductases exert antioxidant actions through catalyzing the reduction of oxidized thioredoxin, using NADPH as the electron donor, or by directly reacting with hydrogen peroxide and hydroperoxides.
In the last period, many different studies have also characterized Selenium as an element capable to limit proliferation of tumor cells and to inhibit microbiological infections. These proprieties permit to use it also for cancer treatment and as antimicrobial agent, respectively.[7]

SeNPs

In order to use Selenium for biological and biomedical applications, in the last years scientists have investigate the possibility to find a non-toxic or lower toxic form of Selenium. In this sense, they all have recognized that Selenium nanoparticles made by elemental Selenium Se^0 (SeNPs) show higher biocompatibility rather than bulk Selenium.[7]
Generally, nanoparticles (NPs) have unique physical and chemical properties that may be very different from the bulk material. At nanoscale, materials behave very differently compared to larger scales and these different physical properties are caused by their large surface-volume ratio, large surface energy, spatial confinement and reduced imperfections.[11]
Nowadays, one of the most studied characteristics of NPs is their action as antimicrobial agents.[12] Antimicrobial activity is related to compounds that locally kill bacteria, inhibit or slow down their growth, without being in general toxic to surrounding tissues. Usually antimicrobial agents are

chemically modified natural compounds, pure natural products and purely synthetic antibiotics and they are normally use against infectious diseases.[12] However, with their broad use and abuse, the emergence of bacterial resistance to antibacterial drugs has become a common phenomenon.[12] Resistance is most often based on evolutionary processes taking place during antibiotic therapy and leads to inheritable resistance. In addition, horizontal gene transfer by conjugation, transduction or transformation can improve bacterial resistance to antibiotics.[12] Thus, infectious diseases continue to be one of the greatest health challenges worldwide and this problem has prompted the development of alternative strategies to treat bacterial diseases.[12] Among them, NPs have emerged as novel antimicrobial agents: they are able to attach to the membrane of bacteria by electrostatic interaction and disrupt the integrity of the bacterial membrane.[12] Nanotoxicity is generally triggered by the induction of oxidative stress by free radical species formation, but specific mechanisms depend on composition, surface modification and intrinsic properties of NPs and the bacterial species.[12]

Other important characteristics that make NPs suitable as anti-microbial agents are: possibility to use low doses of them for treatments and low toxicity for environment and human rather than normally used antibiotics.[12]

Using these properties, in the last 30 years there was a strong develop of NPs in order to use them as antimicrobial agents. In so doing, one of the most important class of studied NPs was silver NPs (AgNPs). Silver is an element widely used in medical field, thanks to its particular antimicrobial properties due to its metallic nature.[13] Because of its high toxicity to most microbial cells, Silver ions were used in the past as biocide.[14] As other classes of NPs, nanoscale elemental Ag^0 is more toxic as biocide than bulk Ag ions.[14] Despite AgNPs antimicrobial activity against large number of bacteria, use of these NPs present some important problems, such as long-term exposure toxicity for humans (especially impaired night vision and abdominal pain) and treatment of silver contaminated waters (environmental damage and potential uptake into food chain).[14] In order to overcome these problems and to develop strong antimicrobial NPs, in the last years there was development of new NPs classes, such as Gold NPs (AuNPs), Titanium NPs (TiO_2NPs), Zinc NPs (ZnNPs) and Copper NPs (CuNPs).[12]

Recently, strong interest was developed in a particular class of NPs: Selenium NPs. In doing so, the focus of synthetize SeNPs is on possibility to use them for biological and biomedical applications, since SeNPs enhance selenium permeation and retention in tumor tissues and also show potential as antimicrobial agents. [14]

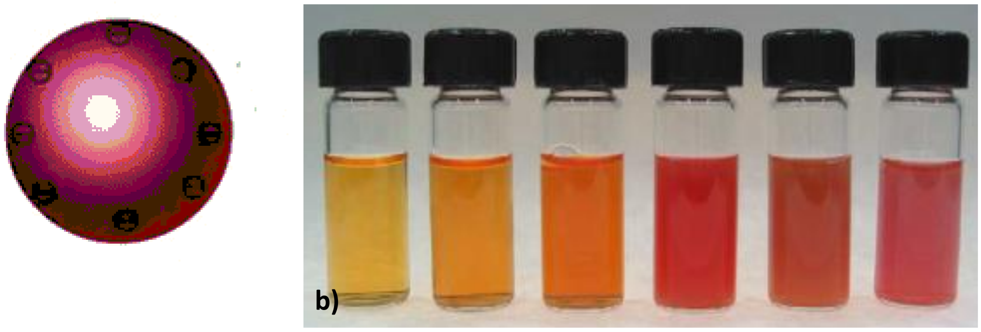

a) b)

Figure 1: a) SeNP structure and **b)** photographic images of six size-distinguishable selenium colloids (*Lin et al 2005*) [10]

An important feature of SeNPs is their high surface-volume ratio: when nanosize decreases, surface atomicity, surface energy, and surface binding energy all increase quickly; as a result, surface atoms become more prone to diffusion, with tendency to combine with other atoms for energy dissipation.[15] SeNPs also possess adsorptive ability, antioxidant functions and marked biological reactivity, including anti-hydroxyl radical efficacy and protective effect against DNA oxidation . [7]

SeNPs action against biofilm

One of the most important and innovative properties of SeNPs is their ability to inhibit or to slowdown biofilm formations. For example, SeNPs have been found to strongly inhibit growth of *Staphylococcus aureus*, a key bacterial pathogen commonly occurring in human infections that grow up thanks to presence of a strong biofilm.[7]

Biofilms are complex microbial communities that form by adhesion to a solid surface and by secretion of a matrix, which cover the bacterial cell community. [16] Biofilm formation is a developmental process characterized of intercellular signals that regulate structure growth (Fig.2).

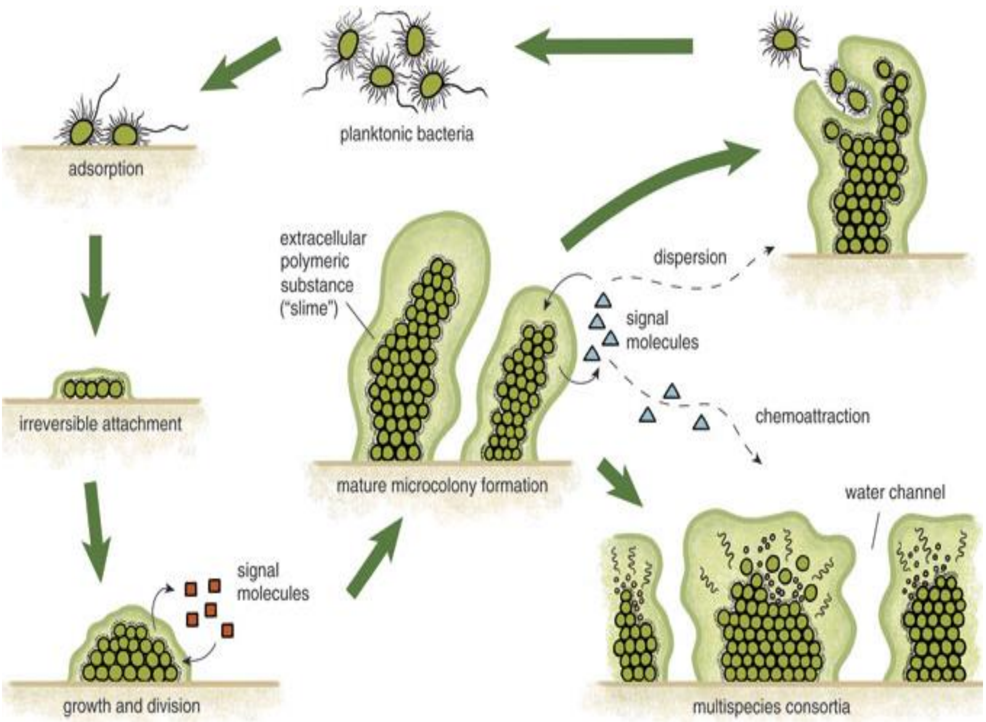

Figure 2: Formation of mature biofilm (*Olson et al 2002*) [17]

When bacteria cells are able to adsorb to a surface and become attached, there is the formation of a typical biofilm. The bacteria then grow and divide to form layers, clumps or stalk and mushroom shaped microcolonies.[17] In these structures, bacteria cells are enclosed in an organic matrix made of water and several macromolecules, such as proteins, glycoproteins, carbohydrates and exopolysaccharides.[18] Once formed, biofilms are difficult to remove as they show an increased tolerance to biocides and antibiotics when compared to the planktonic (free-floating) counterpart.[17]

Biofilm may be found almost everywhere: both in solid or liquid surface and also in soft tissues of living organisms. It's common to find them in hard surfaces in food processing facilities, in water lines of dental equipment in a dentist's office and in medical environment and devices.[18] Normally, biofilms are pathogenic for human body: Center for Disease Control and Prevention estimates that 60% of clinical infections (heart and middle ear infections, infections associated with artificial joints and catheters, tooth decay and gum disease) in the Western world are caused by biofilms.[17] Development of these chronic infections and diseases is possible thanks to biofilm formation, because it's able to protect bacteria cells against antibiotics. [19]

In this sense, SeNPs ability of eradicating biofilms became very important for their possibly biological and biomedical applications.

Chemical SeNPs

SeNPs are normally synthetized by several chemical processes by selenite or selenous acid reduction with various agents: glutathione (GSH), hydrazine, glucose, $NaBH_4$, $SnCl_2$, sodium thiosulfate.[3] In addition, irradiation has also been used to achieve reduction of Selenium precursors by hydrated electrons.

Another method applying for fabrication of SeNPs is laser ablation on various substrates.

However none of these approaches has clearly demonstrated an ability to exert fine control over particle size. Recently, it has been demonstrated that the sizes of SeNPs can be prepared within three size regimes by selenite/GSH chemical reduction approach:

- small (5–15 nm)
- medium (20–60 nm)
- large (80–200 nm) [10]

Some of the most used protocols to synthetize chemical SeNPs are:

- synthesis with Na_2SeO_3 and L-cysteine
- synthesis with Na_2SeO_3 and ascorbic acid
- synthesis with H_2SeO_3, $Na_2S_2O_3$ and SDS

In this project, these 3 methods have been evaluated in order to establish and compare neosynthesized SeNPs characteristics. SeNPs made with these 3 protocols have showed different size, due to change in reagent amounts and reaction conditions.

Anyway, these techniques have limitations: they do not yield narrow size distributions important for industrial applications and they produce particles that are subject to extreme photocorrosion.[19] Furthermore, chemical synthesis of NPs generally have a strong impact both in environment and in human health either as polluting or as toxic, because of use of high pressures and temperatures, energy consume, use of toxic reagents and generation of hazardous by-products. [7]

Biogenic SeNPs:

In order to overcome limitations and dangers of chemical techniques, nowadays the focus is to develop biogenic (or biological) based methods for NPs synthesis. One of the most important innovation in this field is the possibility to use bacteria to produce NPs: bacteria are well known to produce metal and metal oxide NPs of various compositions, sizes and morphologies.[7]

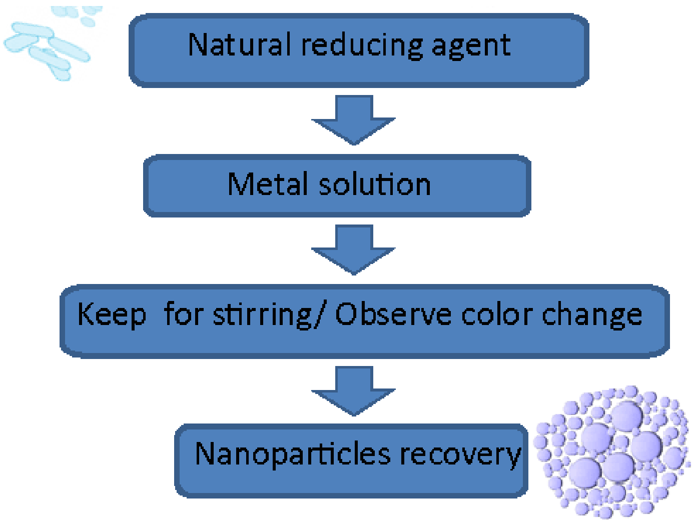

Figure 3: schematic process of biogenic NPs synthesis (*Ingale et al 2013*) [20]

Generally, bacterial synthesis of metallic NPs is often achieved by a reduction step followed by a precipitation step composed of two parts: nucleation and crystal growth. [19]

Some of the most important advantage of biogenic synthesis of NPs is use of non-toxic production agents, limitation in synthesis costs (thanks to the use of bacteria easily available) and production of bio-compatible NPs both for environment and for humans.[19]

In order to use bacteria to synthetize SeNPs, it’s important to consider that microorganisms play a major role in the biogeochemical cycle of selenium in the environment.

A large number of bacterial species, residing in diverse terrestrial and aquatic environments, are resistant to Selenium oxyanions and possess the ability to reduce selenite and selenate into less available elemental Selenium.[7]

The process can occur through both enzymatic or non-enzymatic mechanisms, leading to the formation of Se nanostructured particles (SeNPs) which are deposited inside the cell, within the periplasm or extracellularly.[7]

Microbial reduction of selenite occurs under both anaerobic and aerobic condition, but anaerobic respiration is considered the most likely mechanism for selenite transformation to Se^0 by means of dissimilative metabolism.[7]

Biogenic synthetized SeNPs have shown presence of a macromolecules-based envelope around themselves. Several studies provide evidence that proteins might play a key role in the nucleation and crystal growth of SeNPs. Furthermore, their presence can improve SeNPs affinity for membrane, permitting SeNPs passage outside the cell.[7]

SeNPs synthesis from *Bacillus mycoides* SelTe01

In this project *Bacillus mycoides* SeITE01 has been used for SeNPs synthesis. This bacterium can reduce aerobically selenite into elemental Selenium, forming both extracellular and intracellular (less frequent)

SeNPs spherical in shape and with a size-range from 50 nm to 400 nm, based on incubation time. [7]

Bacillus mycoides is a common road-shape soil bacterium, occurring in the rhizosphere of different plant species. Rhizosphere is a narrow region of soil directly influenced by root secretions and associated with soil microorganisms.[7] This bacterium is called *"mycoides"* just due to fungal-like growth on agar plates with filaments of chained cells projecting radially and turning left or right. [7]

Rate and efficiency of selenite reduction by *Bacillus mycoides* SeITE01 are related to both the initial selenite concentration and the total number of bacterial cells. This process is accompanied by the appearance of a bright red color in the growth medium, due to excitation of the surface plasmon vibrations of new-forming monoclinic selenium (m-Se) particles. [7]

Lampis and co-workers in 2014[7] have established two possible mechanisms for reduction of selenite and formation of SeNPs for *Bacillus mycoides* SeITE01. The main mechanism proposed has involved action of proteins or peptides released by bacterial cells or activated at the plasma membrane. These biological substances can function as oxido-reductase enzymes and selenite can be reduced to elemental Selenium because of interaction with these proteins. After that, Se^0 seed can grow in large SeNPs by aggregation of Selenium atoms.

The second proposed mechanism has concerned an ancillary mechanism of selenite intracellular reduction and also an enzymatic membrane activity. In this case, SeNPs has grown inside cells and after cell lysis can go outside.

In general, SeNPs formation in this strain is a two-step mechanism (Fig.4):

- selenite probably is first reduced by thiol groups of extracellular proteins or peptides, forming selenides
- selenides can be hydrolyzed releasing SeNPs, which undergo extracellular precipitation [7]

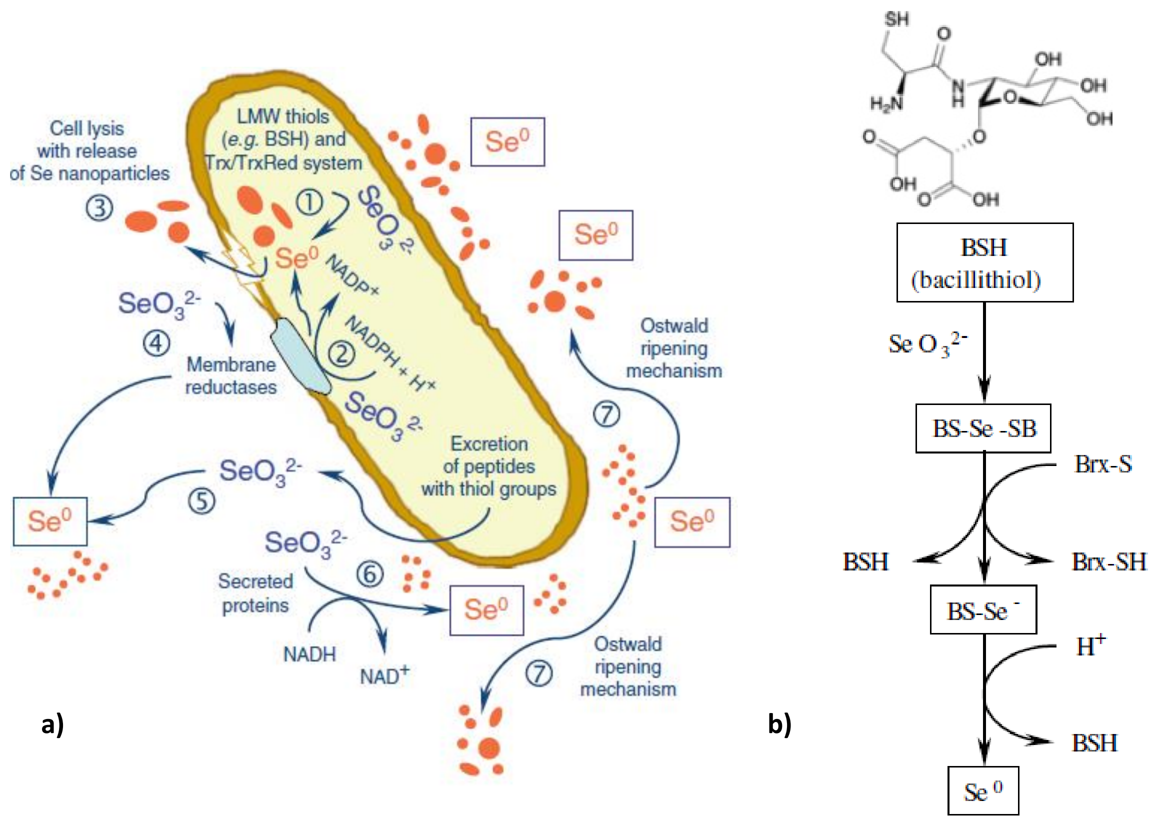

Figure 4: a) Hypothesis of SeNPs formation in *Bacillus mycoides* SelTE01 and **b)** suggesting mechanism of Selenite detoxification in *Bacillus* sp. (*Lampis et al 2014*)[7]

Comparison between chemical SeNPs and biological SeNPs

To prove biogenic SeNPs antimicrobial properties and their advantages in terms of synthesis protocols, final products and possible applications rather than chemically synthetized SeNPs, a comparison between these two kinds of SeNPs has been made.

Firstly, their physical-chemical properties and morphologies have been characterized using DLS, Z potential, SEM and EDS analysis.

Furthermore, both chemical and biogenic SeNPs antimicrobial activity against different biofilms were tested using Minimum Biofilm Eradication Concentration (MBEC) Assay and Calgary Biofilm Device (CBD).

Finally, using Confocal Laser Scanning Microscopy (CLSM) and SEM analysis it was possible to hypothesize a mechanism of SeNPs action against biofilm formation and growth.

MBEC Assay and CBD

MBEC Assay is a high throughput screening test used to determine the efficacy of antimicrobials against biofilms of a variety of microorganisms. The MBEC Biofilm Inoculator is called Calgary Biofilm Device and it's used to determine not only the MBEC, but also minimum inhibitory concentration (MIC) and minimum biocidal concentration (MBC) of several kind of antimicrobial agents.[21]

CBD is made of a polystyrene lid with 96 pegs fitted into a standard 96-well microtiter plate that allow the production of 96 equivalent biofilms (Fig. 5).[22]

Through the use of this method, one batch culture apparatus allows single or multiple species biofilms to be tested against several variables such as growth medium formulations and exposure times.[23]

Biofilms are established on the pegs under batch conditions (no flow of nutrients into or out of an individual well) with gentle mixing.[21] Biofilms form on the pegs of the CBD when planktonic bacteria attach to the surface.

After inoculation of CBD with bacteria cells, it is placed on a gyrorotary shaker in an incubator at 37°C, which provides the shearing force for facilitating the formation of biofilms on the peg lid. In the presence of shear, these bacteria become attached and grow to form mature biofilms.[23]

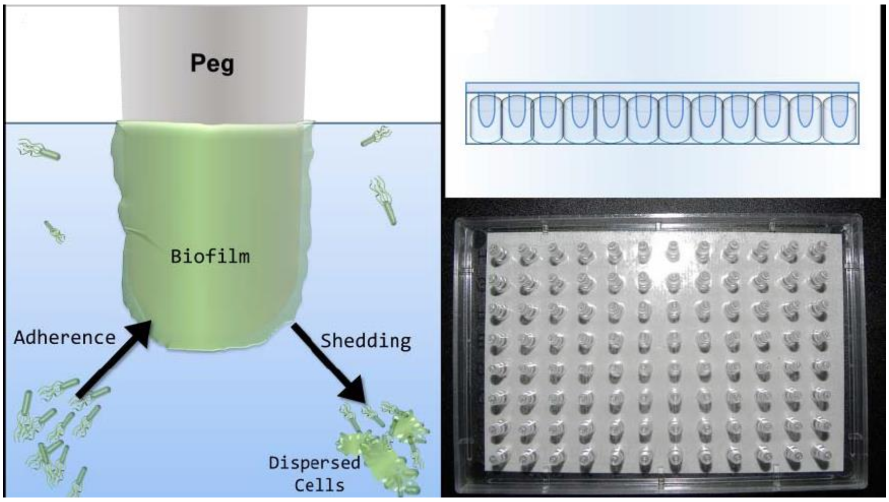

Figure 5: a) biofilm formation on the pegs of CBD when planktonic bacteria adsorb to the surface and **b)** structure of peg lid (*Ceri et al 2001*) [21]

Normally, in the MBEC Assay protocol, the established biofilm is transferred to a new 96 well plate for antimicrobial efficacy testing. The assay design allows for the simultaneous testing of multiple biocides at multiple concentrations with replicate samples, making it an efficient screening tool.[24]

The ability of the CBD to generate a large number of biofilm replicates was used either for the evaluation of a variety of fixing protocols and combinations of fluorescent stains, such as acridine orange, or for the staining of biofilm extracellular polysaccharides with fluorophore-conjugated lectins.[22] It's also possible to select a target biofilm size for antibiotic susceptibility testing and to expose biofilm to multiple antibiotics in a single assay.[22]

CBD is an advantageous tool because of its multiple equivalent biofilms that can be easily used for MBEC Assay, making the process shorter, simple and decreasing possible contaminations.[23] Using MBEC Assay, the availability of multiple testing sites greatly reduced the time required to determine the antibiotic susceptibilities to 3 days.[24]

Finally, it can also prove to be important in the development of new antibiotics selected for their efficacies against biofilms.[21]

In order to both evaluate growth ability of biofilms and antimicrobial agents ability, it's possible to coat CBD with several polymers and materials.[22] One of the most interesting modified CBD, is a particular plate coated with hydroxyapatite. Hydroxyapatite is a biopolymer and it's the principal component of human bones and teeth. In this project, using hydroxyapatite coated CBDs, chemical and biogenic SeNPs action have been tested against several pathogenic biofilms. Furthermore, thanks to hydroxyapatite structures and presence in human body, it was possible to figure out the use of SeNPs coating onto hydroxyapatite surfaces, in order to inhibit formation of biofilms on biomedical devices, such as artificial teeth, bones or joints.

Hydroxyapatite (HA)

Hydroxyapatite is a naturally occurring mineral formed of calcium apatite $Ca_5(PO_4)_3(OH)$ with a recognized crystalline structure.[25]

HA is the key inorganic component of bones and hard tissues of vertebrae in mammals: nanosized hydroxyapatite is the main component of mineral bone.[25] Furthermore, it's also an important bioactive ceramic materials: it's able to promote regenerative bone growth, direct chemical bonding with bone and osteo-integration (interaction in absence of connective tissue on the interface between material and bone) without breaking down or dissolving when used in orthopedic, dental and maxillofacial applications. In this sense, HA can be define as biomaterial, meaning that is a biocompatible and efficient material that can be used in biomedical applications, such as osteo-implants.[26]

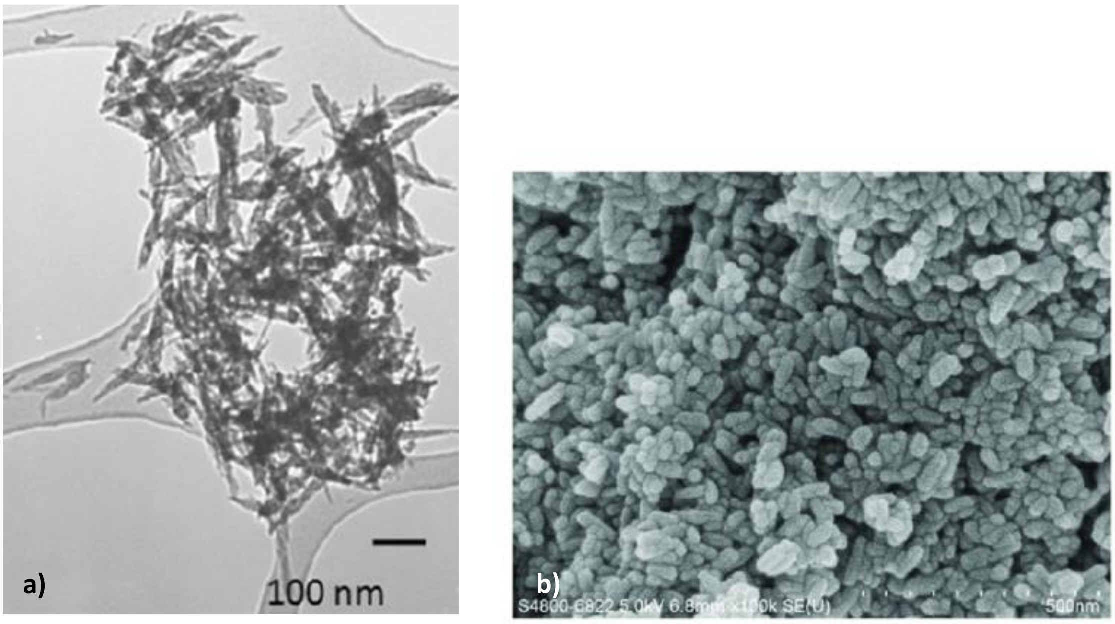

Figure 6: a) TEM image of HA synthetic crystals and **b)** SEM image of HA ceramic powder (http://www.azom.com/article.aspx?ArticleID=107) [26]

HA is a thermally unstable compound, decomposing at temperature between 800°C to 1200°C. Because of its chemical and crystal structure, HA is characterized by substitution processes. The most common substitutions involve carbonate, fluoride and chloride substitutions for hydroxyl groups. These processes can affect biological and physic-chemical properties of native HA.[26]

Structure

Even if HA has monoclinic structure, it's normally considered to have hexagonal crystalline symmetry structure, because dividing unit cell in two halves, they're equivalent.[27] The factor that defines the symmetry of a unit cell is the arrangement of OH- ions.[24] The crystallographic unit cell of HA normally contains ten calcium cations arranged in two non-equivalent sites called Ca(I) and Ca(II). The structural hydroxyl groups are located in columns, where oxygen atoms are too distant (3.44 Å) to form hydrogen bonds.[27]

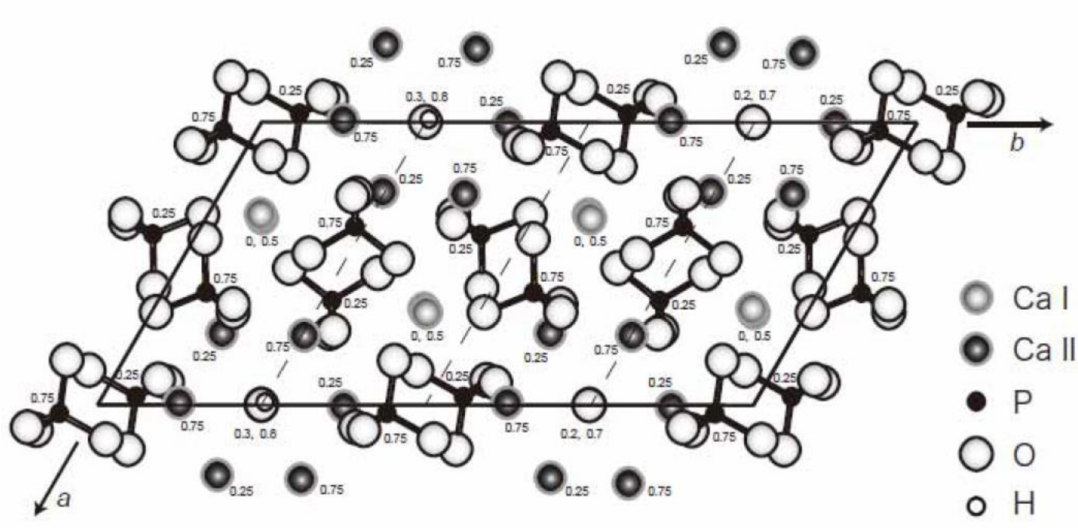

Figure 7: crystal structure of HA (*Suetsugu et al 2013*) [25]

The structure of HA is broadly determined by the positions of Ca^{2+} and PO_4 ions.[24] It's important to note that all chemical substitutions in HA structure can cause lattice distortion, vacancies or crystal defects.[27]

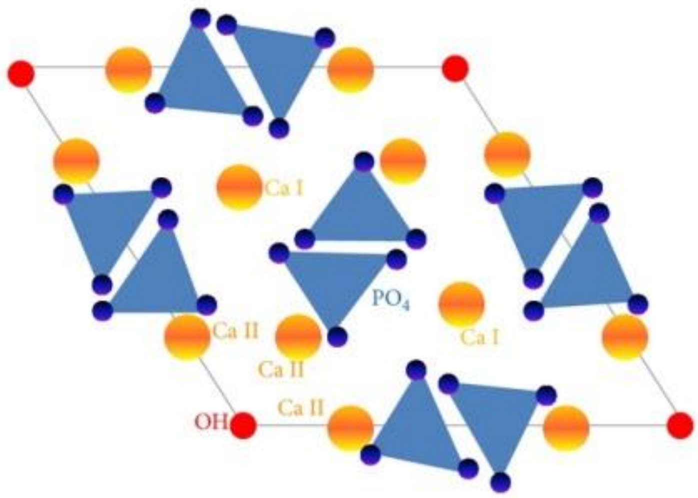

Figure 8: schematic view of HA structure (*Kolmas et al 2015*) [27]

The core framework of the structure is constituted mainly of the PO_4^{3-} tetrahedron, with two types of channel structures that lie parallel to the c –axis (perpendicular to the plane of the paper). Eight of the 20 Ca^{2+} in the unit cell are located at the Ca^{2+} site (Ca I), with the remaining 12 Ca^{2+} located on Ca II site.[24]

There is Ca^{2+} exposed on the crystal surface, giving to HA physical-chemical properties such as surface charge ability to interact with organic compounds.[24]

However, at high temperatures impurities or holes could be included in HA structure and this neat arrangement could be disordered.[24]

Applications

HA, thanks to its high biological activity, biocompatibility, osteo-conductivity, adaptation under in vivo conditions and similar composition to the inorganic fraction of mineralized tissues, play a crucial role in bone and teeth reconstructive surgery.[27] In so doing, HA had significant success in strengthening the fixation between the implant and bone tissue, reducing the healing period during orthopedic implantation practice.

The primary feature of HA is its ability to be doped with various ions in order to change physical, chemical and biological properties of apatites .[28] In this sense, HA is a polymer normally susceptible to exchange ions chemistry and is able to interact with ions similar both for charge and for size to those that compose it: Calcium, Phosphate and Hydroxide ions.[27] HA can interact with huge class of different ions: Calcium cations may be partially replaced by Mg^{2+}, Mn^{2+}, Zn^{2+}, Sr^{2+} or Ag^{+}; Hydroxide anions can be substituted by Cl^{-}, F^{-}, CO_3^{2-}, O^{2-} or S^{2-}; PO_4^{3-} may be replaced by CO_3^{2-} or SiO_4^{4-}. [27]

Normally HA is used as sintered body, powder, porous block or bead to fill bone defects, especially when large sections of bone have had to be removed (bone cancers) or when bone augmentations are required (maxillofacial reconstructions or dental applications). HA acts as scaffold and promotes rapid filling of the void by naturally forming bone. It's also able to become part of the bone structure and to reduce healing times.[25] Improvements to these materials are being made with regards to their mechanical properties and bioactivity by compounding with organic polymers.

HA usually has a coating material over titanium-based implants, as this has been discovered to be invaluable due to its mechanical strength characteristics.[24]

Even if HA exhibits biological activity and efficacy as artificial bone material, there are still problems in using it to replace physiological bone, especially for mechanical strength, brittleness and excessive wear with time.[24] Furthermore, to use HA in order to replace bones and teeth, it's necessary to develop new materials able to inhibit bacterial growth, development of infections and, if it's possible, cancer reoccurrence and osteoblast apoptosis.[29] In this sense, it's important to incorporate in bone implants materials with chemo-preventive and antimicrobial actions, in order to improve their biocompatibility and biomedical effects.[29]

In last few years there was strong interest in possibility to develop HA modified structures enriched of ions with antimicrobial properties, such as Ag^{+} , Au^{2+} and SeO_3^{2-} ions.[27] In so doing, it may be possible to create new class of HA based materials with strong antimicrobial activity, that can be useful in biomedical applications, such as bones and teeth reconstruction.

Effectively, one of the most important problem of this process is the possibility to develop infections due to pathogenic biofilms that are able to grow onto surgery tools, catheters or HA structures, even if they are under sterilized conditions. In this sense, HA polymers coated of strong antimicrobial agents could have a key role in orthopedic applications.

AIM OF THE STUDY

The principal aim of this project was to evaluate both biogenic and chemical SeNPs antimicrobial abilities to inhibit biofilm formation and eradication. In so doing, it was necessary to:

- synthetize both biogenic SeNPs and chemical SeNPs
- physically-chemically characterize them, in order to underline their differences and similarities

At the same time, a comparison between antimicrobial properties of these 2 SeNPs classes has been made testing their action against pathogenic biofilms with CBDs coated of HA. Using together MBEC assay, CLSM, SEM and EDS analysis, it was possible to verify antimicrobial properties of SeNPs and to compare data from different classes of them. SEM and EDS analysis were used also to study HA structure and possible interaction with SeNPs. Finally, use of SeNPs as antimicrobial coating in biomedical applications has been evaluated, using as model of study HA coated CBDs able to mime bone and teeth structure and artificial implants.

MATERIALS AND METHODS

Materials

Nutrient Broth, Agar Technical, sodium chloride (NaCl) were obtained by Oxoid Ltd, Basingstoke Hampshire, England.
Sodium selenite (Na_2SeO_3), Octanol, L-cysteine, Ascorbic Acid, selenous acid (H_2SeO_3), L-Histidine, Reduced Glutathione was obtained by Sigma Aldrich, St. Louis, MO, USA.
Tris-HCl 1,5 mM was obtained adding 0,091 g of Trizma Base (Sigma Aldrich) to 500 mL of water and then using chloridic acid (HCl) from Sigma Aldrich, pH was adjusting to 7,0.
0,5 McFarland Barium Sulfate Turbidity Standard used in MBEC assay was prepared by Biofilm Research Group of University of Calgary.
Bacillus mycoides SeITE01 has been isolated previously from the rhizosphere of Se-hyperaccumulator plant *Astragalus bisulcatus.*[7]
E. coli NCTC 12241, P *aeruginosa* NCTC 12934 and S*. aureus* ATCC 25923 used were obtained from Prof. Douglas Morck, full professor of Faculty of Veterinary Medicine in University of Calgary.
CBDs were obtained by Innovatech Inc., Edmonton, Canada.
Platform shaker was obtained by New Brunswick Scientific.
Ultrasonic cleaner (water bath sonicator) model 250T was from VWR Scientific.

Chemical synthesis of SeNPs

Figure 9: a) L-cysteine SeNPs, **b)** Ascorbic acid SeNPs and **c)** Lin&Wang protocol SeNPs

Synthesis of Ch-SeNPs with L-Cysteine and Na_2SeO_3[30]

Reaction of L-Cysteine and Na_2SeO_3 is immediate: adding of Na_2SeO_3 to L-Cysteine lead to reduction of SeO_3^{2-} ions and to formation of SeNPs.

In this work we synthetized SeNPs using 500 µL of Na_2SeO_3 100 mM added to 500 µL of L-Cysteine 50 mM (Fig.9a).

Synthesis of Ch-SeNPs with Ascorbic Acid and Na_2SeO_3[31]

Ascorbic acid reacts with Na_2SeO_3 in order to reduce SeO_3^{2-} ions and to produce SeNPs. Reaction with ascorbic acid is longer than that with L-Cysteine, as we have observed in experiments.

In this work we have prepared SeNPs adding 1,00 mL of ascorbic acid 30 mM to 200 µL of Na_2SeO_3 100 mM (Fig.9b).

Synthesis of Ch-SeNPs with H_2SeO_3, $Na_2S_2O_3$ and SDS (Lin & Wang 2005)[10]

Using Lin & Wang protocol published in 2005, we have synthetized SeNPs with a 6-hours incubation of reducing solutions made by $Na_2S_2O_3$ and SDS at different concentrations with H_2SeO_3, in order to obtain SeNPs with different size. Reducing solution is made by 10 mL of SDS 0,01 M adding to

3,289 g of $Na_2S_2O_3$ dissolved in 40 mL of milliQ water, getting a final solution concentration of 520 mM. In order to synthetize SeNPs with same size of other protocols, I made a solution of 750 µL H_2SeO_3 5 mM to 216 µL of reducing agent 150 mM and 534 µL of milliQ water to obtain a final volume solutions of 1,5 mL (Fig.9c).

Biological synthesis of SeNPs

Firstly, *Bacillus mycoides* has been grown in inoculating tubes with 4 mL of Nutrient Broth for minimum 24 hours under stirring. Inoculating tubes were later added each one in 1,00 L flasks containing 400 mL of Nutrient Broth and 8 mL of filtered Na_2SeO_3 (100 mM). Therefore, *Bacillus mycoides* cultures has been grown at 27°C under stirring, in presence of sodium selenite for 24 hours in order to permit reduction of SeO_3^{2-} ions in Se^0 (Fig.10).

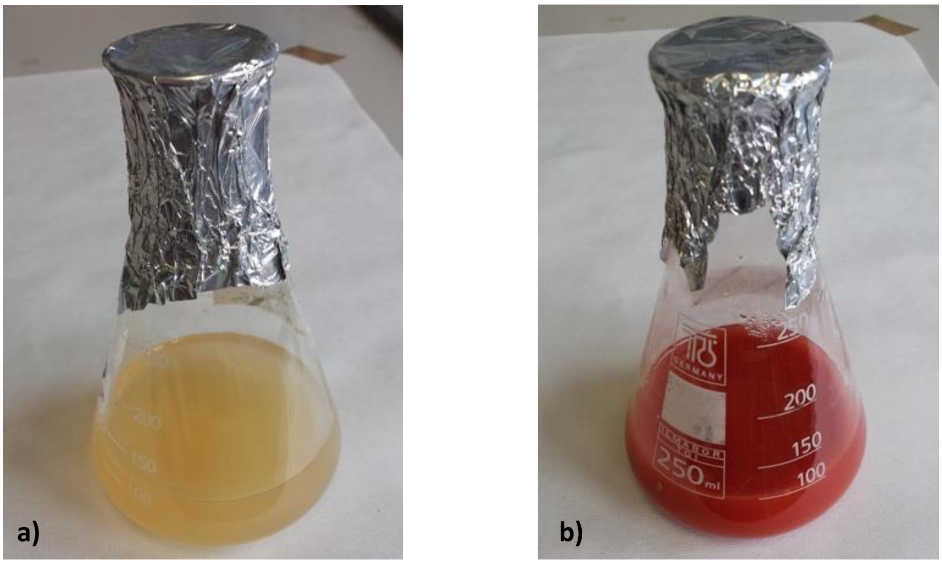

Figure 10: growth of *Bacillus mycoides* SelTE01 in presence of Na_2SeO_3 **a)** at incubation time (t = 0 h) and **b)** after 24 h of exposure

Evaluation of selenite reduction and selenium formation

Efficiency of selenite reduction was determined for *Bacillus mycoides* SeITE01 in rich growth medium (Nutrient Broth). All microbiological tests were carried out in 250-ml Erlenmeyer flasks containing 100 ml of growth medium incubated at 27°C on an orbital shaker (200 rpm). Each flask was inoculated with aliquots from stationary-phase microbial cultures 1 to reach a final optical density of 0.01. Assays were performed in the presence of 2 mM Na_2SeO_3. Culture samples collected at different times were analyzed for bacterial growth, residual selenite in the medium, and formation of elemental Se.

Microbial growth estimation

Bacterial growth was evaluated by counting the colony forming units (CFU) on agarised Nutrient Broth plates seeded with aliquots of bacterial cultures. All analyses were performed in triplicate. Bacterial growth in presence of SeO_3^{2-} was checked vs. control cultures incubated in Nutrient Broth with no Na_2SeO_3 added.

SeO_3^{2-} content determination

SeO_3^{2-} concentration in culture medium was measured spectrophotometrically by using the method described by Kessi et al in 1999.[32] This method was carried out as follow: first 10 ml of 0.1 M HCl, 0.5 ml of 0.1 M EDTA, 0.5 ml of 0.1 M NaF, and 0.5 ml of 0.1 M of disodium oxalate were mixed in a 50 ml glass bottle. A 50- to 250-µl sample containing 100 to 200 nmol of selenite was added, and then 2.5 ml of 0.1% 2,3-diaminonaphthalene in 0.1M HCl was amended. The bottles were incubated at 40°C for 40 min and then cooled to room temperature. The selenium-2,3-diaminonaphthalene complex was extracted with 6 ml of cyclohexane by shaking the bottles vigorously for about 1 min. The absorbance at 377 nm of the organic phase was determined by using a spectrophotometer Heλios β, Unicam. Sterile cultures were also tested for SeO_3^{2-} concentration as negative controls. All manipulations were done in the dark.

Calibration curves were performed by using 0, 50, 100, 150, 200 nmol of selenite in Nutrient broth.

Se^0 content determination

Se^0 concentration was measured spectrophotometrically by using the method described by Biswas et al in 2011.[33] A standard for elemental selenium was prepared by reducing selenite to amorphous red Se^0 as follows: aliquots of a 0.1M sodium selenite solution were placed in test tubes to give a range of 1 to 10 µmol selenite per tube. 25 µmol of $HN_2OH{\cdot}HCl$ (Sigma-Aldrich) were then added to each tube containing selenite, to obtain a quantitative reduction of SeO_3^{2-} to Se^0. The tubes were gently mixed and after 1 hour, the intensity of the red-brown selenium solution was measured at 490nm. To establish the Se^0 standard, average values of triplicate samples were used.

To determine the amount of selenium produced by *Bacillus mycoides* SeITE01 strain, the bacterial culture along with the insoluble red elemental selenium was gently mixed and 10 ml was transferred to polycarbonate centrifuge tubes. After centrifugation at 5000 x g, bacterial cells and elemental selenium were collected as a pellet. To remove non-metabolized selenite, pellets were washed twice with 10 ml of 1 M NaCl.

The red colloidal selenium in the pellet was dissolved in 10 ml of 1 M Na_2S and after centrifugation to remove bacterial cells, absorption of the red-brown solution was measured at 490 nm.

SeNPs extraction from *Bacillus mycoides* SeITE01 cultures

After 24 hours of incubation under stirring, flasks containing Bacillus mycoides have shown red coloration due to effective reduction of Selenite ions to elemental Selenium.
In order to extract SeNPs from *Bacillus mycoides* cultures, content of each flask was divided in 8 falcon with 50 mL of capacity and they were centrifuged at 6000 rpm for 10 minutes. Pellets were washed twice with 0.9% NaCl solution, resuspended in Tris/HCl buffer (pH 8.2) and then disrupted by ultrasonication at 100 W for 5 min. The suspension was then centrifuged at 10000 x g for 30 min to separate disrupted cells (pellet) from NPs (supernatant). NPs were recovered after centrifugation at 40000 x g for 30 min, washed twice and resuspended in deionized water.

SeNPs characterization

To determine both biogenic and chemical SeNPs morphology and physical-chemical properties, severals techniques has been used:

- Absorbance spectrophotometer
- DLS
- Z potential
- SEM and EDS

Absorbance spectrophotometer

To collect absorbance spectra of biogenic SeNPs produced by *Bacillus mycoides* SelTE01 after 6h, 24h and 48 h of Na2SeO3 exposure, Cary 60 UV-Vis by Agilent Technology (California, USA) was used.

DLS and Z potential

In order to measure DLS and Z potential value of all 5 SeNPs classes, Zen 3600 Zetasizer Nano ZS from Malvern Instruments (Worcestershire, UK) was used.

SEM and EDS

Both biogenic and chemically synthesized SeNPs were analyzed through scanning electron microscopy (SEM). SeNPs were fixed, dehydrated with increasing ethanol concentrations and dried through the critical point method by using liquid CO2. They were mounted on metallic specimens stubs and then directly observed through XL30 ESEM (FEI-Philips) equipped with an EDS micro-analytical system.

SeNPs antimicrobial properties

To proof antimicrobial ability of biogenic SeNPs and to make a comparison with those chemically synthetized, some techniques has been used:

- MBEC assay
- CLSM analysis
- SEM and EDS analysis

MBEC assay

In order to verify both biogenic and chemical SeNPs antimicrobial properties, MBEC assay with CBDs coated of hydroxyapatite was used, following MBEC Assay Procedural Manual written by Innovatech Inc. in 2012.

SeNPs action against 3 different biofilm strains grown at 37°C has been tested:

- *E. coli* NCTC 12241
- *P. aeruginosa* NCTC 12934
- *S. aureus* ATCC 25923

Pathogenic biofilms were grown on hydroxyapatite plates in 2 different conditions:

- 24 h growth of pathogen biofilms added of SeNPs
- 24 h pre-growth of pathogen biofilms and exposure of MBEC plate to SeNPs for 24 h

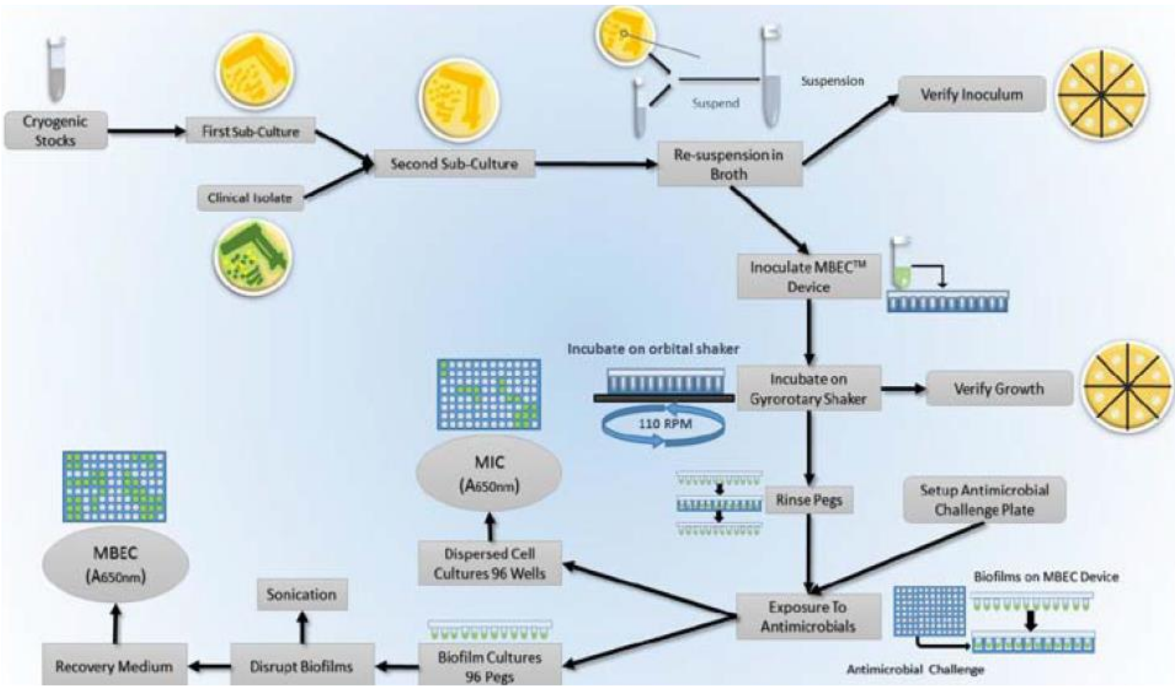

Figure 11: flow diagram representing the steps in the experimental process for 96 well base antimicrobial susceptibility testing using MBEC assay (*Ceri et al 2001*) [21]

Using MBEC assay, it was possible to evaluate action of 11 different SeNPs concentrations, going from 2,5 mg/mL to 0,0025 mg/mL with serial dilutions 1:2.

In order to obtain numerable results from MBEC assay 12 serially dilutions Nutrient Agar plates (1 as control and 11 for different SeNPs concentrations) for each SeNPs classes were prepared.

After 18 h of incubation, it was possible to count number of colonies present on plates and to convert these values in CFU/mL (Colony Forming Unit):

$$CFU = \frac{n° \text{ colonies} * \text{dilution factor}}{\text{plated volume}}$$

Using Log[CFU/mL], curves of these values versus SeNPs concentrations have been obtained. This procedure has been repeated 3 times as statistical analysis for each SeNPs class.

CLSM

CLSM model DM IRE2 was obtained by LEICA and images were processed using Imarisx64 from Bitplane, USA.

Pegs prepared on hydroxyapatite CBDs were break off with alcohol flamed pliers. They were rinsed with 200 µL of 0,9% NaCl solution in a microtiter plate twice and after were stained with Live/Dead BacLight staining kit obtained by Molecular Probes, Burlington (Ontario), Canada for 30 minutes before analysis.

SEM and EDS

SEM used both for SEM and EDS analysis in University of Calgary was FEI XL30, obtained by Philips.

Samples for SEM analysis were pre-grown for 24 hours on hydroxyapatite coated CBDs and after they were deep in 0,1 M Cacodylate buffer (pH=7,2) for 2 h at room temperature, then air dried for 120 h.

Sodium Cacodylate Trihydrate used to prepare SEM analysis buffer was obtained by Electron Microscopy Sciences.

RESULTS AND DISCUSSION

Evaluation of selenite reduction, elemental selenium formation and *Bacillus mycoides* SeITE01 growth

The ability of *Bacillus mycoides* SeITE01 of both growing in presence of SeO_3^{2-} ions and reducing selenite ions into elemental Selenium (Se^0) is reported in Figure 12.

Firstly, growing ability of *Bacillus mycoides* SelTE01 without selenite ions was evaluated as negative control. Consequently, strain growth with Selenite in media, presence of Selenite ions and elemental Selenium in the media have been established, in order to proof *Bacillus mycoides* SelTE01 ability to produce SeNPs (Fig.12).

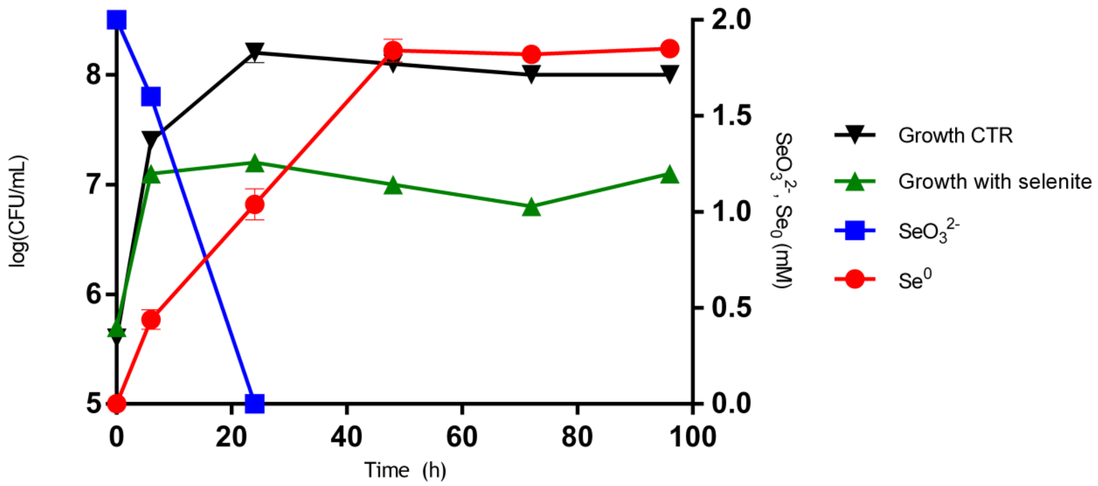

Figure 12: evaluation curve of Bacillus mycoides SelTE01 reduction of SeO_3^{2-} and production of Se^0

Even if number of *Bacillus mycoides* SelTE01 colonies grown in presence of 2 mM SeO_3^{2-} was less than control growth, both samples showed same growth dynamics. Evaluating SeO_3^{2-} presence in growth media, at t = 0 (when there's no effective bacterial growth), there was highest amount of

Selenite, that progressively decreased during time course till it becomes 0 after 24 h of growth.

At the same time, considering Se^0 production, it had 0 value at the beginning (t = 0), while it constantly increased reaching its highest value after 40 h of bacteria growth. After this time, production of Se^0 became stable, reaching 85% presence of Se^0.

These results permit to establish that *Bacillus mycoides* SelTE01 was effectively able to growth in presence of Selenite ions in growth media. At the same time, increasing amount of Se^0 produced by bacteria and decreasing of SeO_3^{2-} ions in media are proves of *Bacillus mycoides* SelTE01 ability to produce nontoxic SeNPs.

SeNPs characterization

Absorbance spectrum

Absorbance spectroscopy measures absorption of radiation in function of wavelength, due to its interaction with samples.[34] Normally samples are able to absorb energy from radiating field and intensity of absorption depends on frequency.[34]

Variation of absorption gives as result absorbance spectrum, usually used in order to underline presence of a particular substance or element in analyzed samples. [34]

Figure 13 shown absorbance spectrum of biogenic SeNPs produced by *Bacillus mycoides* SelTE01 after 6h, 24 h and 48 h of Na_2SeO_3 exposure.

As it's possible to notice analyzing this spectrum, 3 curves of different biogenic SeNPS solutions show same trend in function of wavelength, even if with different absorbance values.

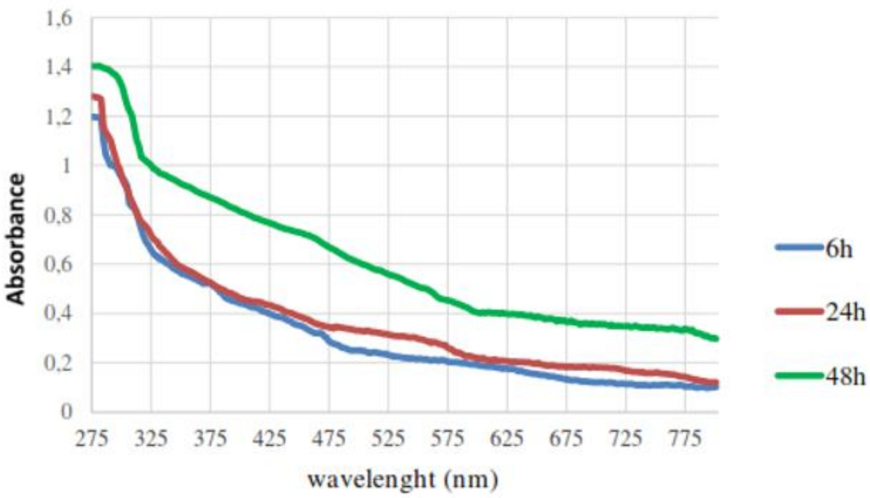

Figure 13: absorbance spectra of SeNPs produced by *Bacillus mycoides* SelTE01 after 6h, 24 h and 48 h

In all 3 analyzed samples absorbance peaks indicating highest values of absorbance corresponds to 275-280 nm region of UV spectrum. It's also important to notice that even if absorbance values of samples are different, biogenic SeNPs produced after 6 h and 24 h of Na_2SeO_3 exposure show very similar absorbance plot. Meanwhile, 48 h sample highlights different plot: absorbance values are higher rather than other 2 samples. However, since all 3 samples have same absorbance spectrum trend, it's possible to affirm that all of them are made of same biogenic SeNPs.

To evaluate *Bacillus mycoides* SelTE01 products as SeNPs, it's possible to analyze SeNPs produced by other strains. Consequently, it can be useful to make a comparison between previously analyzed biogenic SeNPs and those synthetized by *P. aeruginosa* JS-11 in Dwivedi et al. work of 2013.[35] Comparison of absorbance results shows in both classes of SeNPs presence of wide absorbance peaks between 275 nm-300 nm (UV region).

However, in Dwivedi et al. spectrum there's also present another wide absorbance peak around 520 nm, probably due to Surface Plasmon Resonance band of Selenium.[35]

DLS

DLS is a technique for measuring size of particles in submicron region. It measures Brownian motion (random movement of particles due to interaction with solvent molecules) and it relates it to size of particles. Velocity of Brownian motion is defined by translational diffusion coefficient.[36] DLS is a technique that gives measurement of hydrodynamic diameter, which is a value refers to diameter of a sphere with the same translational diffusion coefficient of particle.[36]

Using DLS, a plot of relative intensity of light scattered by particles is obtained, called intensity size distribution. However, in order to overcome problems about background, shape and number of peaks, it's possible to obtain a volume and a number size distribution. [36]

In order to determine hydrodynamic diameter of SeNPs, DLS was used both with biogenic SeNPs samples and chemical SeNPs samples. Because of the presence of clear peaks for shape and intensity, number size distribution of SeNPs has been analyzed.

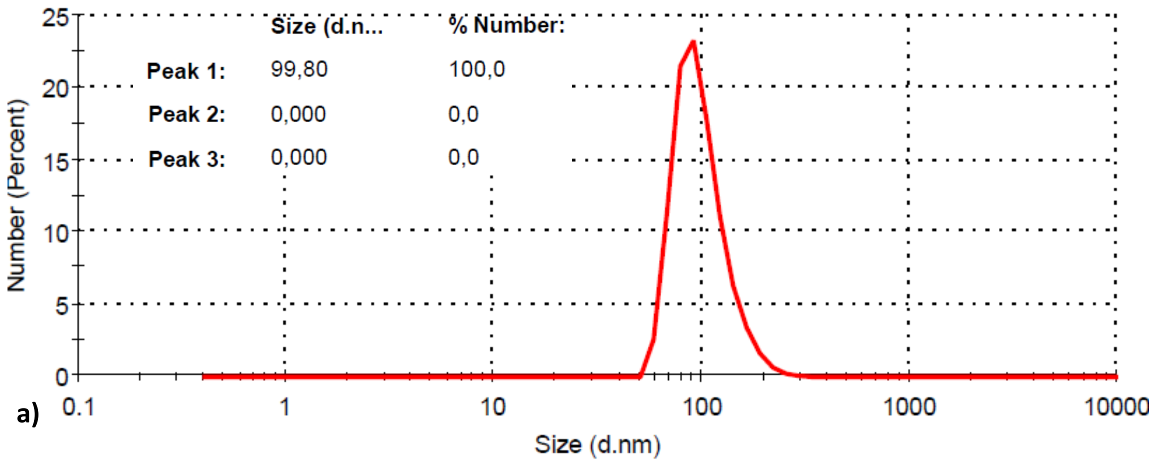

a)

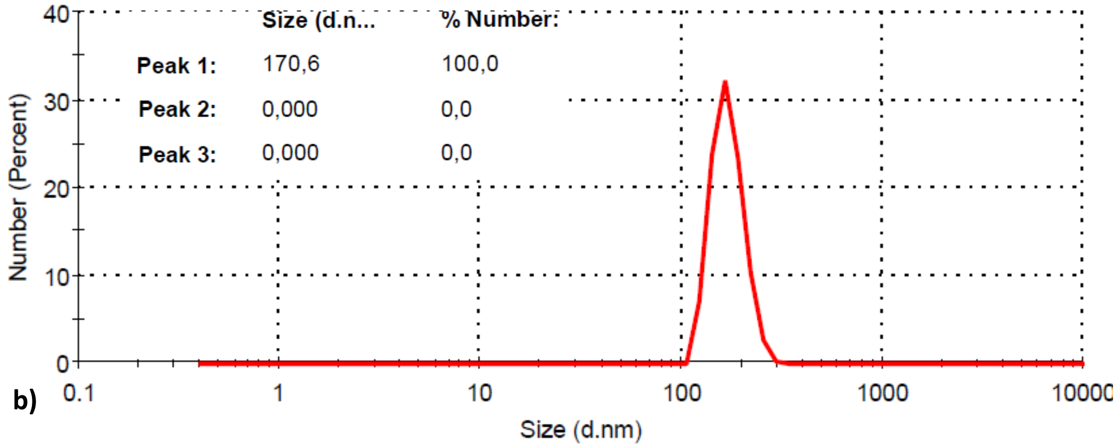

b)

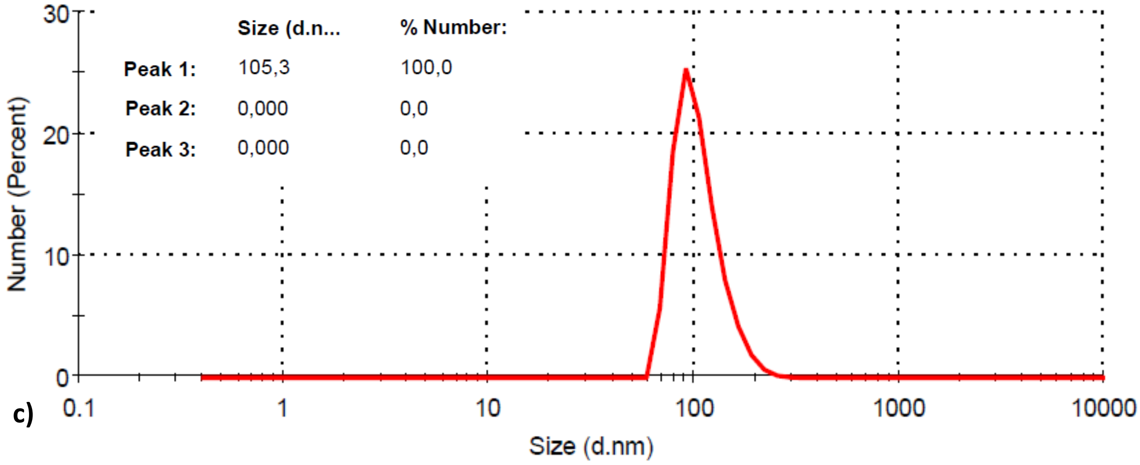

c)

Figure 14: number size distribution of **a)** SeNPs made with L-cysteine **b)** SeNPs made with ascorbic acid **c)** SeNPs made with Lin and Wang protocol

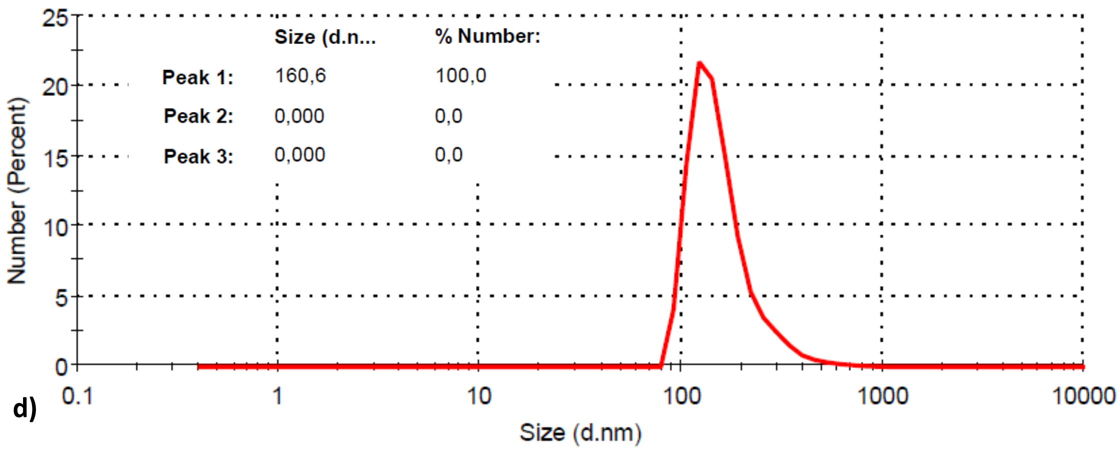

d)

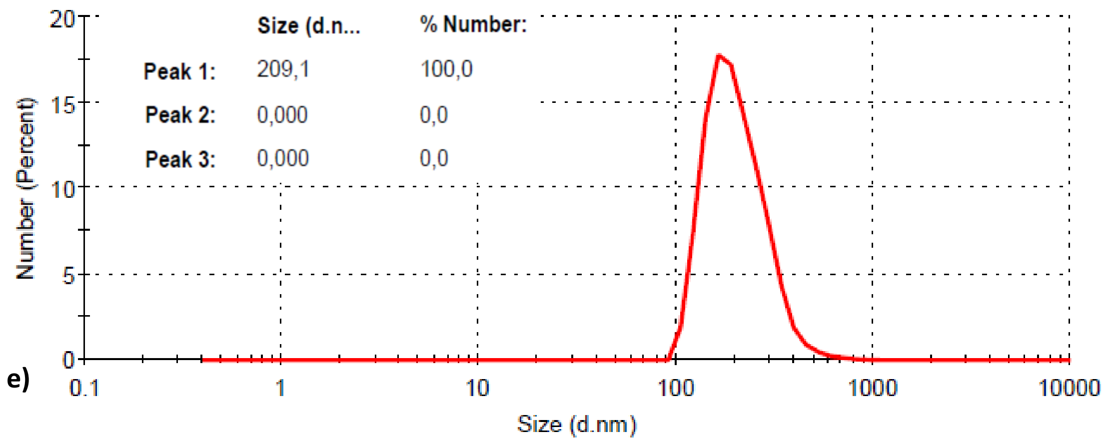

Figure 15: number size distribution of **d)** SeNPs made by *Bacillus mycoides* SelTE01 after 6 h of Na_2SeO_3 exposure **e)** SeNPs made by *Bacillus mycoides* after 24 h of Na_2SeO_3 exposure

Comparing DLS number size distributions of 3 chemically synthesized SeNPs and 2 biogenically synthesized SeNPs, it's easy to observe that they're comparable in size, except for SeNPs made by *Bacillus mycoides* SelTE01 after 24 h of exposure to Na_2SeO_3. 3 chemical SeNPs and those biogenically synthesized after 6 h of exposure of *Bacillus mycoides* to Na_2SeO_3 show peaks going from 99,80 nm to 170 nm, while the other one has a shift in the peak to 209 nm in size.

As correlation with size, normally large particles have slower Brownian motion, while those small move faster.

Chemically synthesized SeNPs with ascorbic acid have highest percentage value of population with same size: 30%, while other 4 classes of SeNPs have value ranging from 17% to 25%. Since these values are similar, it's possible to compare chemical and biogenic SeNPs both for intensity of peaks and size distribution: biogenic SeNPs have similar DLS size distribution to chemical ones.

It's useful also to make a comparison between biogenic SeNPs synthesized using different bacteria strains, in order to analyze differences and similarities in size and shape. As suggested by Antonioli et al. work (2007), *Stenotrophomonas maltophila* SeITE02 is one of the most important bacteria used in order to produce biogenic SeNPs: it's capable of resisting to high concentrations of SeO_3^{2-} , reducing it in nontoxic elemental selenium (SeNPs) under aerobic conditions.[37] Zonaro et al. in 215 analyzed SeNPs produced by Stenotrophomonas maltophila SelTE02 after 24 h of Na_2SeO_3 exposure.[38] Size and distribution of population are similar both to chemical SeNPs and to those synthetized using *Bacillus mycoides* SeITE01: 30% of SeNPs population has 170 nm in size. Both intensity of peak and size are the same of chemical SeNPs made with ascorbic acid.

Another interesting strain able to produce SeNPs in presence of Selenite ions in growth media is *Pantoea agglomerans* UC-32.[39] In 2012, Torres et al. studied biogenic SeNPs produced by this particular strain. In so doing, DLS analysis revealed that *Pantoea agglomerans* UC-32 is able to produce 25% of population of SeNPs with 120 nm of hydrodynamic diameter. Comparing this result with *Bacillus mycoides* SelTE01 DLS number size distribution, it's possible to establish that both intensity of peaks and size of SeNPs are similar for the two strains.

Z potential

Z potential is a physical property exhibited by colloidal systems (heterogeneous systems made of dispersed phase with very fine particles and dispersion medium).

In a liquid colloidal system, liquid layer surrounding particle is formed by 2 different parts: Stern layer (inner region), where ions are strongly bound, and diffuse layer (outer region), where ions are less bound.[40] Inside diffuse layer it's possible to recognize a notional boundary called surface of hydrodynamic shear, where ions and particles form a stable entity.[40] When particles move, ions in the boundary move and the potential at the hydrodynamic shear is the Z potential.

Magnitude of Z potential is used to determine stability of colloidal system: particles with large negative or positive Z potential don't have tendency to aggregate, while systems with low Z potential values don't have force to avoid aggregation and flocculation.[40] Normally, particles with Z potential values more positive than +30 mV or more negative than -30 mV are considered stable.[40]

Result of Z potential measurement is a plot of total counts Z potential values and it's called Z potential distribution.

In order to establish SeNPs stability in water solution, Z potential of all different SeNPs has been measured.

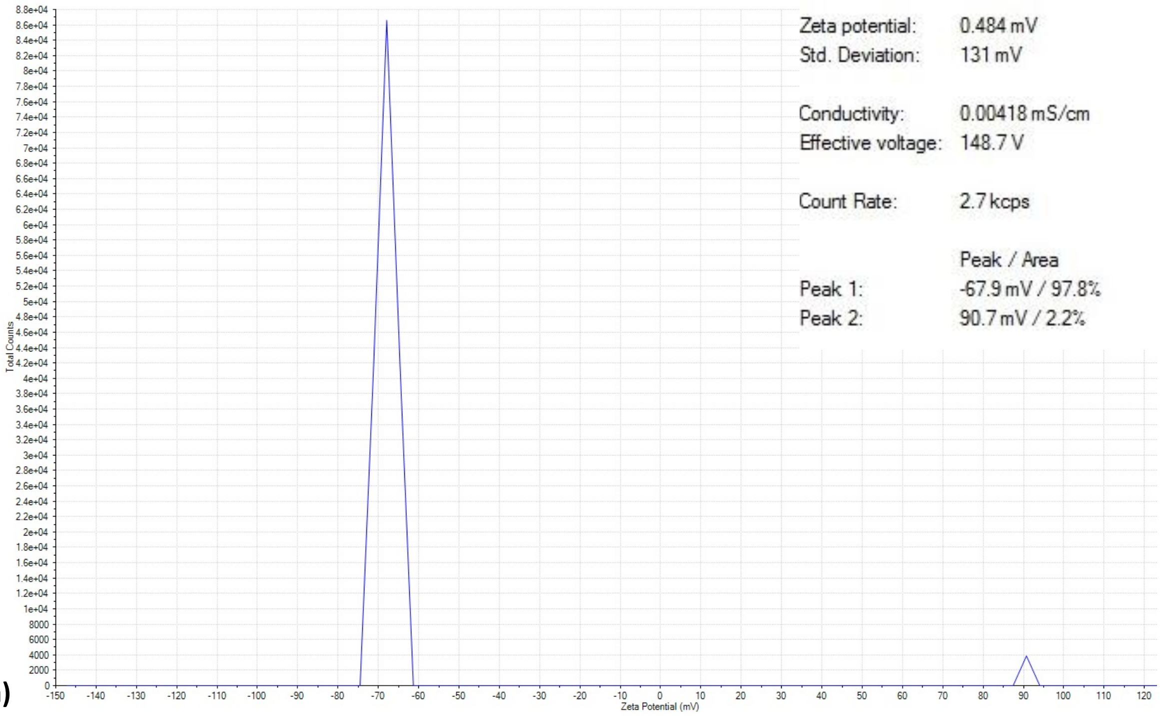

a)

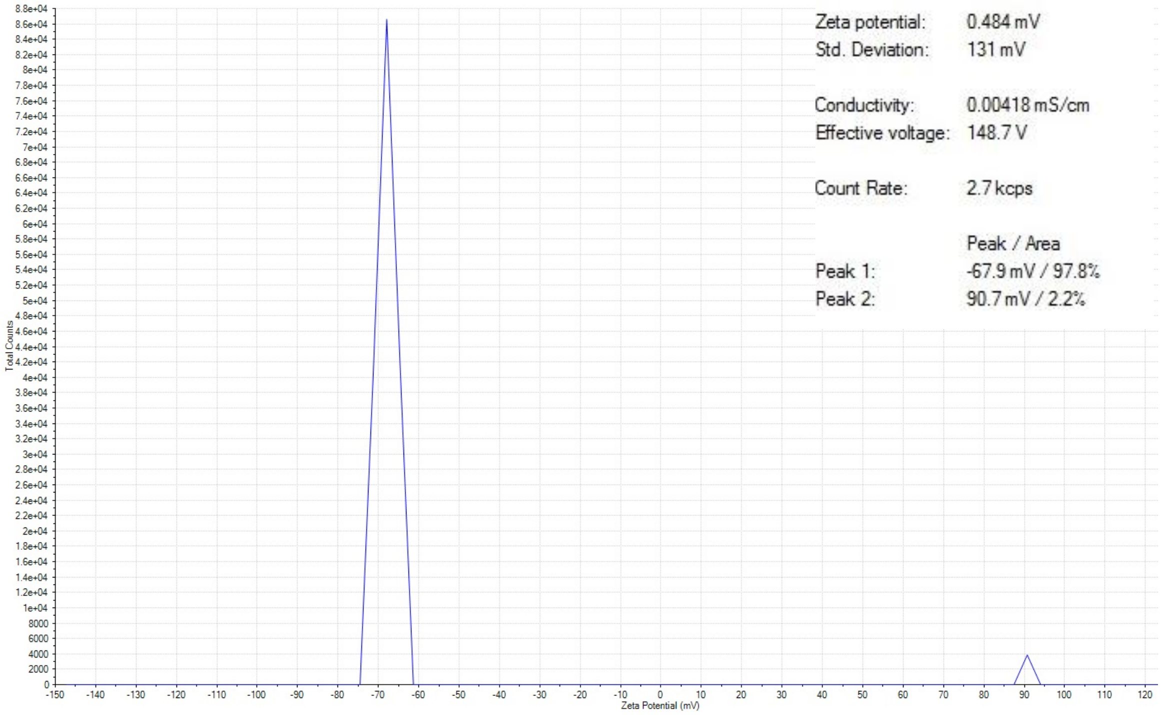

Zeta potential: 0.484 mV
Std. Deviation: 131 mV
Conductivity: 0.00418 mS/cm
Effective voltage: 148.7 V
Count Rate: 2.7 kcps
Peak / Area
Peak 1: -67.9 mV / 97.8%
Peak 2: 90.7 mV / 2.2%
Total Counts
Zeta Potential (mV)

b)

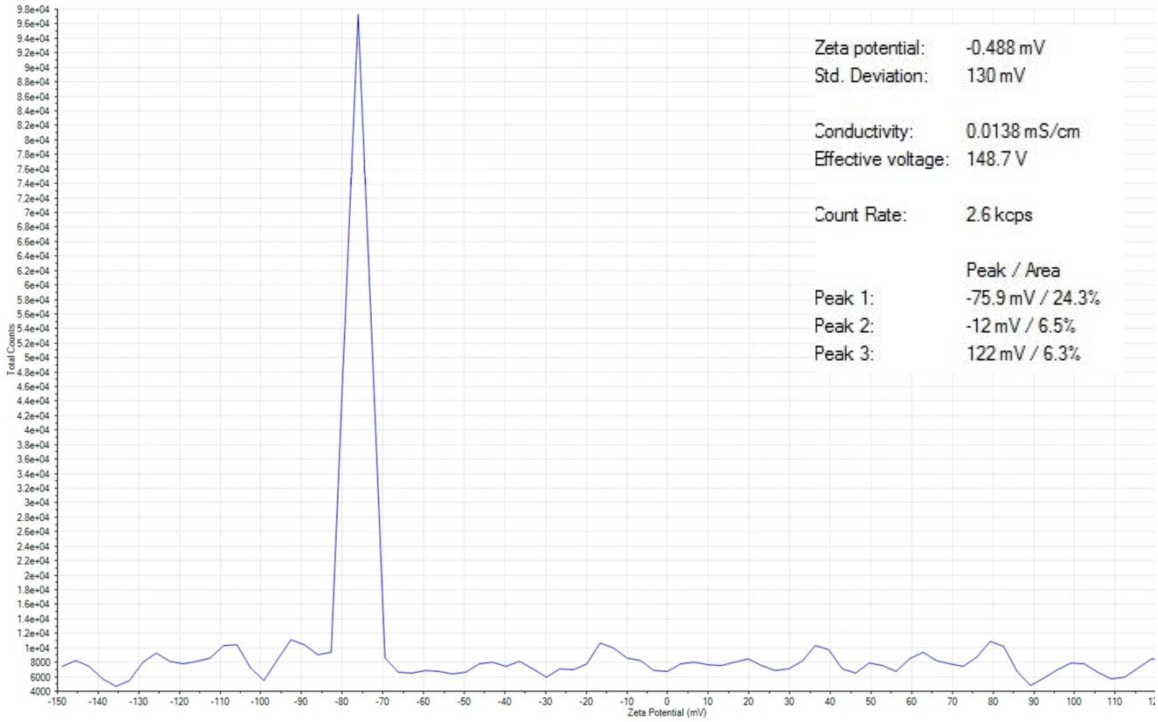

Zeta potential: -0.488 mV
Std. Deviation: 130 mV
Conductivity: 0.0138 mS/cm
Effective voltage: 148.7 V
Count Rate: 2.6 kcps
Peak / Area
Peak 1: -75.9 mV / 24.3%
Peak 2: -12 mV / 6.5%
Peak 3: 122 mV / 6.3%
Total Counts
Zeta Potential (mV)

c)

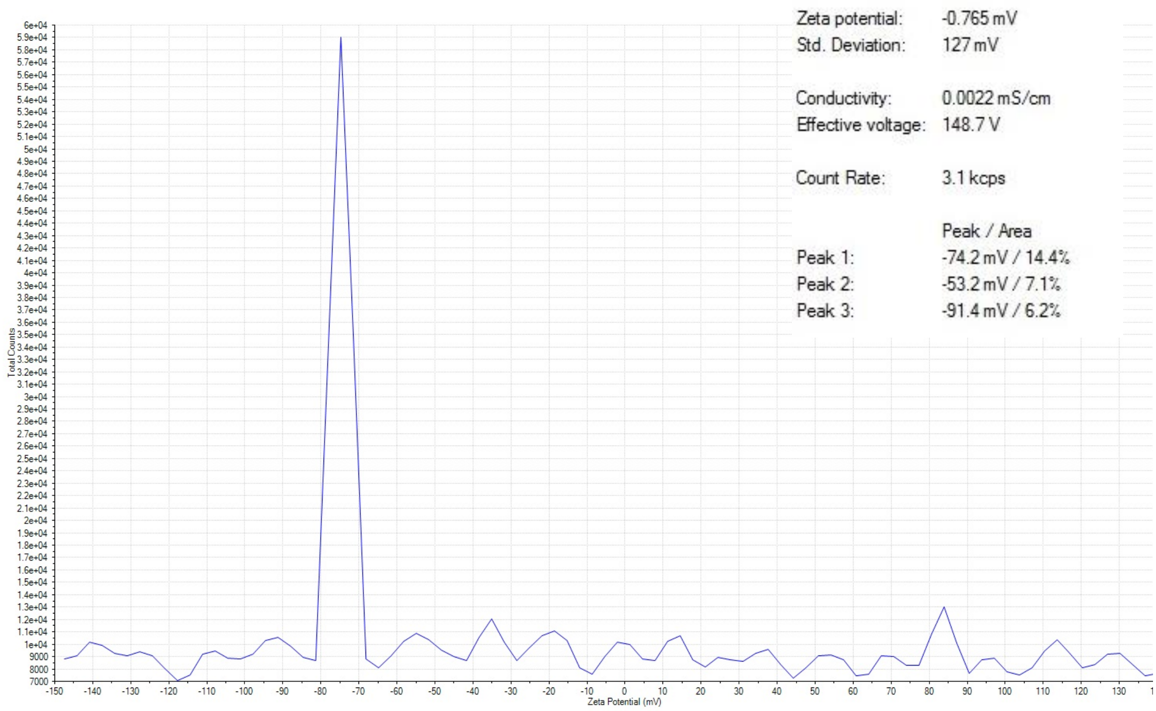

d)

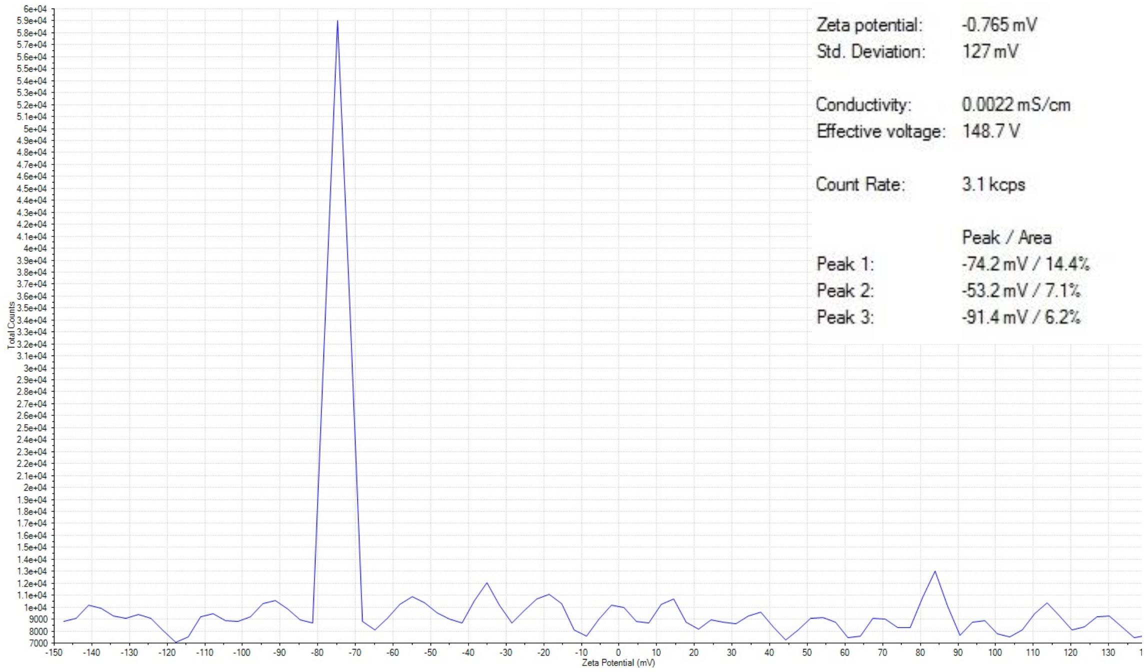

e)

Figure 16: Z potential distribution of **a)** SeNPs made with L-cysteine **b)** SeNPs made with ascorbic acid **c)** SeNPs made with Lin and Wang protocol **d)** made by *Bacillus mycoides* SelTE01 after 6 h of Na_2SeO_3 exposure **e)** made by *Bacillus mycoides* SelTE01 after 24 h of Na_2SeO_3 exposure

As shown in figure 16, all 5 different synthesized SeNPs have strong negative Z potential values. All principal peaks of distributions have similar values, going from -67 mV to -75 mV. According to Z potential theory, these values show strong stability of SeNPs colloidal systems.
It’s also important to notice that Z potential distribution of SeNPs made with Lin & Wang protocol shows same plot of SeNPs made with L-cysteine. Moreover, plots of both biogenic synthesized SeNPs show same Z potential distributions.
Considering Z potential plots, a common behavior of biogenic and chemically synthesized SeNPs with ascorbic acid has been notice. Their Z potential distributions are not so clear as the other 2 classes, with presence of important background signals, probably because of big steric groups surrounding the nanoparticles.
It’s also important to notice the presence of a little peak at +90 mV in all samples, except in SeNPs made with ascorbic acid.
In order to compare different biogenic SeNPs, analysis of Z potential measurement of SeNPs produced by different strains have been made. In so doing, *Stenotrophomonas maltophila* SelTE02[38] (Zonaro et al. 2015) and *P. aeruginosa* JS-11[35] (Dwivedi et al. 2013) biogenic SeNPs Z potential values have been evaluated and analyzed.
Comparison between Z potential distributions of SeNPs produced by *Stenotrophomonas maltophila* SelTE02 and *Bacillus mycoides* SelTE01 permits to observe the presence of a strong negative principal peak with similar Z potential values: -75,9 mV for SeNPs made with *Stenotrophomonas maltophila* SelTe02 and -74,2 mV for SeNPs made using *Bacillus mycoides* SelTE01. At the same time, both distributions

show presence of background signals, probably caused by bacterial macromolecules surrounding SeNPs.

Furthermore, Z potential distribution of biogenic SeNPs made using *Stenotrophomonas maltophila* SeITE02 is similar to one of chemical SeNPs made with ascorbic acid, suggesting possible similarities of NPs envelops.

SeNPs produced by *P. aeruginosa* JC-11 show an high Z potential negative value of -42,1 mV, allowing to affirm that they're stable in solution. However, Z potential value of these SeNPs is less negative than one of SeNPs produced by *Bacillus mycoides* SelTE01. This difference can be explained considering that probably these two classes of SeNPs are surrounded by different kind of macromolecules, that can give diverse contribute stability of NPs in solution and, in so doing, different Z potential values.

Although SeNPs previously analyzed showed similar Z potential values, there are also some of them with completely different behavior, such as biogenic SeNPs produced by *Bacillus licheniformis* JS2.[41] This strain is able to synthetize SeNPs under exposure for 24 h of Na_2SeO_3.[41] In 2014 Sonkusre et al. studied this class of biogenic SeNPs, highlighting Z potential value of 0 mV, probably due to different nature of cap surrounding SeNPs.

Comparing Z potential values of biogenic SeNPs produced by different strains, it's possible to suppose that generally biogenic SeNPs have strong negative Z potential values, meaning that they're stable in solution. However, in some cases Z potential values of biogenic SeNPs could be completely different, ranging from positive to neutral charge and changing SeNPs stability.

SEM analysis

SEM is one of the most widely used techniques in characterization of nanomaterials, thanks by its resolution of few nanometers and the possibility to use magnifications from 10 to over 300,000. [42]

In a typical SEM, a source of electrons is focused into a beam, with a very fine spot size of *5* nm and an energy ranging from a few hundred eV to 50KeV that is allocated over the surface of the specimen by deflection coils. When electrons strike and penetrate the surface, a number of interactions occurs and result in the emission of electrons and photons from the sample. SEM images are produced by collecting the emitted electrons on a cathode ray tube (CRT). [42] Combining different kind of images, SEM provides information about morphology, microstructures, chemical composition and distribution of bulk and nanomaterials. [42]

In order to characterize SeNPs principally in size, shape and distribution, both chemically and biogenically synthesized SeNPs were analyzed through SEM. In particular, focus of SEM analysis were chemical SeNPs made with L-cysteine and biogenic SeNPs made with *Bacillus mycoides* SelTE01 after 6 h of exposure of Na_2SeO_3.

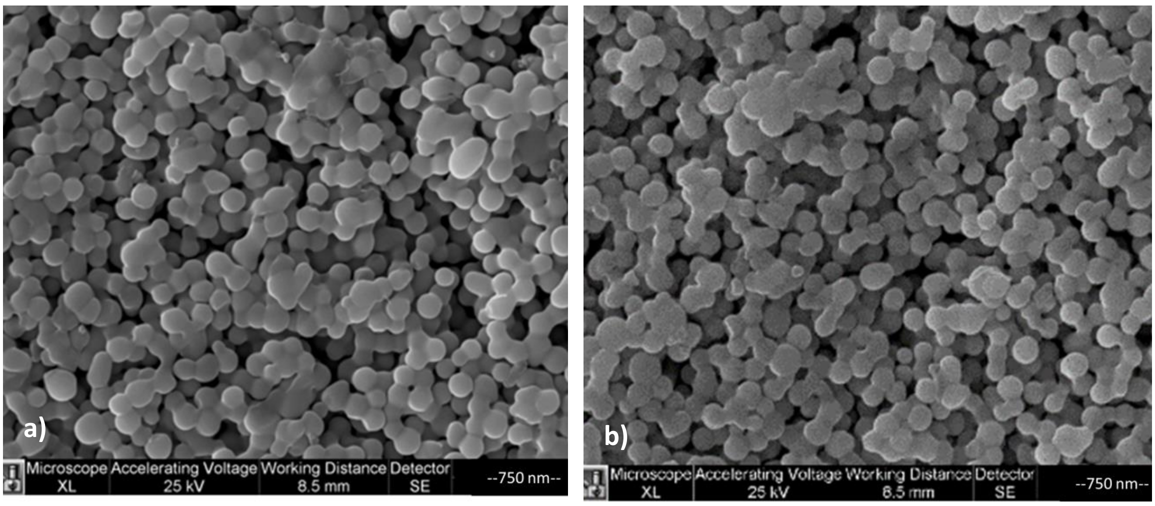

Figure 17: SEM analysis of **a)** biogenic SeNPs made with *Bacillus mycoides* SelTE01 6 h of exposure of Na_2SeO_3 and **b)** chemical SeNPs made with L-cysteine

As shown in Figure 17, physical characteristics of both chemical and biogenic SeNPs are similar: SeNPs seem almost all regularly sferic and monodispersed, with presence of few and isolated aggregates. At the same time, these two classes of SeNPs show also same size (size range value is the same in both images). In so doing, it's possible to determine that they've both same size and morphology.

In order to make a comparison between different biogenic SeNPs, it's useful to analyze SEM images of SeNPs produced by different strains, such as *Stenotrophomonas maltophila* SelTE02[38] and Shewanella sp. HN-41 [43]. Analyzing SEM images of Zonaro et al. work (2015) about Stenotrophomonas maltophila SelTE02 ability to produce SeNPs, it's possible to determine presence of both differences and similarities between these SeNPs and those produced by *Bacillus mycoides* SelTe01. Firstly, SeNPs made with *Stenotrophomonas maltophila* SelTE02 show no regular shape: it's easy to observe presence of many aggregates of different shape, even if there are also many monodispersed SeNPs. At the same time, there's difference also in size of these two classes of biogenic SeNPs: *Stenotrophomonas maltophila* SeITE02 SeNPs seem to be bigger than those synthetized using *Bacillus mycoides* SeITE01, probably because the latter don't produce so much aggregates.

Another comparison between biogenic SeNPs produced by *Bacillus mycoides* SelTE01 is possible considering SeNPs produced by *Shewanella* sp. HN-41.[43] This strain is able to anaerobically produce SeNPs from aqueous selenite solutions on cellular membranes.[43] Tam et al. work of 2010 shows SEM analysis of SeNPs produced by *Shewanella* HN-41 in presence of sodium lactate as electron donor after 24 h of incubation. Analyzing these biogenic SeNPs permits to affirm that they're different both in size and shape rather than other discussed classes. Effectively, SEM image shows bigger SeNPs rather than those produced by *Bacillus mycoides* SelTE01 and *Stenotrophomonas malophila* SelTE02.

It's also possible to observe non homogeneous shape in SeNPs produced by *Shewanella* HN-41: most of them are spherical, even if relatively high number of SeNPs seems to have non regular shape.

EDS analysis

EDS is an analytic technique that allows to identify composition of samples and elements relative proportions. EDS is useful to identify different elements based on particular property for which every element has a unique atomic structure, that is recognizable analyzing its X-ray emission spectrum.[44]

Practically, an incident charged particles beam is focused into the sample. This incident beam is able to excite an inner electron in ground state of sample, ejecting it from its shell and creating an electron hole.[42] Firstly, an electron from an outer shell with higher energy can fill the hole and difference in energy between two shells is released in form of X-ray. Then, number and energy of emitted X-rays can be collected and measured, determining elemental composition of a sample.[42]

In order to determine both biogenic and chemical SeNPs elemental composition using EDS, two different samples have been analyzed: first one made of biogenic SeNPs produced by *Bacillus mycoides* SelTE01 after 6 h of exposure to Na_2SeO_3, and second one made of chemical SeNPs synthetized with L-cysteine.

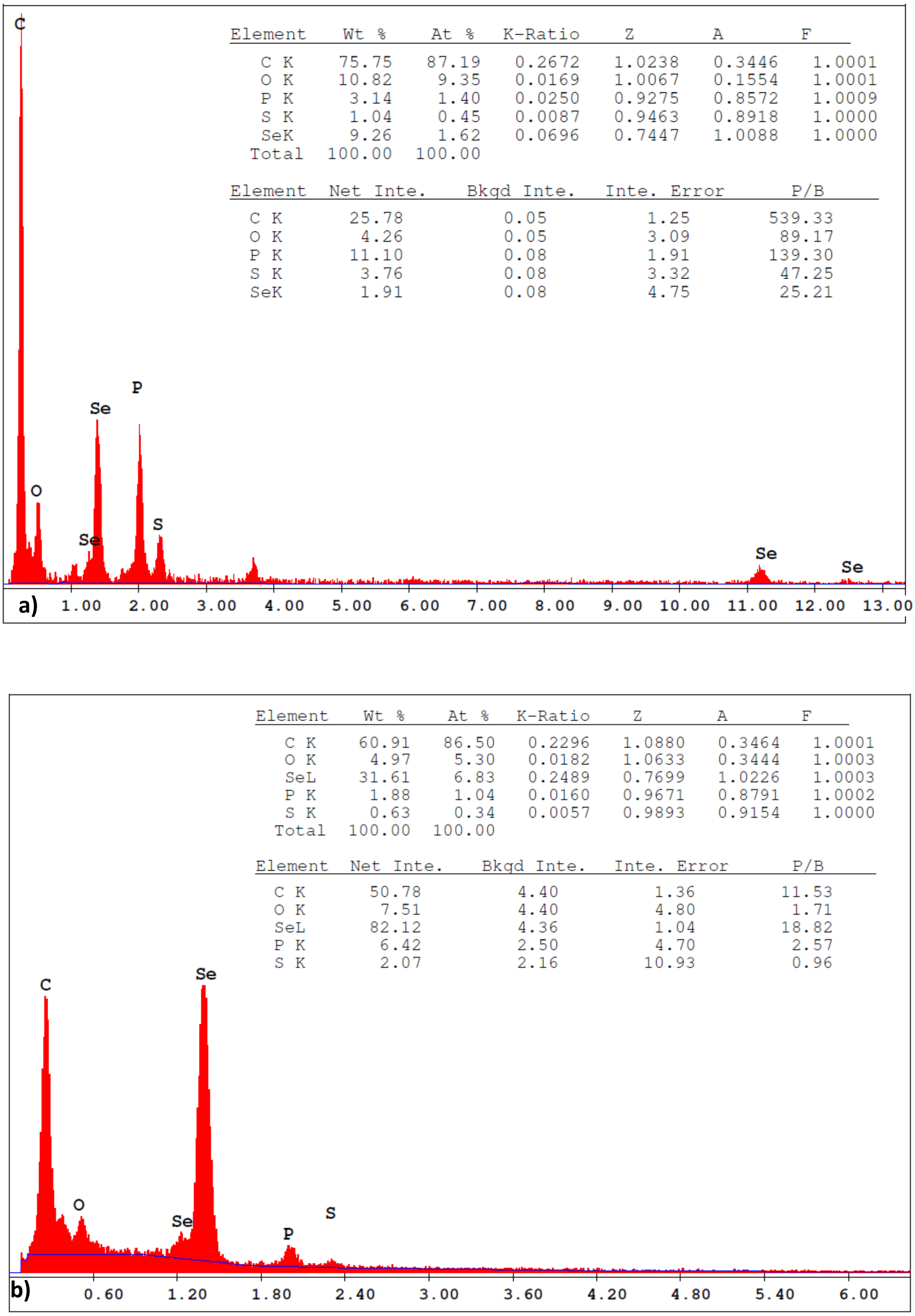

Figure 18: EDS analysis of **a)** Biogenic SeNPs produced by *Bacillus mycoides* SelTE01 after 6 h of Na_2SeO_3 exposure **b)** chemical SeNPs synthetized with L-cysteine

As shown by EDS spectra and quantification data, both samples present typical Se peaks, even if in different percentage and forms. Biogenic SeNPs have 9,26% in weight of Selenium present with 3 different peaks, due to different electronic conformation of Selenium atoms inside NPs. L-cysteine SeNPs show 31,61% in weight of Selenium in 2 different electronic conformations, arising in two different Selenium peaks.

Furthermore, analysis of other elements present in SeNPs is also important: biogenic SeNPs are made of Carbon (75, 75& in weight), Oxygen (10, 82% in weight), Phosphorous (3,14% in weight) and a little amount of Sulfur (1,04% in weight). This particular composition suggests presence of biological macromolecules surrounding biogenic SeNPs, because all these elements are typical of biological compounds. Based on presence of Carbon and Oxygen, it's possible to suppose that biogenic SeNPs cap include proteins or enzymes, also considering little Sulfur amount typical of Cysteine, some cellular residues and phospholipids of cellular membrane, evaluating presence of Phosphorous peak.

In L-cysteine SeNPs there are same elements of biogenic SeNPs, but in different percentage: 60,91% in weight of Carbon, 4,97% in weight of Oxygen, 1,88% in weight of Phosphorous and 0,63% in weight of Sulfur. This particular composition suggests presence of some organic groups all around chemical SeNPs, but not as biomolecules. Even if there's an high percentage of Carbon, Oxygen amount is not enough to suppose presence of biological cap surrounding SeNPs. Probably, in this envelop there are cysteine residues due to synthesis process (made of Carbon, Oxygen and Sulfur) and some phospholipids (low amount of Phosphorous, Carbon and Oxygen).

In order to understand biogenic SeNPs nature, it's useful to compare other classes of SeNPs produced by different bacteria strains, such as S*tenotrophomonas maltophila* SelTE02[38] and Bacillus licheniformis JS2[41].

Considering Zonaro et al. (2015)[38] EDS analysis, it's noticeable that Selenium is present in two different electronic configurations, arising in two different peaks with different intensity. Even if Selenium peaks position is the same as L-cysteine SeNPs one, amount of Selenium present in the sample is more similar to biogenic SeNPs produced by *Bacillus mycoides* SeITE01: 12,57% in weight for SeNPs made by *Stenotrophomonas maltophila* SeITE02 and 9,26% in weight for those made with *Bacillus mycoides* SelTE01.

As in the other two samples, both EDS spectrum and quantification data show presence of other elements in SeNPs: 76,21% in weight of Carbon, 9,23% in weight of Oxygen, 1,54% in weight of Phosphorous and 0,45% in weight of Sulfur. Making a comparison between two biogenic SeNPs classes, it's possible to notice that compositions are almost the same, supporting hypothesis of presence of biomolecular cap all around biogenic SeNPs.

Furthermore, in 2014 Sonkusre et al. have done EDS analysis of SeNPs produced by *Bacillus licheniformis* JS2. [41] EDS spectrum of this biogenic SeNPs is similar to those already analyzed. Selenium is present in two different electronic configurations, such as in SeNPs produced by *Stenotrophomonas maltophila* SelTE02 and Selenium amount is similar to both of other biogenic SeNPs.

Even if there's presence of other elements, percentage and composition of this SeNPs class is different than others. Carbon and Oxygen are present in the sample, but with lower percentage rather than Selenium. Moreover, it's possible to notice peaks indicating presence of Nitrogen and Chlorine. Normally, presence of Nitrogen and Chlorine in this kind of analysis is due to X-ray source and they are not considered as part of the sample.

However, Carbon and Oxygen amount in the sample suggest presence of a biomolecular cap surrounding biogenic SeNPs, but maybe with different composition than the one present around SeNPs produced by *Bacillus mycoides* SelTE01.

SeNPs antimicrobial properties

MBEC assay

MBEC assay is a microbiological tool that permits multiple growth and screening of a large amount of pathogenic biofilms, thanks to the use of CBDs.[22]

Considering CBD as incubator plate, it's possible to growth together different biofilm strains and to evaluate their differences and similarities in growth rate using same or different media.[22]

Normally, MBEC test is used to monitor biofilm growth or death and to test antimicrobial ability of several substances against pathogenic biofilms.[23]

CBD pegs can be also coated with different polymers and substances, in order to evaluate biofilms ability to growth in different environment.

To evaluate antimicrobial properties of all 5 classes of different produced SeNPs, MBEC assay analysis on hydroxyapatite coated CBDs has been made.

Firstly, in order to investigate and to establish possible different growth rate between different CBDs, biofilm growth ability both on normal and hydroxyapatite coated CBDs has been tested. In so doing, *P. aeruginosa* NCTC 12934 biofilm was grown on both different plates for 24 h. Consequently, CFU/mL counting colonies number have been evaluated on Nutrient Agar plates.

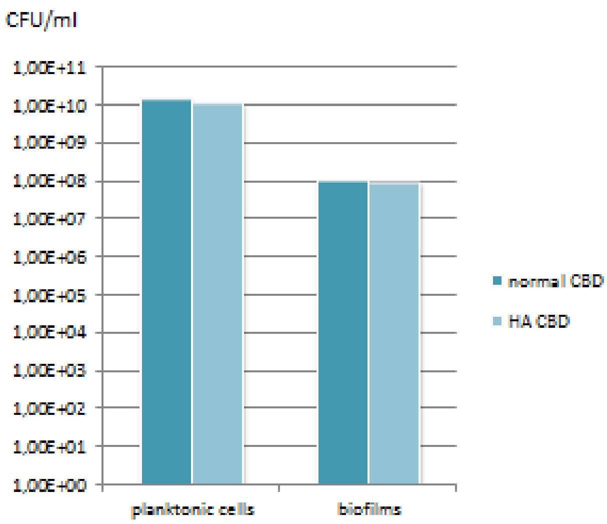

Figure 19: evaluation of *P. aeruginosa* NCTC 12934 biofilm and planktonic cells growth on normal and HA coated CBDs

As shown in figure 19, CFU/mL of both normal and HA coated CBDs are almost the same, meaning that number of bacteria colonies able to growth on different CBDs is the same. Considering this results, probably the most important difference between two diverse CBDs is not the ability of biofilm to growth, rather than different distribution of cells onto pegs. However, growth profile permits to suppose that number of *P. aeruginosa* NCTC 12934 colonies present on both CBDs is the same.

Using these results it's possible to make a comparison between MBEC results of biofilms and planktonic cells of same strain grown in 2 different CBDs, because rate of growth is the same.

MBEC curves give a plot of CFU/mL in function of solutions with different concentration of antimicrobial agents, including a negative control.

Using MBEC curves, it's possible to figure out the Minimal Inhibitory Concentration (MIC) for tested antimicrobial agents. MIC is defined as lowest concentration of an antimicrobial agent that inhibits growth of the bacterium being investigated, theoretically giving cells death.[46] MIC values are normally used to determine susceptibilities of bacteria to drugs and also to evaluate the activity of antimicrobial agents.[46]

In order to verify SeNPs ability to inhibit and to stop biofilm growth, MBEC assay has been done onto 3 different pathogens able to grow as biofilm:

- *E. coli* NCTC 12241
- *P. aeruginosa* NCTC 12934
- *S. aureus* ATCC 25923

These biofilms were grown in presence of the five different classes of SeNPs for 24 h, in order to establish their ability to inhibit biofilm formation. Furthermore, SeNPs ability to stop biofilm growth and eradication using SeNPs against 24 h pre-formed biofilms has been evaluated. Finally, SeNPs action against planktonic cells of these 3 pathogens grown together with NPs has been also tested.

MBEC assay against pathogenic biofilm exposed to SeNPs

Figure 20 shows MBEC curves for action of biogenic SeNPs produced by *Bacillus mycoides* SelTE01 after 6 h of Na_2SeO_3 exposure against 3 pathogens.

In this case, 3 pathogens were grown using hydroxyapatite coated CBDs together with different concentrations of SeNPs for 24 h.

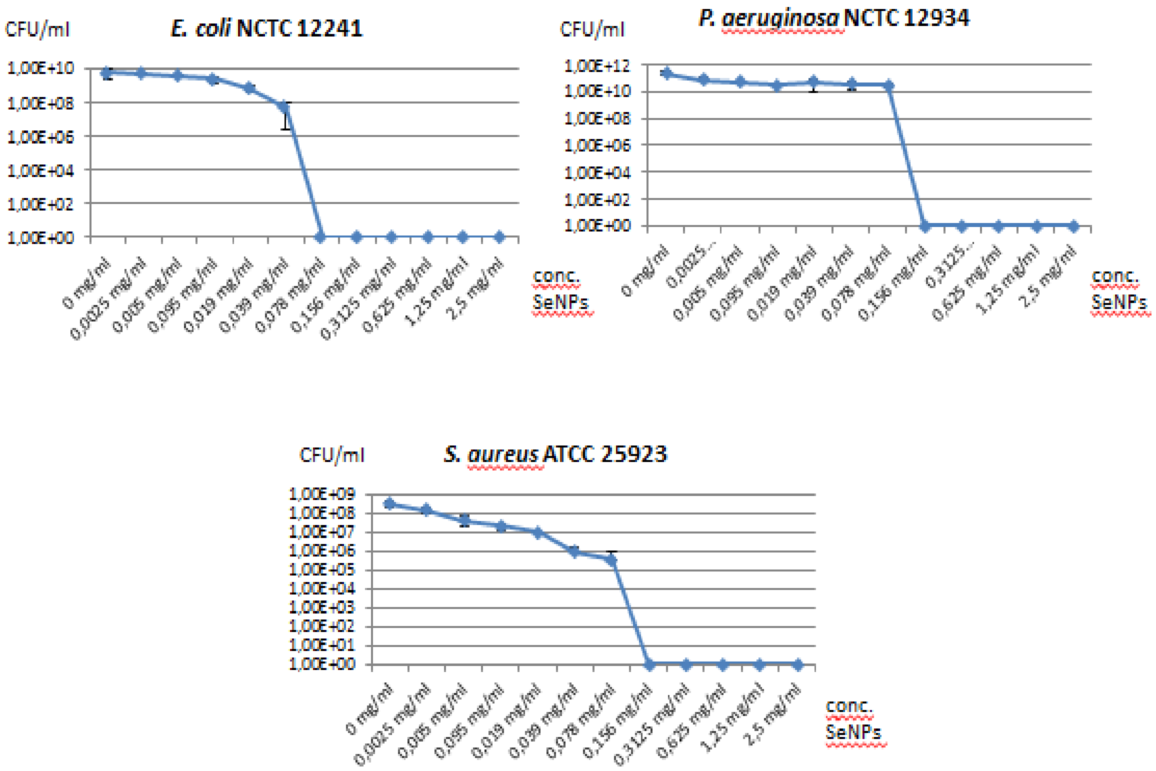

Figure 20: MBEC curves of biogenic SeNPs produced by *Bacillus mycoides* SelTE01 after 6 h of Na_2SeO_3 exposure against 3 pathogenic biofilms

As shown, in all of 3 MBEC curves is possible to clearly determine MIC value of biogenic SeNPs:

- MIC for *E. coli* NCTC 12241 = 0,039 mg/mL – 0,078 mg/mL
- MIC for *P. aeruginosa* NCTC 12394 = 0,078 mg/mL
- MIC for *S. aureus* ATCC 25923 = 0,078 mg/mL

All curves go to 0 values after MIC, indicating strong biogenic SeNPs ability to inhibit biofilm formation killing all bacteria cells with relatively low concentrations.

It's also important to notice that MIC values of this class of biogenic SeNPs are similar for all 3 pathogens. In particular, MICs are the same for *P. aeruginosa* NCTC 12394 and for *S. aureus* ATCC 23923, while *E. coli* NCTC 12241 MIC is lower, probably because this biofilm is not as strong as other two analyzed, so it's easier to kill.

Similar result is obtained testing biogenic SeNPs action produced by *Bacillus mycoides* SelTE01 after 24 h of exposure to Na_2SeO_3.

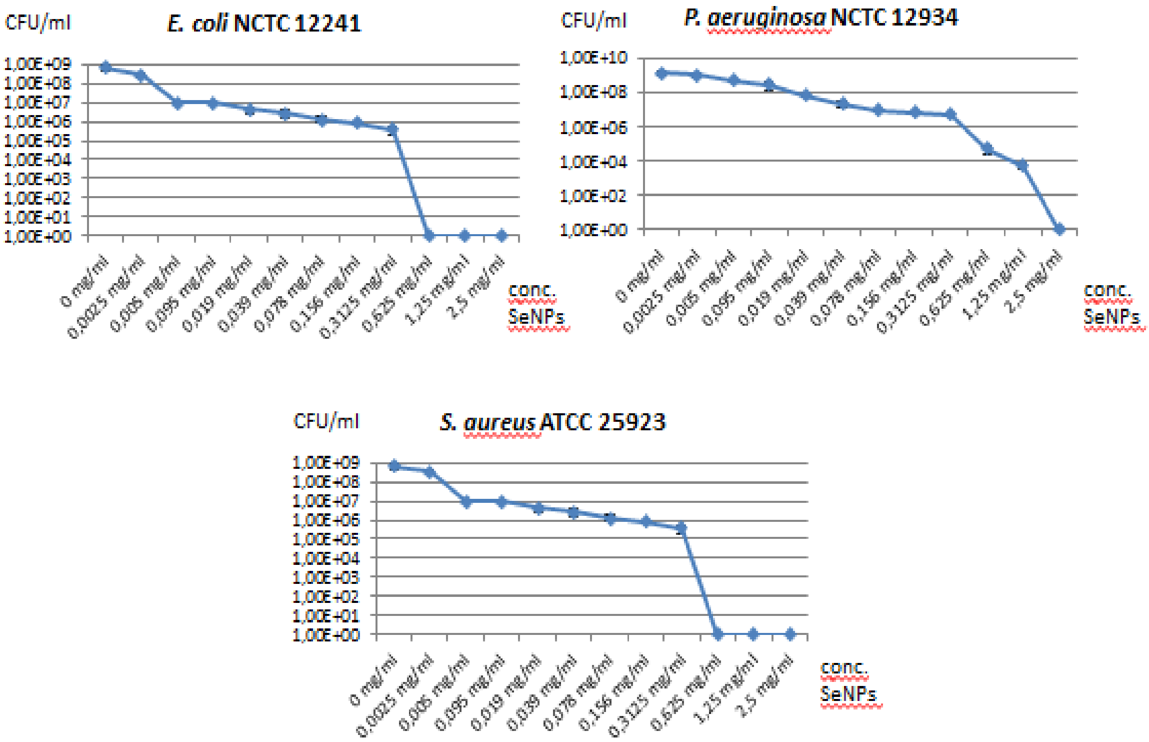

Figure 21: MBEC curves of biogenic SeNPs produced by *Bacillus mycoides* SelTE01 after 24 h of Na_2SeO_3 exposure against 3 pathogenic biofilms

In this case, MIC results are different than first one analyzed:

- MIC for *E. coli* NCTC 12241 = 0,3125 mg/mL
- MIC for *P. aeruginosa* NCTC 12394 = 1,25 mg/mL
- MIC for *S. aureus* ATCC 25923 = 0,3125 mg/mL

Probably, strong difference between MIC values of 2 classes of biogenic SeNPs is due to their different characteristics, such as size and presence of some aggregates in those synthesized after 24 h of exposure to Na_2SeO_3. Considering these MIC values, it's possible to hypothesize that biogenic SeNPs may not have bacteria-specificity and they're able to act against all these 3 tested pathogens. Effectively, both *E. coli* NCTC 12242 and *P. aeruginosa* NCTC 12394 are Gram-negative, aerobic rods belonging to

Gamma Proteobacteria, while *S. aureus* ATCC 25923 is a Gram-positive, spherical bacteria that occur in microscopic clusters resembling grapes belonging to Bacilli class. [47]

Inhibition of biofilm growth using biogenic SeNPs it's particularly interesting considering both *P. aeruginosa* NCTC 12934 and *S. aureus* ATCC 25923.

Pseudomonas aeruginosa has become increasingly recognized as an emerging opportunistic pathogen of clinical relevance.[47] It's an opportunistic pathogen of humans, because it exploits some break in the host defenses to initiate an infection.[47] The bacterium almost never infects uncompromised tissues, yet there is hardly any tissue that it cannot infect if the tissue defenses are compromised in some manner.[47] *Pseudomonas aeruginosa* is recognized as one of the most important nosocomial antibiotics resistant opportunistic pathogens, meaning that its infections principally occur in the hospital.[47] It causes a variety of systemic infections (urinary tract, respiratory system, soft tissue, bone and joint infections) particularly in patients with severe burns, cancer, cystic fibrosis and AIDS patients who are immunosuppressed.[47]

S. aureus is a key bacterium for many human infections, that can be serious when they occur on surgical wounds, bloodstream or in the lungs.[45] Because of its ability to growth as strong biofilm, it's very difficult to treat *S. aureus* infections and, at the same time, it becomes increasingly resistant to many common antibiotics.[45] In this sense, biogenic SeNPs ability to inhibit *P. aeruginosa* and *S. aureus* biofilms formation becomes important in order to prevent development of several human infections.

Evaluating MBEC curves of chemical SeNPs carried out at the same experimental conditions, results are completely different from what we obtained from biogenic SeNPs.

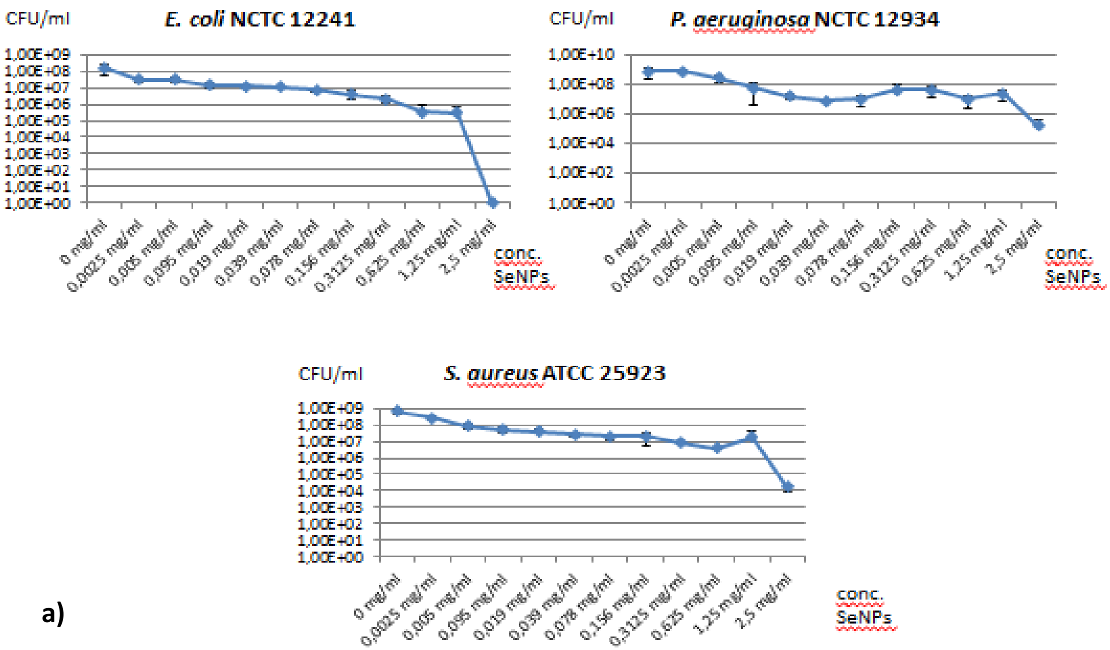

a)

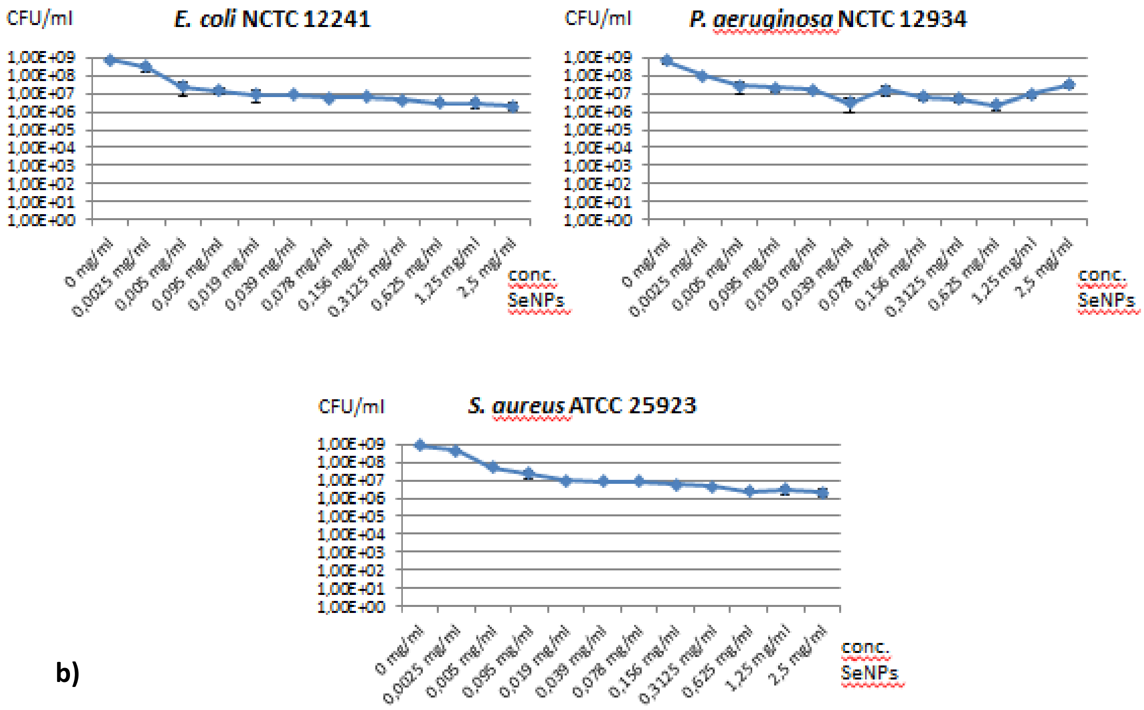

b)

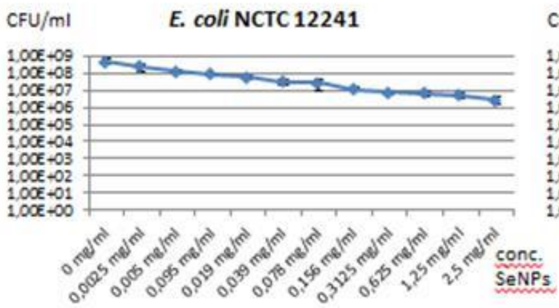

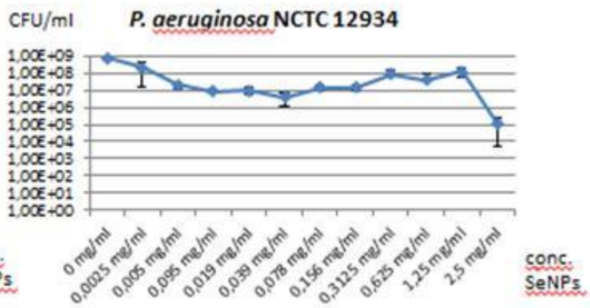

c)

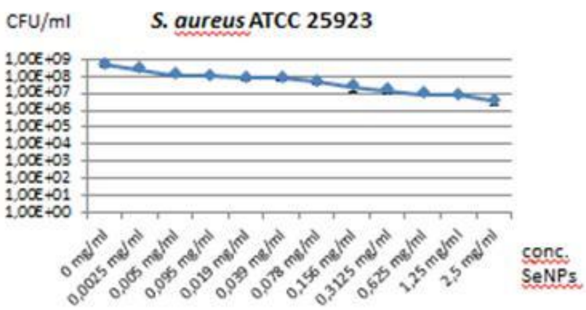

Figure 22: MBEC curves against 3 pathogenic biofilms of chemical SeNPs produced with **a)** L-cysteine **b)** Ascorbic Acid and **c)** Lin&Wang protocol

As shown in MBEC curves, chemical SeNPs are not able to strongly inhibit formation of pathogenic biofilms and, as result, it's not possible to determine a real MIC for action of all 3 SeNPs classes.

However, analyzing MBEC results of action of SeNPs made with L-cysteine, it's noticeable that this class of SeNPs is able to inhibit growth of *E.coli* NCTC 12241 with a MIC value of 1,25 mg/mL of SeNPs concentration.

L-cysteine SeNPs antimicrobial activity is stronger for *P. aeruginosa* NCTC 12394 and *S. aureus* ATCC 25923 than the other chemical SeNPs, showing similar curve trend of a typical kill-curve.

Other two classes of chemical SeNPs are never able to partially kill bacteria cells and to inhibit biofilm formation.

Considering SeNPs nature, different antimicrobial ability of biogenic and chemical SeNPs is probably due to different cap surrounding NPs. Both chemical and biogenic SeNPs are formed of Selenium, that it's known as good antimicrobial element: the only difference between biogenic SeNPs and those chemically synthetized is due to the presence of different elements and in different amount all around NPs. Probably biogenic SeNPs have a biomolecular cap, as also suggested from EDS analysis, that can have double functions of stabilizing SeNPs, avoid formation of aggregates and preventing bacteria cells adhesion during biofilm formation.

Considering together EDS and MBEC results, it's possible to suppose that biogenic SeNPs are surrounded of proteins and phospholipids, that can be able to interact with biofilm in formation. Proteins of biogenic SeNPs cap may be particular enzymes able to inhibit adhesion of bacteria cells together, stopping formation of biofilm. At the same time, presence of phospholipids in SeNPs may be important in order to stabilize these nanomaterials, to improve their availability and their rate of penetration in biofilm during formation process.

Obtained results permit to hypothesize that biogenic SeNPs are able to inhibit biofilm formation because they're able, both using Selenium antimicrobial ability and cap characteristics, to interact with bacteria cells and to inhibit matrix development.

MBEC assay against 24 h pre-grown pathogenic biofilms exposed to SeNPs

In order to verify possible SeNPs ability to inhibit biofilm eradication and growth and to kill living biofilms, SeNPs action against 24 h pre-grown pathogenic biofilms has been also evaluated.

In this case, MBEC assay has been done exposing 3 pre-grown pathogenic biofilms previously mentioned to both biogenic and chemical SeNPs.

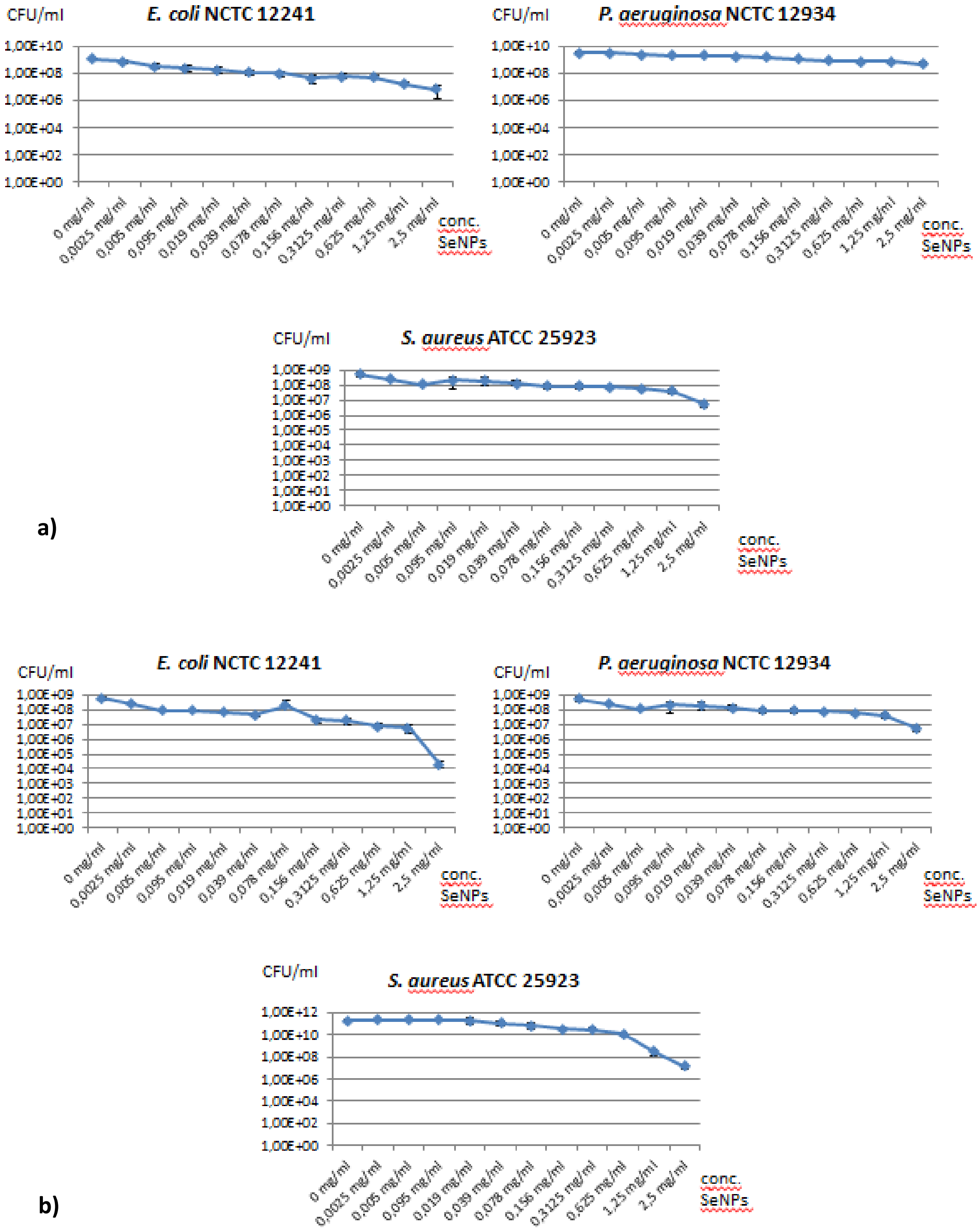

Figure 23: MBEC curves against 3 pathogenic pre-grown biofilms of **a)** biogenic SeNPs produced by *Bacillus mycoides* SelTE01 after 6 h of Na_2SeO_3 exposure and **b)** biogenic SeNPs produced by *Bacillus mycoides* SelTE01 after 24 h of Na_2SeO_3 exposure

As shown in MBEC curves for both biogenic SeNPs, there's no evidence of strong antimicrobial activity able to kill pre-grown pathogenic biofilms.

Analyzing these results it's not possible to establish a real MIC. As previously described, biogenic SeNPs seem to have more activity on *E. coli* NCTC 12241 because this particular biofilm is not so stable and strong as those of other two pathogens. However, both biogenic SeNPs classes don't show ability to stop the growth of living biofilm.

The same kind of results are obtained analyzed action of all 3 chemical SeNPs against pre-grown pathogenic biofilms.

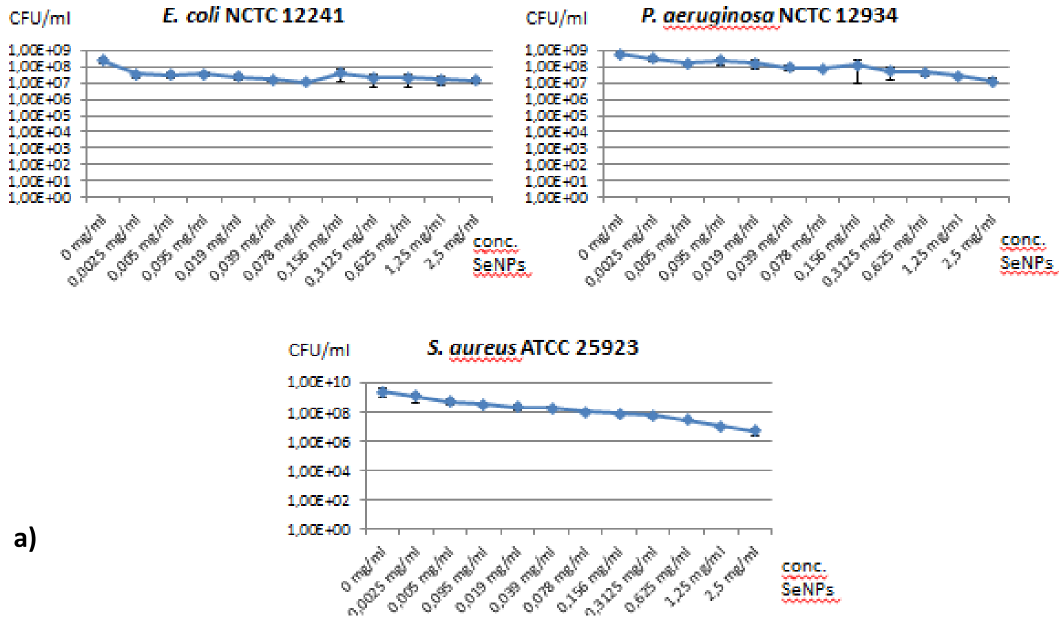

a)

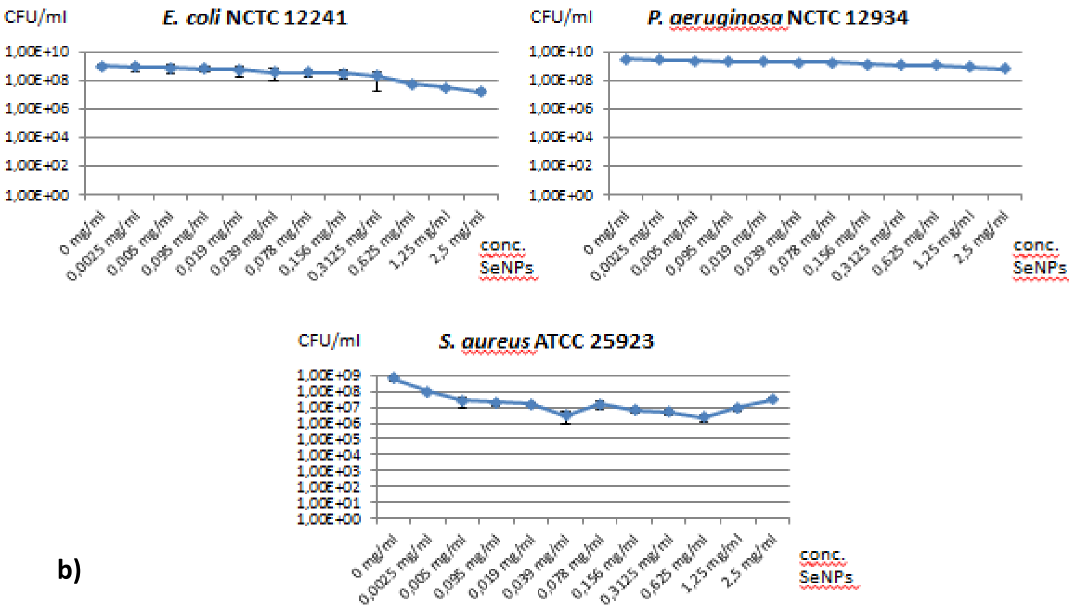

b)

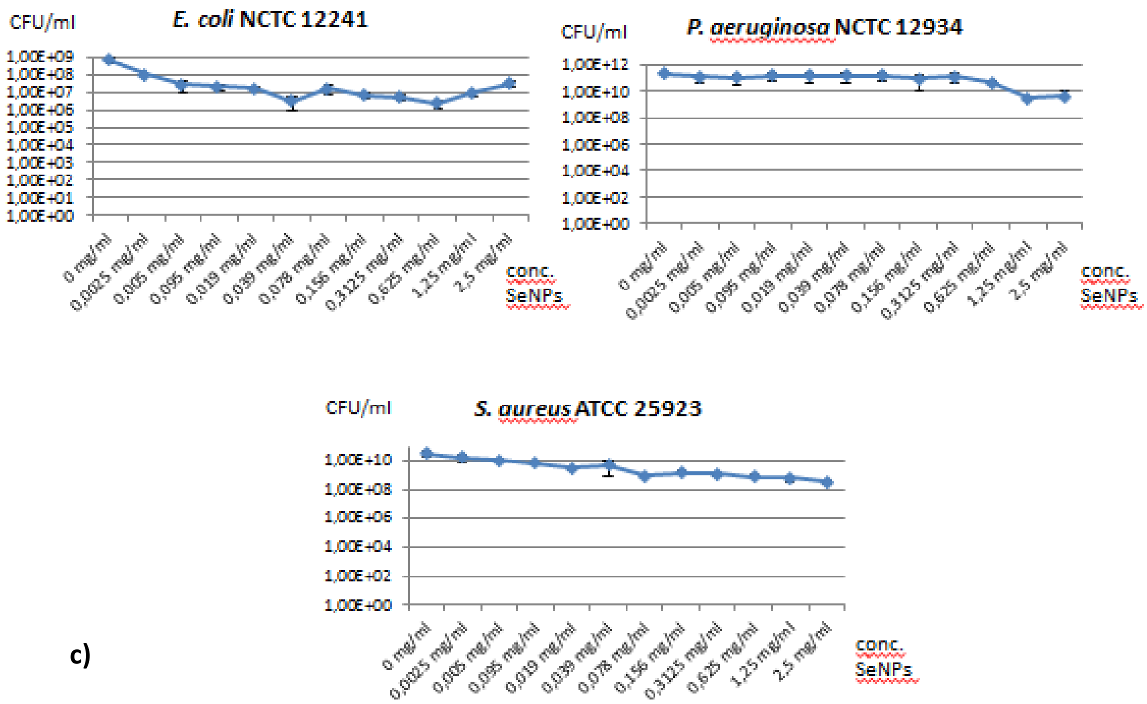

Figure 24: MBEC curves against 3 pathogenic pre-grown biofilms of chemical SeNPs produced with **a)** L-cysteine **b)** Ascorbic Acid and **c)** Lin&Wang protocol

Also in these 3 situations, it's not possible to determine a real MIC and they have similar MBEC curves of chemical SeNPs tested against biofilm in formation.

This time, all 5 classes of SeNPs have similar MBEC results, giving the hypothesis that they're not strong enough to kill living biofilms. A mature biofilm is similar to an absorptive sponge, that is able of capturing chemical and biological components in its vicinity.[48] Probably this is due to structure of biofilms: they're made of a strong matrix, that protects bacteria cells living inside, leaving few ways to SeNPs to penetrate. Biofilm matrix is made of extracellular polymeric substances (EPS), that include wide variety of proteins, glycoproteins, glycolipids, polysaccharides and, in some cases, extracellular DNA. [49] Thanks to its composition, EPS matrix is an efficient binding matrix for different substances: it has the potential to bind ions, charged molecules or NPs.[48] Considering these binding properties, it's possible to suppose that biofilms are efficient chelators for physical-trapping and binding of colloidal forms of metals and organic matter.[48]

Normally, both biogenic and chemical NPs are not made of one element, but they are surrounded of different chemical groups or molecules, forming a cap all around NPs. This cap normally include chemical residues due to synthesis process of NPs, that are able to interact with EPS matrix.

As previously described with EDS results, both biogenic and chemical SeNPs have a complex chemical structure, in which real SeNPs is surrounded of different chemical residues or biomolecules. Analyzing nature of SeNPs cap, it's possible to suppose that SeNPs cap is able to chemically interact with EPS matrix, changing its conformation and becoming trapped in matrix itself.

Both biogenic classes of SeNPs have a similar cap, probably made of proteins and phospholipids. These compounds easily interact chemically with EPS matrix, using protein-protein interaction or organic groups of phospholipids. At the same time, all 3 chemical SeNPs can easily bind EPS matrix compunds, thanks to their cap composition:

- L-cysteine SeNPs can interact with EPS proteins using Cysteine residues and –SH groups all around NPs
- SeNPs made with ascorbic acid can bind EPS matrix using chemistry reaction of ascorbic acid residues both with proteins and lipids
- SeNPs produced using Lin & Wang may interact with EPS positive charged proteins because of presence of negatively charged SDS residues and $Na_2S_2O_3$ residues

Because of these possible interactions between SeNPs and EPS matrix, it's conceivable that all 5 SeNPs are able to strongly interact with EPS biofilm matrix and to be trapped there, inhibiting their antimicrobial ability to kill bacteria biofilm cells.

Considering large amounts of bacteria strains able to produce SeNPs, it's useful to understand if there are difference and similarities between their antimicrobial mechanisms of action. In so doing, it's possible to compare antimicrobial ability of biogenic SeNPs produced by *Bacillus mycoides* SelTE01 and *Stenotrophomonas maltophila* SelTE02[38].

Zonaro et al in 2015 evaluated antimicrobial action of different concentration of SeNPs produced by *Stenotrophomonas maltophila* SelTE02 after 6 h, 24 h and 48 h of Na_2SeO_3 exposure.[38]

Biogenic SeNPs antimicrobial ability has been tested growing in presence of SeNPs 3 pathogenic biofilms:

- *E. coli* JM109
- *P. aeruginosa* PAO1
- *S. aureus* 25923

Analysis of Zonaro et al. results permits to determine clear MIC values for all 3 experiments. MICs change dramatically considering all 3 biogenic SeNPs classes in a time-dependent way: MIC values of biogenic SeNPs made after 6 h of Na_2SeO_3 exposure are lower rather than MIC values of those produced after 48 h of Selenite precursor inoculation. This time-dependent trend is the same previously discussed for MBEC results of SeNPs made by *Bacillus mycoides* SelTE01.

Comparing antimicrobial ability of SeNPs produced by 2 different strains, it's noticeable how SeNPs action made by *Bacillus mycoides* SelTE01 is higher than those made with *Stenotrophomonas malthopila* SelTE02. Even if kill-curves of latter SeNPs classes are good, MIC values of them are almost double of SeNPs produced by *Bacillus mycoides* SelTE01. This trend is verified both for SeNPs made after 6 h and after 24 h of exposure of Selenite precursor. So high difference in antimicrobial ability of these 2 class of biogenic SeNPs may be due to difference in cap structure of them. Based on previously described SEM characterization data results of these 2 SeNPs, SeNPs produced by *Bacillus mycoides* SelTE01 have higher antimicrobial ability because of their higher regularity in size and shape and their higher monodispersion. At the same time, caps surrounding the two different SeNPs may have different composition: it's possible that percentages of proteins and phospholipids present all around SeNPs are different in those synthetized using *Bacillus mycoides* SelTE01 than *Stenotrophomonas maltophila* SelTE02. Changing caps composition may have strong effect both on antimicrobial ability and stabilization of biogenic SeNPs.

MBEC assay against planktonic pathogenic cells exposed to SeNPs

Once understood SeNPs antimicrobial activity against biofilm, SeNPs ability to kill also planktonic pathogenic cells has been evaluated. Planktonic cells are defined as "free flowing bacteria in suspension" [50] and they practically are free bacterial cells living in different environments.

In order to understand differences in SeNPs action and antimicrobial properties, all 5 SeNPs classes were used against planktonic cultures of:

- *E. coli* NCTC 12241
- *P. aeruginosa* NCTC 12934
- *S. aureus* ATCC 25923

These strains were grown for 24 h in presence of different SeNPs concentrations.

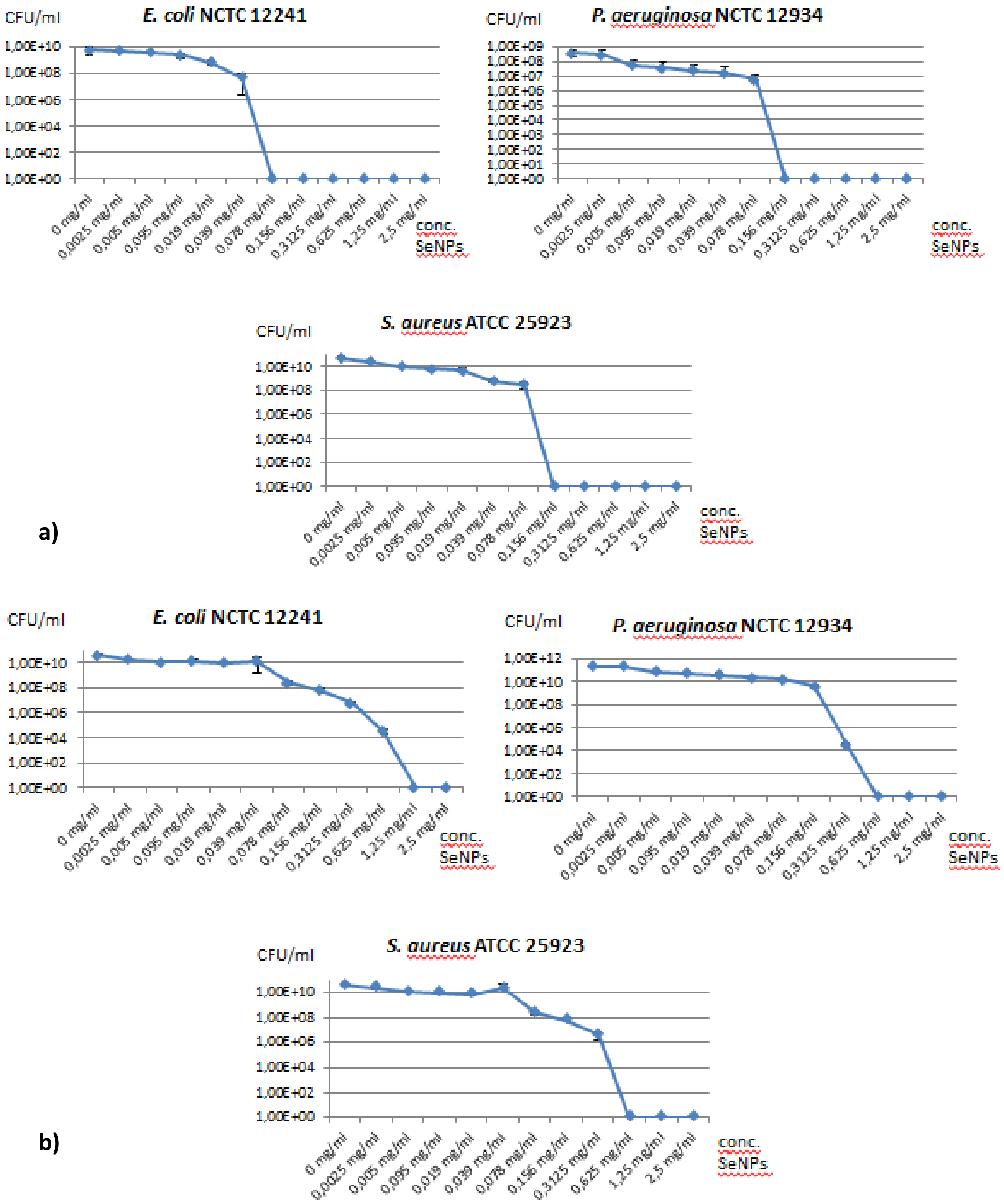

Figure 25: MBEC curves of against planktonic pathogenic biofilms with **a)** biogenic SeNPs produced by *Bacillus mycoides* SelTE01 after 6 h of Na_2SeO_3 exposure **b)**) biogenic SeNPs produced by *Bacillus mycoides* SelTE01 after 24h of Na_2SeO_3 exposure

MBEC results for biogenic SeNPs show a stronger antimicrobial activity also against planktonic cells, with almost same trend of biofilms.

Considering action of SeNPs produced by *Bacillus mycoides* SelTE01 after 6 h of Na_2SeO_3 exposure, MIC values are very similar to those of pathogenic biofilms, showing also same kill-curve trend. However, analysis of MBEC curve of SeNPs made by same strain after 24 h of Na_2SeO_3 exposure is more different than that of pathogenic biofilms. Even if MIC values are almost the same, trend of curve before raising MICs is completely changed, showing both in *E.coli* NCTC 12241 and *S. aureus* ATCC 25923 higher irregularity.

Furthermore, because of planktonic cells structure, theoretically SeNPs could have stronger antimicrobial activity: single cells able to growth in a media as planktonic cells are weaker than biofilms, especially because planktonic cells don't have an EPS matrix as protection.

Anyways, analysis of MBEC curves for biogenic SeNPs doesn't show strong difference in action against planktonic cells rather than biofilms. This particular behavior may be attributable to different numbers of planktonic cells than those of biofilms: probably, at the beginning of MBEC test number of planktonic cells were higher rather than biofilms cells.

Figure 26 shows evaluation of chemical SeNPs antimicrobial activity against planktonic cells.

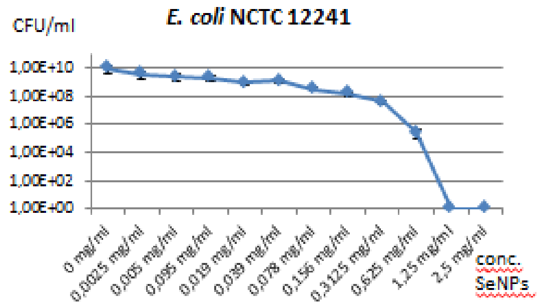

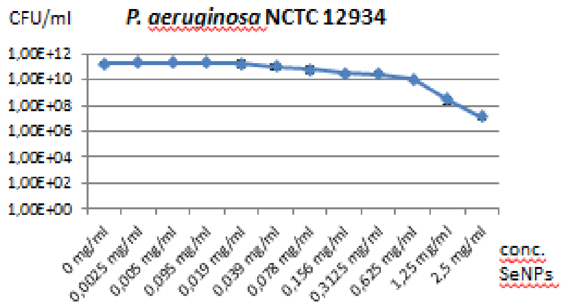

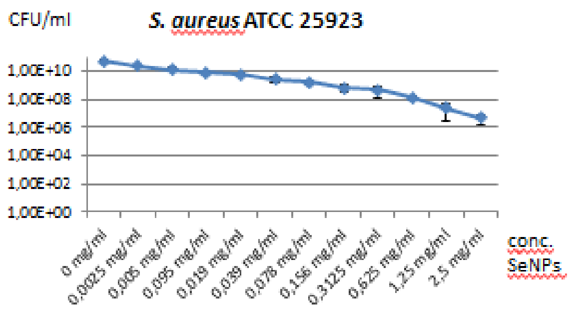

a)

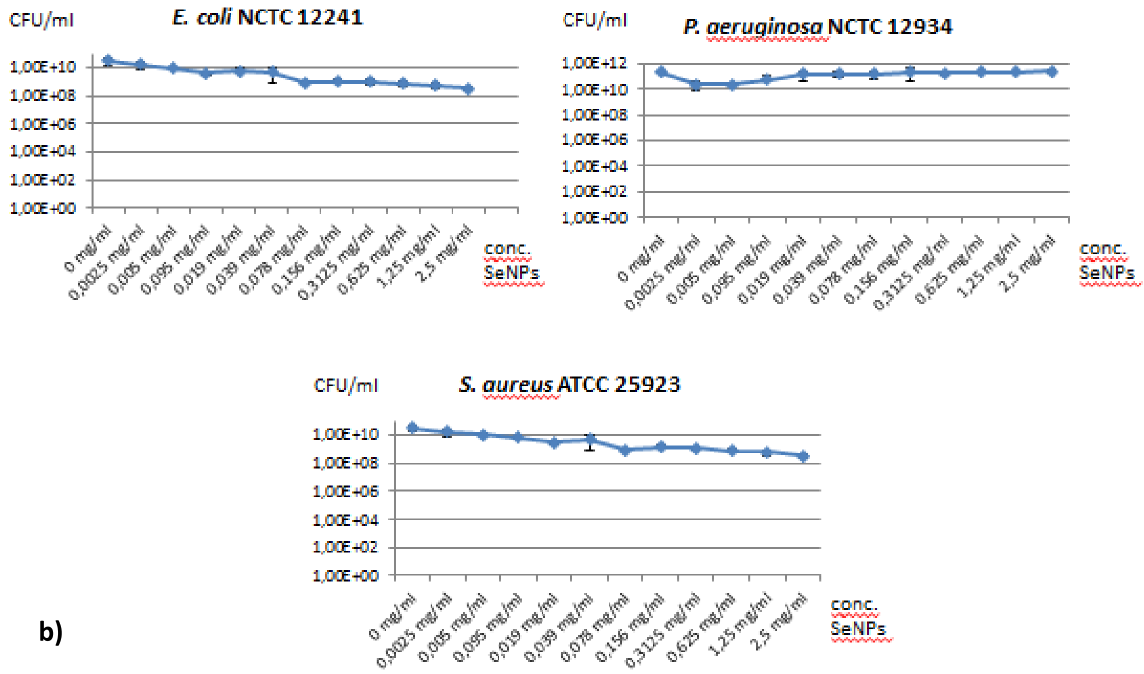

b)

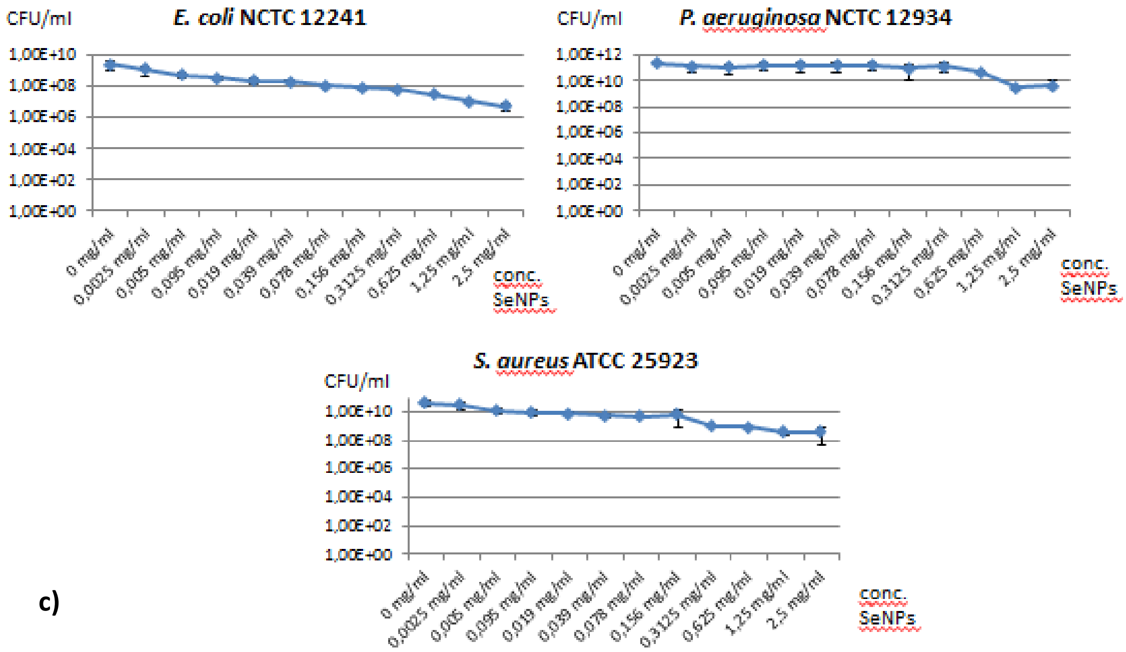

c)

Figure 26: MBEC curves against pathogenic planktonic cells of chemical SeNPs produced with **a)** L-cysteine **b)** Ascorbic Acid and **c)** Lin&Wang protocol

As shown in MBEC curves, chemical SeNPs are not able to kill planktonic cells and, as result, it's not possible to determine a real MIC for action of all 3 SeNPs classes, giving same results of chemical SeNPs against biofilms. However, analysis of MBEC results of action of L-cysteine SeNPs suggests that they've antimicrobial activity against *E.coli* NCTC 12241 plantkonic cells with a MIC value of 0,625 mg/mL. As in evaluation of action against biofilms, the other two classes of chemical SeNPs are not able to kill bacteria cells. There's no such difference in action and antimicrobial ability of all 5 SeNPs against planktonic pathogenic cells rather than pathogenic biofilms.

Furthermore, it's possible to make a comparison of different biogenic SeNPs action against planktonic cells using Zonaro et al (2015)[38] work about SeNPs produced by *Stenotrophomonas maltophila* SelTE02. MBEC results of this class of biogenic SeNPs action against planktonic cells are the same of those obtained against pathogenic biofilms, with no evident differences. Comparison between MBEC curves of SeNPs produced by *Stenotrophomonas maltophila* SelTE02 and those of SeNPs produced by *Bacillus mycoides* SelTE01 have same differences and similarities to MBEC curves for biofilms.

<u>Summary</u>

Thanks to use of MBEC assay, strong antimicrobial activity of biogenic SeNPs has been determined, together with weaker one of those chemically synthetized. Furthermore, also SeNPs antimicrobial properties against pre-grown biofilms has been evaluated, understanding that they're not stronger enough to stop growth and to kill bacteria cells of mature biofilms.

Comparing these results with those obtained using SeNPs made by *Stenotrophomonas maltophila* SelTE02[38], it's possible also to verify how biogenic classes of SeNPs produced by *Bacillus mycoides* SelTE01 were stronger antimicrobial agents rather than those other analyzed.

Finally, comparison between SeNPs action against planktonic cells and biofilms has been made, in order to verify stronger biogenic SeNPs antimicrobial ability against planktonic cells.

CLSM analysis

CLSM analysis permits to obtain high-resolution optical images with depth selectivity.[51] This microscope is able to make an optical sectioning: it acquires point-by-point images from selected depths. Images are then reconstructed with a software, allowing to have 3D images of complex objects. [52]

Using CLSM it's possible to control depth of field, to eliminate background information from focal plane and to collect serial optical sections. It's also useful in order to improve optical resolution both in optical axis and specimen plane, avoiding secondary fluorescence emissions by samples. [52]

CLSM analysis permits also to stain samples using fluorescence ability of dyes and cellular components.

In this study, CLSM analysis have been used in order to investigate both biogenic and chemical SeNPs antimicrobial ability to inhibit formation of *P. aeruginosa* NCTC 12934 biofilms. *P. aeruginosa* strain was chosen because of:

- its production of strong and mature biofilm
- its character as harmful and powerful opportunistic human pathogen
- its normally use as biofilm model

Completely CLSM analysis has been conducted using 2 different classes of SeNPs: those biogenically synthetized NPs using *Bacillus mycoides* SelTE01 after 6 h of exposure of Selenite precursor and those chemically synthetized with L-cysteine.

Evaluation and study of these two classes of SeNPs have been chosen in order to make a comparison between biogenic and chemical SeNPs antimicrobial properties. In so doing, analysis of both biogenic and L-cysteine SeNPs has been selected since they exhibited best MBEC results comparing with other classes.

In order to investigate SeNPs antimicrobial activity, CLSM analysis has been made onto different samples:

- HA coated peg as negative control (without *P. aeruginosa* NCTC 12934 inoculation) to be sure to not have contamination and to understand hydroxyapatite structure on CBD pegs used to growth biofilm
- HA coated peg as positive control inoculated with *P. aeruginosa* NCTC 12934 strain in order to establish biofilm formation and to understand the mature biofilm structure
- 3 samples (before MIC, MIC and after MIC) of HA coated pegs for biogenic SeNPs produced by *Bacillus mycoides* after 6 h of Na_2SeO_3 exposure in order to investigate stress conditions and changing in biofilm structure with varying SeNPs concentration
- 3 samples of HA coated pegs with L-cysteine SeNPs in order to investigate stress conditions and changing in biofilm structure with varying SeNPs concentration

Normally, CLSM images have been taken using 20x objective lens.

In order to analyze biofilm morphology, samples were stained using Live/dead Baclight staining kit. This kit is made of SYTO 9, that is a green-fluorescent nucleic acid stain, and propidium iodide, red-fluorescent one. These stains have different spectral characteristics and they're able to differentially penetrate bacterial cells.[53] SYTO 9 generally labels all bacteria cells in population, while propidium iodide penetrates only

bacteria cells with damaged membranes. In so doing, when they're used together, fluorescence of SYTO 9 is reduced in damage cells.[53] As result, live bacteria with intact cell membranes show green fluorescence, while dead bacteria with damage membranes have red fluorescence.[53]
Use of Live/Dead kit is important in order to investigate biofilm conditions of growth in presence of antimicrobial agents, such as SeNPs. It permits also to establish presence of stress conditions in biofilm and to monitor development of SeNPs action increasing their concentration.

HA coated peg as negative and positive P.aeruginosa NCTC 12934 growth control

Figure 27 shows comparison between negative and positive control of *P. aeruginosa* NCTC 12934 biofilm growth.

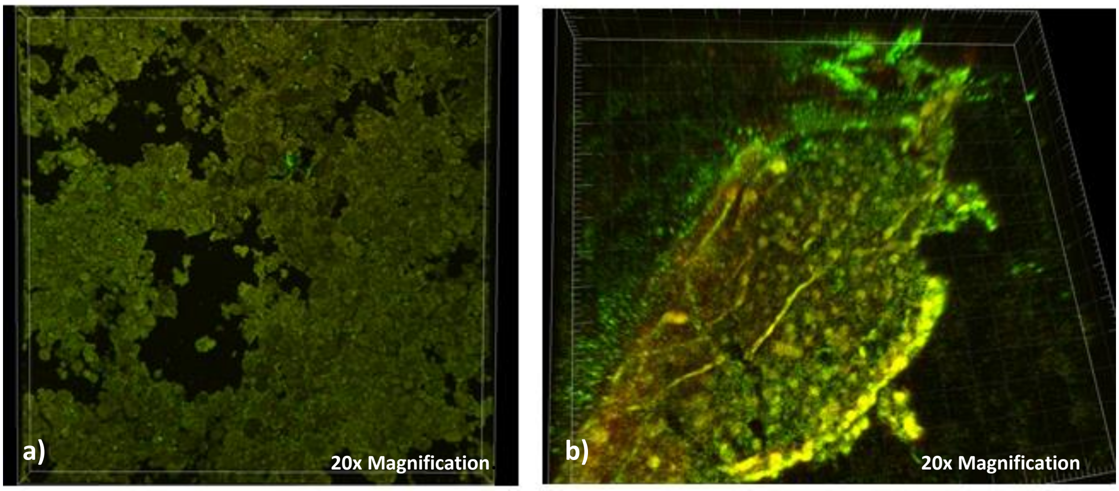

Figure 27: CLSM images of **a)** negative control and **b)** positive control of *P. aeruginosa* NCTC 12934 biofilm presence

As it's easy to observe, there's no presence of contamination in negative control: there's no fluorescence signal due to live (green) or dead (red) cells.

It’s also important to notice presence of some background noise in the negative control (dark green color in peg). Usually, Live/Dead kit doesn’t give background signal and pegs are black with fluorescence due to live or dead cells. However, presence of dark green color may be due to HA coating of CBDs: HA is subject to exchange ions chemistry and it’s able to bind with positive charge ions. In so doing, HA it’s able to partially bind with nucleic acid stain, that are positive charge because they have to detect DNA presence (DNA is negative charge), giving some background fluorescent signal.

HA fluorescence is completely different than bacteria cells: it arises in dark stifled green or red color, while bacteria cells give strong and brilliant green and red fluorescence observable in positive *P. aeruginosa* NCTC 12934 control.

In Fig.27b, it’s easy to recognize presence of strong and live biofilm, thanks to high number of brilliant green stained cells (live cells). There are not so many dead cells (red color), probably because *P. aeruginosa* biofilms are normally strong and able to growth with high number of bacterial cells, forming thick cells layers.

Darker fluorescent signal present especially with red color is due to presence of HA coating on CBD plates.

It’s important to notice also in both negative and positive control that HA coating is not uniformly distributed onto pegs: this is easy to observe for presence of black zones similar to black holes. In these zones there’s no coating of HA onto peg and, as consequence, there’s no fluorescent signal due to cells or to HA presence.

Furthermore, HA seems to coat CBD pegs forming organized structure similar to clusters. This is possible due to HA structure itself: it has crystal organization and probably thanks to this property HA is able to organize crystals together, forming big clusters.

P. aeruginosa NCTC 12934 biofilm positive control shows that living cells are present almost on the edge of different HA clusters, as it's possible to observe by watching the different intensity of fluorescent signals. Probably, HA clusters, thanks to their conformation and volume, act like mechanical obstacle to biofilm cells growth. In so doing, biofilm cells are able to growth better and stronger in pegs areas in which there's no HA coating. It's also possible to notice presence of bacteria cells near and onto HA clusters, but with a lower density.

Biogenic SeNPs action against P.aeruginosa NCTC 12934 biofilm grown onto HA coated peg

In order to investigate SeNPs antimicrobial properties and to understand their action at MIC, 3 samples of biogenic SeNPs produced by Bacillus mycoides SelTE01 after 6 h of Na_2SeO_3 exposure have been analyzed:

- sample exposed to 0,039 mg/mL SeNPs solution (lower than MIC = 0,078 mg/mL)
- sample inoculated with 0,078 mg/mL SeNPs concentration corresponding to MIC value
- sample grown in presence of 1,25 mg/mL SeNPs solution (higher than MIC = 0,078 mg/mL)

These samples have been chosen to investigate 3 different stress situations for bacteria cells and to evaluated biogenic SeNPs efficacy.

As shown in figure 28, completely different biofilm conformation is noticeable using different biogenic SeNPs solutions.

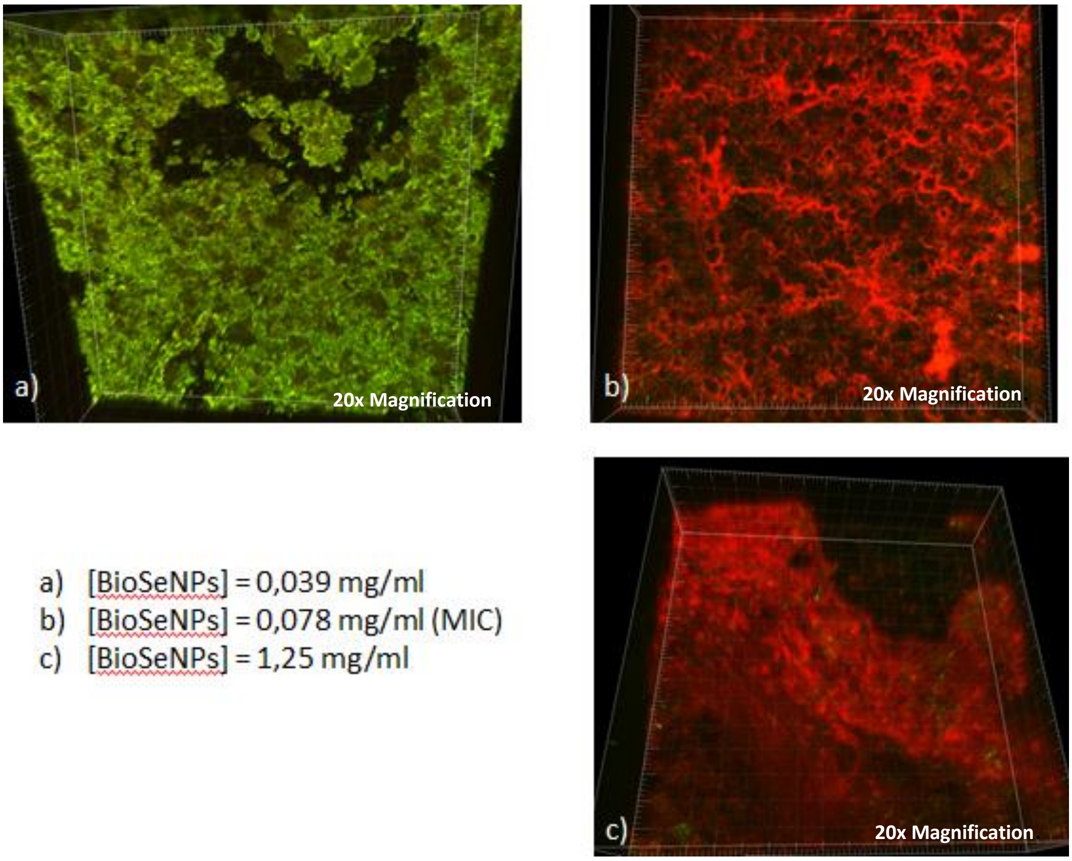

Figure 28: evaluation of live/dead cells ratio of *P. aeruginosa* NCTC 12934 biofilm exposed to different concentration of biogenic SeNPs

In figure 28.a is shown *P. aeruginosa* NCTC 12934 biofilm grown in presence of a solution of SeNPs at 0,039 mg/mL, concentration value immediately lower than MIC value. Watching this figure it's noticeable strong green fluorescent signal, indicating presence of high number of biofilm living cells. There are also darker fluorescent signals due to HA coating not uniformly distributed on peg. Analyzing action of this SeNPs solution onto biofilm cells, there's no evidence of strong antimicrobial activity of NPs: bacteria cells are present in high number and they're all alive (green fluorescent signal). It's also possible to notice that *P. aeruginosa* NCTC 12934 seems able to growth in thick layer that covered HA peg.

Biofilm conformation completely changed when it’s grown in presence of higher SeNPs solution concentrations (fig.29b and 29c).
Considering MIC value (0,078 mg/mL) determined by MBEC assay, CLSM analysis has been conducted exposing *P. aeruginosa* NCTC 12934 to SeNPs solution with MIC concentration, in order to detect biofilm changing in structure. As shown in figure 28.b, most cells have strong red fluorescent signal, indicating that they’re almost all died, confirming MBEC results. Even if it’s possible to notice presence of background fluorescent signal due to HA coating, brilliant red fluorescence signal is preponderant in all peg sections analyzed. Furthermore, there’s no strong evidence of green fluorescent signal presence, symptom that there’s just few alive bacteria cells present in *P. aeruginosa* NCTC 12934 analyzed biofilm. This result permits both to confirm MBEC results and to suppose that biogenic SeNPs at this concentration show very strong antimicrobial activity.
Finally, *P. aeruginosa* NCTC 12934 biofilm grown in presence of SeNPs solution with higher concentration (1,25 mg/mL) rather than MIC has been analyzed. Figure 28.c is similar to one with SeNPs solution at MIC value: almost all fluorescent signal is red, symptom that all bacteria cells are died. At the same time, in this sample there is a stronger brilliant red signal rather than the second one at MIC value. This is probably due to strong ability of 1,25 mg/mL SeNPs solution to kill bacteria cells also in thick layers or, at the same time, to higher presence of biofilm in this analyzed peg.
However, as in other 2 samples, it’s possible to notice presence of red background signal, due to HA coating, even if in this sample this is lower than in the others analyzed before.

In order to better investigate biofilm structure in presence of SeNPs solution at same concentration of MIC, CLSM images using 63x objective lens (higher magnification rather than that at 20x) have been analyzed.

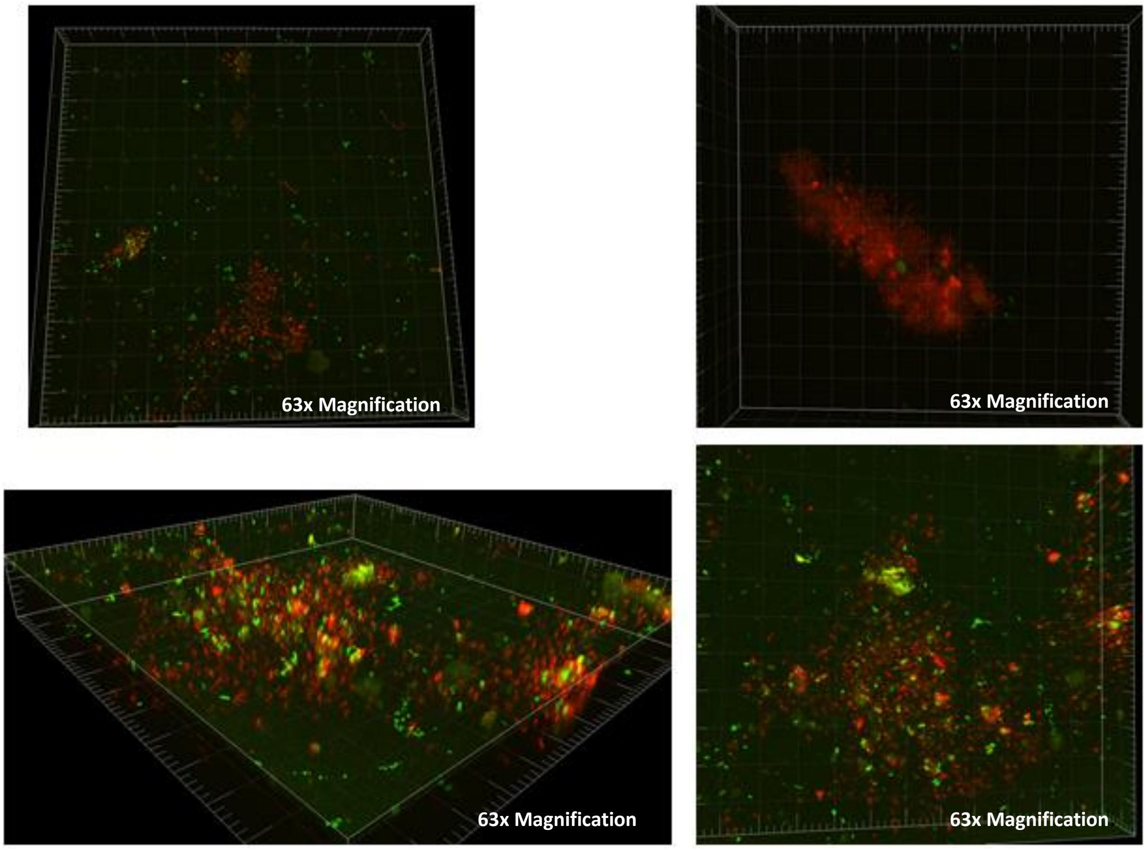

Figure 29: 63x objective lens CLSM images of biogenic SeNPs solution at MIC acting against *P. aeruginosa* NCTC 12934 biofilm

Figure 29 shows difference peg section of *P. aeruginosa* NCTC 12934 growth in presence of 0,078 mg/mL SeNPs solution (MIC). It’s noticeable that in all 4 pictures red fluorescent signal is preponderant rather than green one, symptom that number of died cells are higher than those still alive. All 4 pictures confirm both MBEC results and previously CLSM analysis made with 20x objective lens.

However, these CLSM images permit also to determine presence of few bacteria cells still alive (brilliant green fluorescent signal) that using 20x objective lens is not possible to detect.

It's also important to consider that using higher magnification leads to lose HA coating structure: in all 4 pictures is not possible to find darker background fluorescent signal due to HA but only alive or dead cells. Probably this is due to magnification power of lens: 63x one have resolution power bigger than HA cluster size, permitting to analyze section of sample also from too close clusters.

In order to understand strength of SeNPs synthetized using *Bacillus mycoides* SelTe01 as antimicrobial agents, it's useful also to make a comparison with biogenic SeNPs made using different strains. However, in scientific literature there's no other papers describing use of HA coated CBDs to evaluate biofilm growth and SeNPs antimicrobial action together. However, considering previously analysis of growth of *P. aeruginosa* NCTC 12934 biofilm onto normal and HA coated CBDs, Zonaro et al (2015) work about use of SeNPs produced by *Stenotrophomonas maltophila* SelTE02 could be used as comparison.[38] CLSM analysis are made on *P. aeruginosa* PAO1 biofilm grown on CBD peg without SeNPs (positive control) and with 60 mg/L solution of biogenic SeNPs.[38] Positive control image showed typical biofilm conformation, in which there's strong brilliant green fluorescent signal due to presence of high number of living cells.

P. aeruginosa PAO1 biofilm exposed to 60 mg/L biogenic SeNPs solution analysis exhibited almost all dead cells, thanks to detection of strong red fluorescent signal. There's no presence of darker background fluorescent signal, because there's no HA coating on CBDs. Furthermore, it's important to consider differences between biogenic concentration of biogenic SeNPs solutions: while SeNPs solution made by *Bacillus mycoides* SelTE01 have concentrations between 0,039 mg/mL to 1, 25 mg/mL, Zonaro and coworkers tested 0,06 mg/mL SeNPs solution. Comparing images of both classes of biogenic SeNPs, it's possible to note that *P. aeruginosa* biofilm grown in presence of SeNPs produced by *Bacillus mycoides* SELTE01 shows higher number of red dead cells rather than SeNPs made by *Stenotrophomonas maltophila* SelTE02. This permits to suppose that even if biogenic SeNPs produced by *Stenotrophomonas maltophila* SelTE02 show strong antimicrobial activity, this is always lower rather than SeNPs synthetized using *Bacillus mycoides* SelTE01, as previously described with MBEC results discussion.

L-cysteine SeNPs action against P.aeruginosa NCTC 12934 biofilm grown onto HA coated peg

In order to compare biogenic SeNPs antimicrobial properties and activity, 3 samples of *P. aeruginosa* NCTC 12934 biofilm growth in presence of L-cysteine SeNPs solutions with different concentration has been analyzed. Considering MBEC results, it was no possible to determine a clear MIC value for L-cysteine SeNPs action against this biofilm. However, CLSM analysis has been take exposing pathogenic biofilm to 3 different SeNPs solutions, using MBEC curve as reference:

- sample exposed to 0,625 mg/mL SeNPs solution (lower than solution with antimicrobial activity similar to an MIC value)
- sample inoculated with 1,25 mg/mL SeNPs concentration similar to an MIC value (higher antimicrobial properties)
- sample grown in presence of 2,5 mg/mL SeNPs solution (higher than solution similar to MIC)

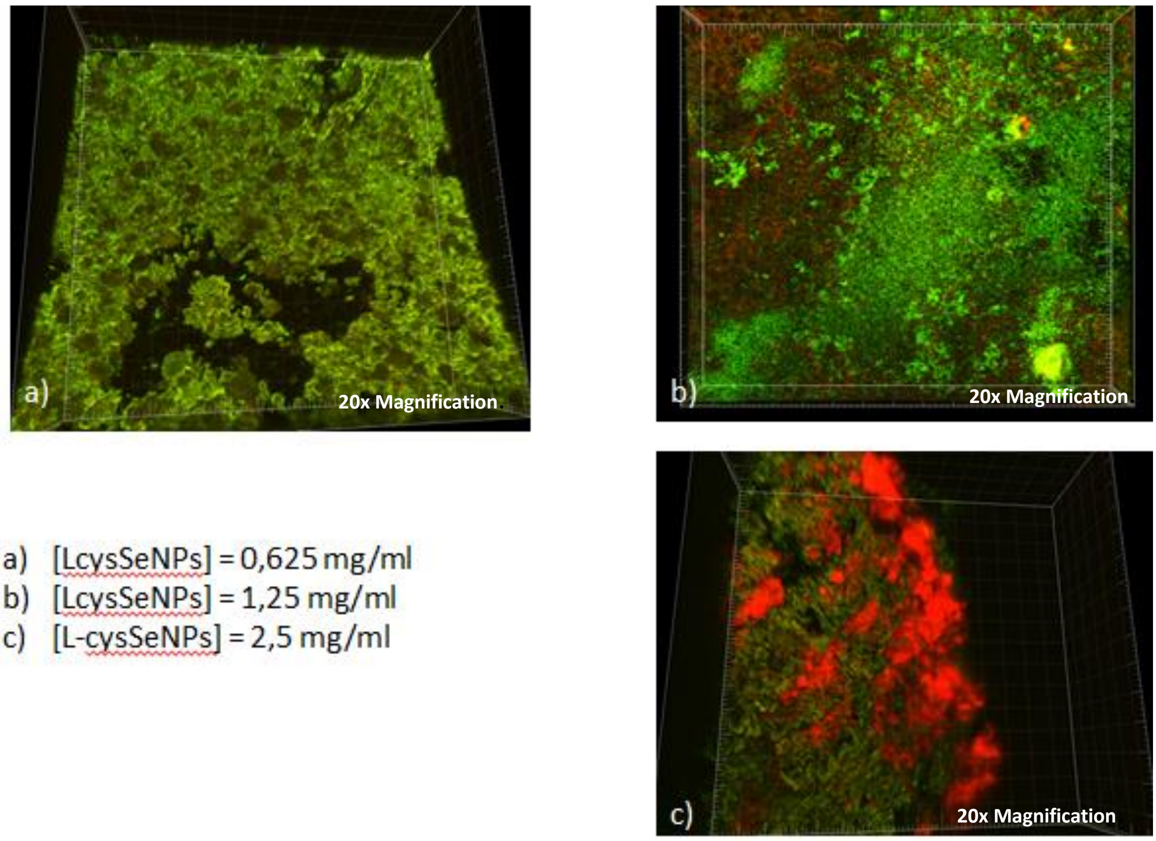

Figure 30: evaluation of live/dead cells ratio with exposure of *P. aeruginosa* NCTC 12934 biofilm to different chemical SeNPs solutions

Figure 30.a evaluates SeNPs solution action with concentration of 0,625 mg/mL, that, considering MBEC curve, doesn't have strong antimicrobial ability to inhibit biofilm growth. As validation of MBEC results, figure 30.a shows a strong mature biofilm, thanks to brilliant green fluorescent signal recognizable in all analyzed section of the peg. This sample resembles typical *P. aeruginosa* NCTC 12934 biofilm structure with high number of bacteria cells organized in thick layers. As in other samples analyzed before, it's possible to determine presence of non-uniform HA coating thanks to its dark background fluorescent signal and black holes.

Analyzing *P. aeruginosa* NCTC 12934 biofilm growth in presence of SeNPs solution with higher concentration (1,25 mg/mL, fig.30b), it's possible to note changing in biofilm structure: even if there is still strong brilliant green fluorescent signal, on the left part of peg section there are also high

number of red bacteria cells, symptom that L-cysteine SeNPs are able to kill some of them. However, number of alive cells green colored is, without doubt, higher rather than number of those red colored (dead), indicating that L-cysteine SeNPs are not so strong antimicrobial agents.
Finally, testing action of 2,5 mg/mL L-cysteine SeNPs solution (fig.30c) shows presence of both brilliant green and red fluorescent signal. In this situation, the ratio between alive (green) and dead (red) bacteria cells is different: almost half of cells are green and other half are red. Considering this results, probably it's possible to achieve all bacteria cells death by increasing L-cysteine SeNPs concentration of solutions.
CLSM images of L-cysteine SeNPs action against *P. aeruginosa* NCTC 12934 biofilm confirms MBEC curve results: they've antimicrobial activity, but not stronger enough to completely inhibit biofilm growth with tested range of SeNPs concentrations.
In order to analyze SeNPs action inside a mature biofilm, CLSM images of *P. aeruginosa* NCTC 12934 biofilm growth in presence of 1,25 mg/mL L-cysteine SeNPs solution have been taken using 63x objective lens.

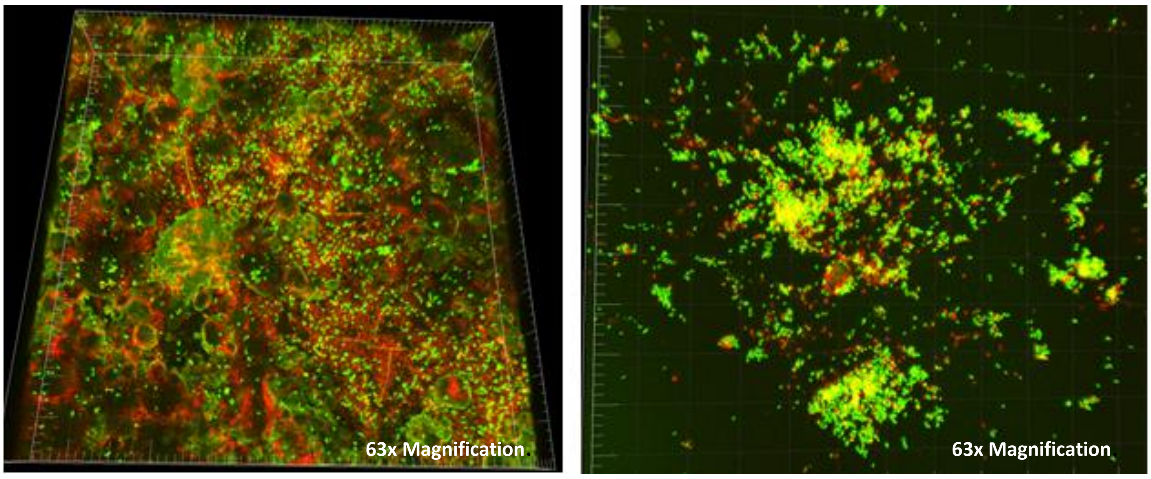

Figure 31: 63x objective lens CLSM images of L-cysteine SeNPs action at MIC against *P. aeruginosa* NCTC 12934 biofilm

These two images are taken for two different peg sections and, as it's possible to note, biofilm situation and structure is completely different. While left image shows complex biofilm structure, right one has easier cells distribution. Analysis of left image permits to recognize many structures typical both of biofilm and HA peg. There's huge presence of alive cells all around peg section, in particular concentrated in black zone of peg (without HA coating) and on the edge of HA clusters. Despite images took with biogenic SeNPs, presence of HA structure is detectable considering both dark fluorescent signal and live cells distribution. Living cells are present all around spherical big and organize structures, detectable as HA clusters. At the same time, there's a high number of dead cells present in analyzed biofilm, especially detectable in black zone of peg section.

Image on the right shows an easier situation, in which there's no evidence of HA cluster presence and ratio between green and red cells shows presence of higher number of alive cells (green) rather than those dead (red). It's possible to notice also presence of some yellow colored zones, probably due to overlapping of dead cells and alive cells layers.

Summary

Comparison between biogenic and chemical SeNPs confirms previously described MBEC results: biogenic SeNPs have stronger antimicrobial properties rather than those chemically synthetized. Evaluation CLSM images obtained using Live/Dead staining permits to affirm that ratio between green and red cells is completely different considering biogenic and chemical SeNPs. Analysis of both first samples grown with biogenic and chemical SeNPs with low concentration shows same results: presence of strong and mature living biofilm with high number of alive bacteria cells. However, situation drastically changes considering other 4 samples: biogenic SeNPs show stronger antimicrobial properties rather than those synthetized with L-cysteine. Ratio between green and red cells is completely different in these samples: both biofilms grown in presence of SeNPs have almost all dead cells (red color), while samples growth with L-cysteine SeNPs have more living cells (green colored) than those red in biofilm with SeNPs intermediate concentration, and almost half dead and half alive cells in sample growth in presence of SeNPs with higher concentration.

SEM analysis

SEM analysis has been conducted principally in order to better understand HA coating structure, possible interaction between HA and biogenic SeNPs and P. aeruginosa NCTC 12934 ability to grow onto HA pegs.

In particular, SEM analysis has been made of 5 different samples:

- HA coated peg as negative control to establish HA structure and coating onto CBD pegs
- HA coated peg exposed to biogenic SeNPs solution to understand presence of possible interaction between two chemical compounds
- HA coated peg with *P. aeruginosa* NCTC 12934 biofilm grown without SeNPs exposure to verify biofilm ability to grow on this peg
- HA coated peg with *P. aeruginosa* NCTC 12934 biofilm grown with biogenic SeNPs solution at MIC
- HA coated peg with *P. aeruginosa* NCTC 12934 biofilm grown with L-cysteine SeNPs solution at concentration with higher antimicrobial activity

SEM images has been collected using two different magnification lens (75x and 800x) in order to have both general images of pegs structure and images of details of different samples.

HA coated peg

Figure 32 shows SEM image of the first sample: negative control made of HA coated peg.

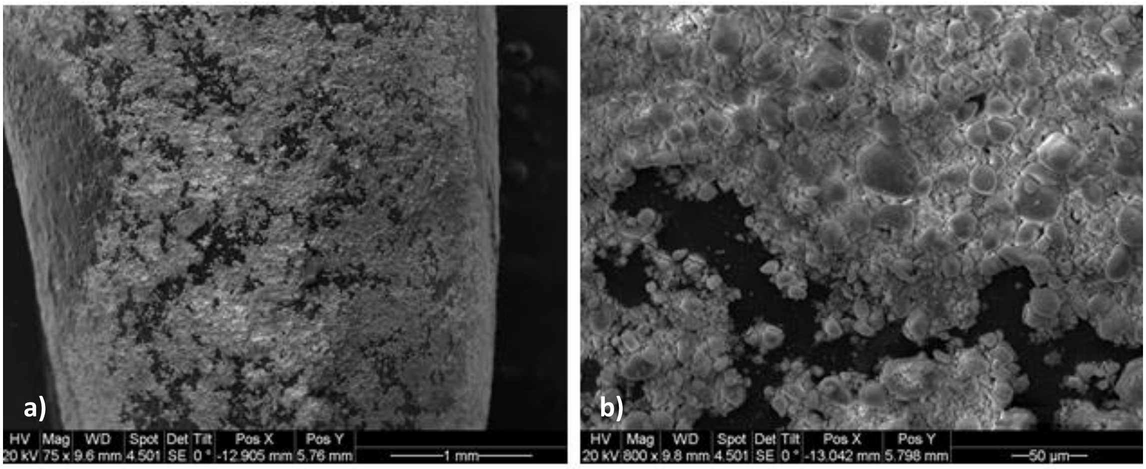

Figure 32: SEM analysis of HA coating on CBD peg at **a)** 75x magnification **b)** 800x magnification

Analysis of figure 32 shows how HA coating on CBD peg is not uniformly present: in both images it's possible to notice presence of black holes, due to absence of HA coating (grey structure). Probably this is due to chemical coating process that is not able to completely fill pegs with HA. Furthermore, image on right permits to confirm CLSM hypothesis of HA organized clusters, recognizable as spherical structures bound all together to form a complex tridimensional matrix, in which both SeNPs and bacteria cells are able to penetrate. Effectively, considering size scale of 800x image, it's possible to suppose that HA clusters are in order of 25-30 µm of diameter, while both bacteria cells of biofilm and SeNPs are smaller (nanometer range).

Ha coated peg exposed to biogenic SeNPs

Considering HA coated pegs as scaffold to growth pathogenic biofilms, it's also useful to study possible chemical interaction between HA and SeNPs. As previously described, in last few years there was development of HA structures and implants coated with antimicrobial agents, such as Ag^{+}, Au^{2+} or SeO_3^{2-} ions. However, thanks to the stronger antimicrobial activity of NPs, nowadays scientific interest is moved to create HA structure coated of NPs or directly to create HA-NPs doped with antimicrobial ions or NPs. Based on recent results, one of the most interesting possibility is to coat HA implants with SeNPs. Considering antimicrobial ability shown in this work, one of the best and innovative option is to create HA structures coated with biogenic SeNPs. In order to understand if SeNPs are naturally able to link and to be trap in HA structure, SEM analysis has been made on a HA coated peg exposed to 0,078 mg/mL (MIC value) biogenic SeNPs produced by Bacillus mycoides SelTE01 after 6 h of Na_2SeO_3 exposure.

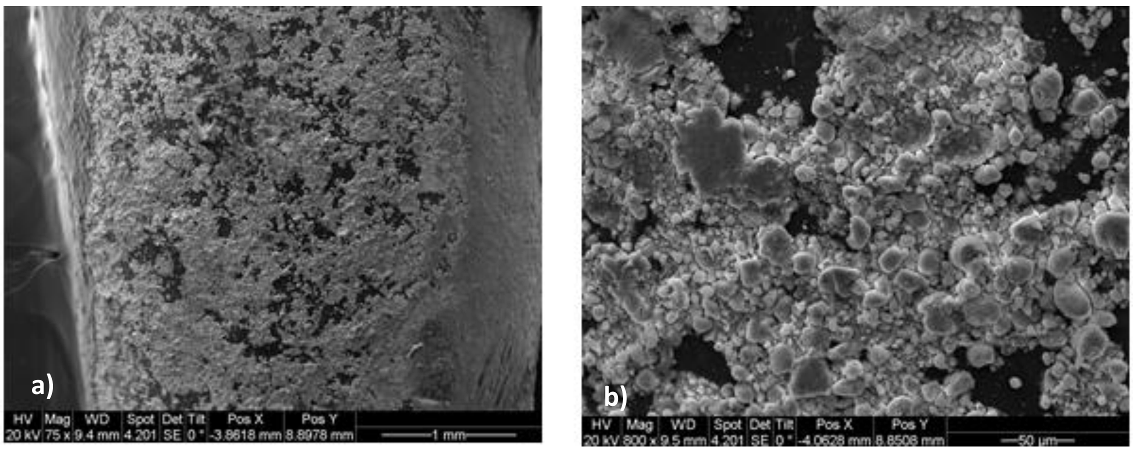

Figure 33: SEM analysis of HA coated peg exposed to 0,078 mg/mL biogenic SeNPs solution at **a)** 75x magnification **b)** 800x magnification

To analyze this sample is important to consider that 75x objective lens image is not so useful to determine presence of SeNPs in HA coating. At the same time, also analysis of 800x image has the same issue: HA clusters are too big (micrometric scale) compared to SeNPs (nanometric scale) and detection of them becomes difficult. One other issue could be that HA clusters are able to form an organized tridimensional structure and, in so doing, it’s possible also that SeNPs remain onto HA coating but on the edge of HA clusters becoming not detectable. However, lack of big visible SeNPs deposits is a positive results, because it permits to suppose that HA and SeNPs are not able to chemically interact, preventing SeNPs to aggregate and form bigger structures.
It’s also possible to affirm that there’s no evidence of SeNPs presence in black zones of peg, in which there’s no HA coating.

P. aeruginosa NCTC 12934 biofilm growth onto HA coated peg

In order to verify biofilm ability to grow onto HA coated peg, a HA coated peg of inoculated *P. aeruginosa* NCTC 12934 strain has been analyzed as positive control with SEM.

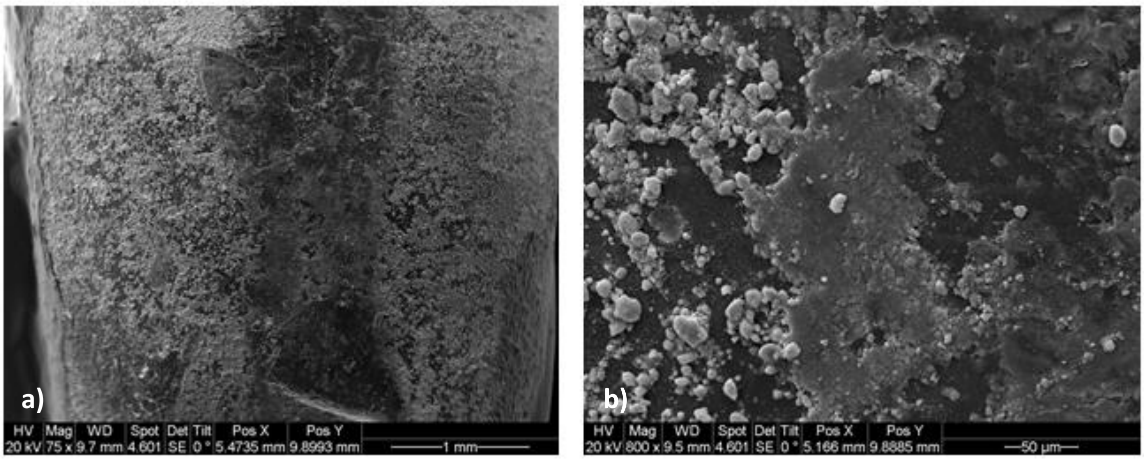

Figure 34: SEM analysis of HA coated peg exposed to *P. aeruginosa* NCTC 12934 at **a)** 75x magnification **b)** 800x magnification

Figure 34 shows HA coated peg with a wide dark area in the middle similar to a stripe recognizable as biofilm. Using 800x objective lens to improve magnification power permits to highlight *P. aeruginosa* NCTC 12934 biofilm existence thanks to bacteria cells presence. Effectively, image on the right points out simultaneously the presence of typical HA structures, detectable by presence of big HA clusters on the left side of image, and presence of bacteria cells, recognizable on the right part of image as thick dark and homogeneous layer. Analysis of size range of image on the rights permits to detect thick dark layer as biofilm: bacteria cells have normally 0,2 µm of diameter and few micrometers in length [48] but, when they are linked together in organic matrix to create biofilm, they can increase total size of structure, becoming a thick and homogeneous layer of cells.

It's also important to consider growth distribution of biofilm onto HA coated peg comparing to a normal one. Usually strong biofilm, such as that of *P. aeruginosa* NCTC 12934, is able to grow in all peg surface, arising in bigger thick homogenous region of overlapping bacteria cells and organic matrix. However, using HA coated peg, biofilm growth situation changes: the strain is able only to grow as wide stripe, in which all bacteria cells are strictly linked together in one region. Probably this is due to HA organized crystalline structure: clusters of HA may be an obstacle to biofilm formation and, in so doing, bacteria cells are able to grow only in areas with low HA amount or on the edge of HA clusters.

P. aeruginosa NCTC 12934 biofilm HA coated peg exposed to biogenic SeNPs

Once determined *P. aeruginosa* NCTC 12934 ability to grow as biofilm onto HA coated peg, HA coated peg with mature biofilm grown in presence of 0,078 mg/mL biogenic SeNPs (MIC value) produced by *Bacillus mycoides* SelTE01 after 6 h of Na_2SeO_3 exposure has been evaluated. Using SEM images evaluation of biogenic SeNPs antimicrobial activity is not univocal, because it doesn't permit to distinguish between living mature biofilms and those dead, but just to detect their presence.

However, in order to establish possible noticeable differences in morphology or peculiarity, this sample has been analyzed.

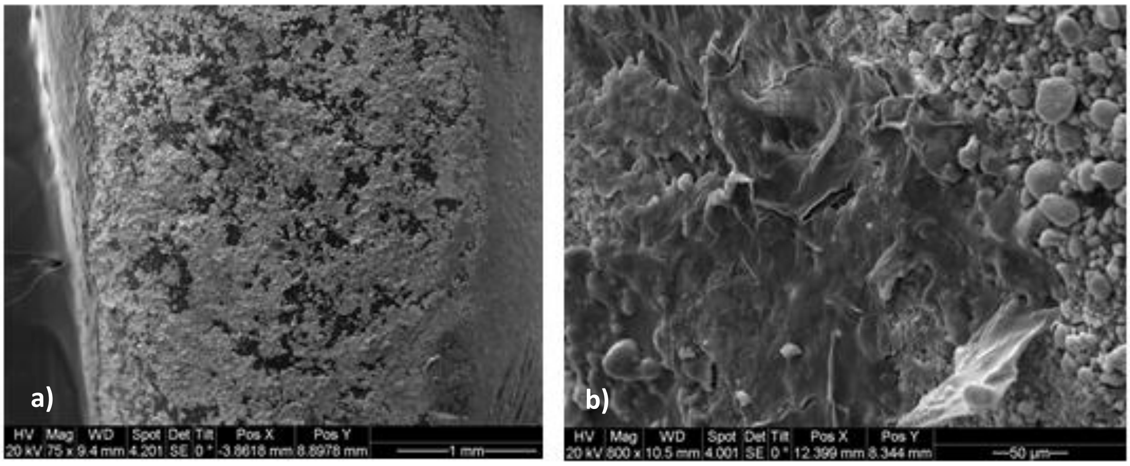

Figure 35: SEM analysis of HA coated peg exposed to *P. aeruginosa* NCTC 12934 grown in presence of biogenic SeNPs at **a)** 75x magnification **b)** 800x magnification

Analysis of SEM image taken using 75x objective lens (left image) permits to have a general view of sample. In so doing, it allows to affirm that in almost all HA peg there's no strong evidence of *P. aeruginosa* NCTC 12934 presence. However, it's possible to notice presence of biofilm structure as stripe on left side of HA peg. Improving magnification power of this area, using 800x objective lens, permits to detect biofilm presence as thick dark and homogeneous layer (image on the right). Structure and morphology of this biofilm is similar to the one observed on positive control previosuly analyzed, allowing to affirm that it is recognizable as *P. aeuginosa* NCTC 12934 biofilm. As in positive control peg both typical HA structure of

clusters and overlapping of bacteria cells together in layers are present. There's no strong evidence of changing in structure and morphology between positive control biofilm and the one exposed to biogenic SeNPs.
Considering SEM tecnique, it's possible that detected biofilm on this sample is both alive or dead. However, biogenic SeNPs solution used in this sample corrisponds to MIC value determined with MBEC assay, value that is also previously confirmed with CLSM analysis.
Using together MBEC, CLSM and SEM analysis it's possible to suppose that *P. aeruginosa* NCTC 12934 biofilm, detected onto this HA coated peg, is probably a dead one.

P. aeruginosa NCTC 12934 biofilm HA peg exposed to L-cysteine SeNPs

To compare biogenic and chemical SeNPs action as antimicrobial agents, *P. aeruginosa* NCTC 12934 biofilm grown onto HA peg in presence of 1,25 mg/mL solution of SeNPs synthetized using L-cysteine (highest antimicrobial value detected with MBEC assay) has been evaluated.

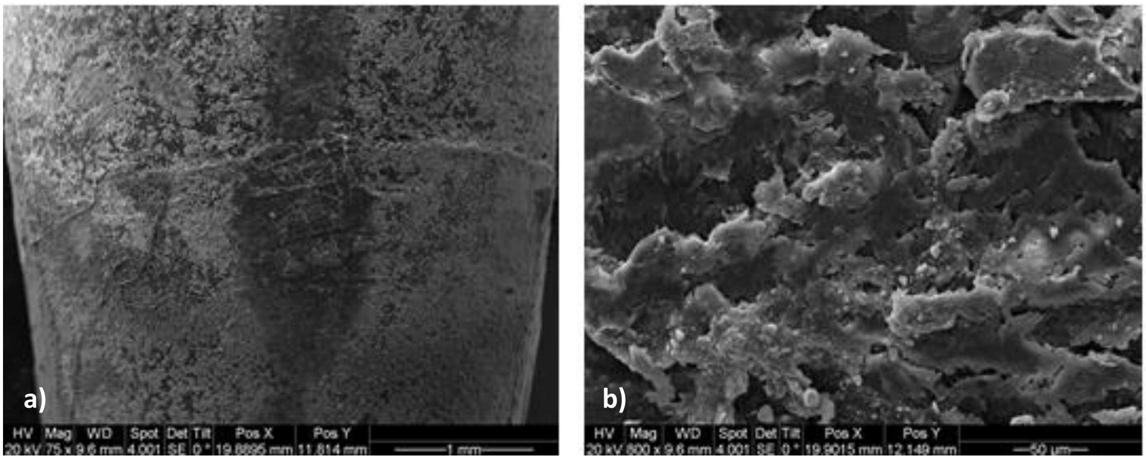

Figure 36: SEM analysis of HA coated peg exposed to *P. aeruginosa* NCTC 12934 grown in presence of L-cysteine SeNPs at **a)** 75x magnification **b)** 800x magnification

As shown in Figure 36a, there's wide area of HA coated peg covered of *P. aeruginosa* NCTC 12934 biofilm. Size and morphology of detected biofilm is similar to one recognized in positive control previously described: big dark area in the middle of HA coated peg that resemble a stripe. Considering this image, it's also important to notice presence of flaws onto HA coating as white stripe present in the middle of peg structure.

Figure 36.b on right side shows magnificated area of detected biofilm stripe with 75x objective lens. As in other samples, it's possible to note the presence of thick dark and homogenous layers of bacteria cells in all section.

Analysis of biofilm morphology shows many differences comparing to biofilms of positive control or the one grown in presence of biogenic SeNPs. In this sample biofilm seems to be damaged and lifted compared to the image plane. Even if it's similar for thickness and homogeneity to the other analyzed, this biofilm shows cuts and incisions in all its surface, arising in a non-conventional structure. Considering together MBEC and CLSM resluts, it's difficult to suppose that this analyzed biofilm corresponds to a dead one, because L-cysteine SeNPs don't show strong antimicrobial activity.

<u>*Summary*</u>

Analysis of HA coated peg permits to affirm that HA coating is not uniformly present onto CBD peg. It's possible also to notice presence of bigger HA clusters linked together in all structure.

Furtermore, SEM images of HA coated peg exposed to biogenic SeNPs solution suggests that there's no evidence of chemical interactin between

HA and SeNPs. In so doing, both HA structure and SeNPs chemistry remain untouched.

Finally, comparison between biofilms exposed to biogenic and L-cysteine SeNPs solutions with SEM analysis shows both differences and similarities. Even if *P. aeruginosa* NCTC 12934 biofilms are able to growth onto HA peg in as thick layer in both situations, sample exposed to biogenic SeNPs shows lower area filled with biofilm structure rather than sample exposed to chemical SeNPs. At the same time, biofilm conformation in these two samples is completely different: while in the one exposed to biogenic SeNPs biofilm has normal structure similar to positive control, in the sample exposed to L-cysteine SeNPs biofilm seems to be damaged.

EDS analysis:

To validate SEM results and to better understand HA, SeNPs and biofilm nature on pegs, all 5 samples have been analyzed with EDS.

<u>*HA coated peg*</u>

Firstly HA coated peg has been evaluated, in order to proof HA presence with chemical composition.

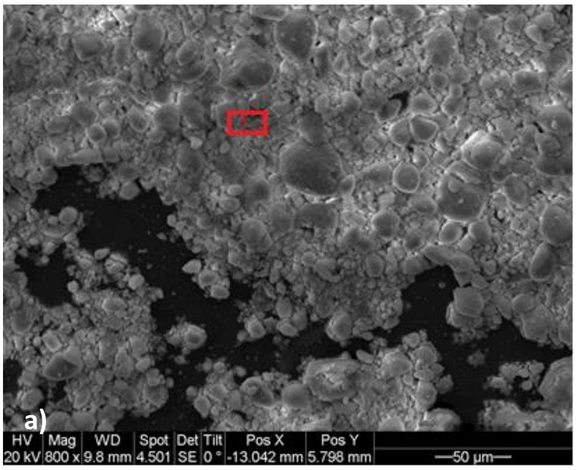

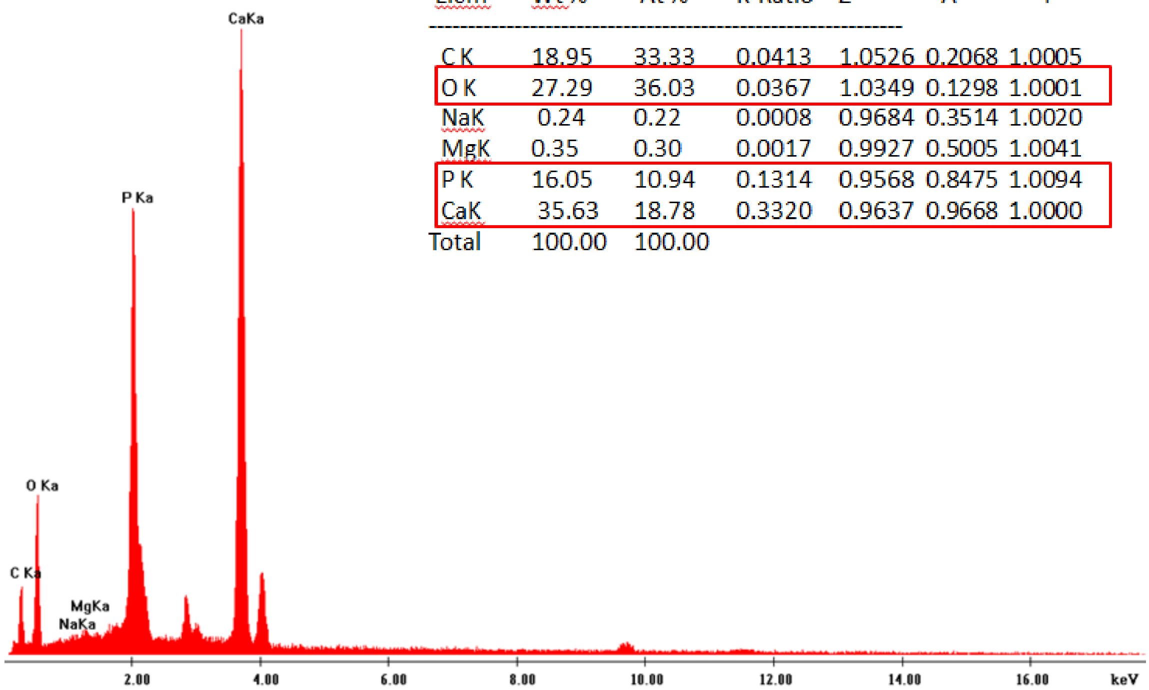

Elem	Wt %	At %	K-Ratio	Z	A	F
C K	18.95	33.33	0.0413	1.0526	0.2068	1.0005
O K	27.29	36.03	0.0367	1.0349	0.1298	1.0001
NaK	0.24	0.22	0.0008	0.9684	0.3514	1.0020
MgK	0.35	0.30	0.0017	0.9927	0.5005	1.0041
P K	16.05	10.94	0.1314	0.9568	0.8475	1.0094
CaK	35.63	18.78	0.3320	0.9637	0.9668	1.0000
Total	100.00	100.00				

b)

Figure 37: a) SEM image of HA coated peg with reference to chosen area for EDS analysis **b)** EDS spectrum and data quantification

Knowing Ha nature and composition, it's possible to confirm HA presence onto CBD pegs. Normally HA is a polumer made of Ca2+ ions, PO42- and OH-.

As shown in EDS spectrum and quantification data, this sample has typical HA composition, with 35,63% in weight of Calcium, 16,05 % in weight of Phosphorous and 27,29% in weight of Oxygen (together form Phosphate group PO_4^{2-} or present as OH^- ions).

Ha coated peg exposed to biogenic SeNPs

Using same process, it's possible also to analyze HA coated peg exposed to 0,078 mg/mL biogenic SeNPs solution produced by *Bacillus mycoides* SelTE01, in order to establish possible ability of SeNPs to bind HA clusters.

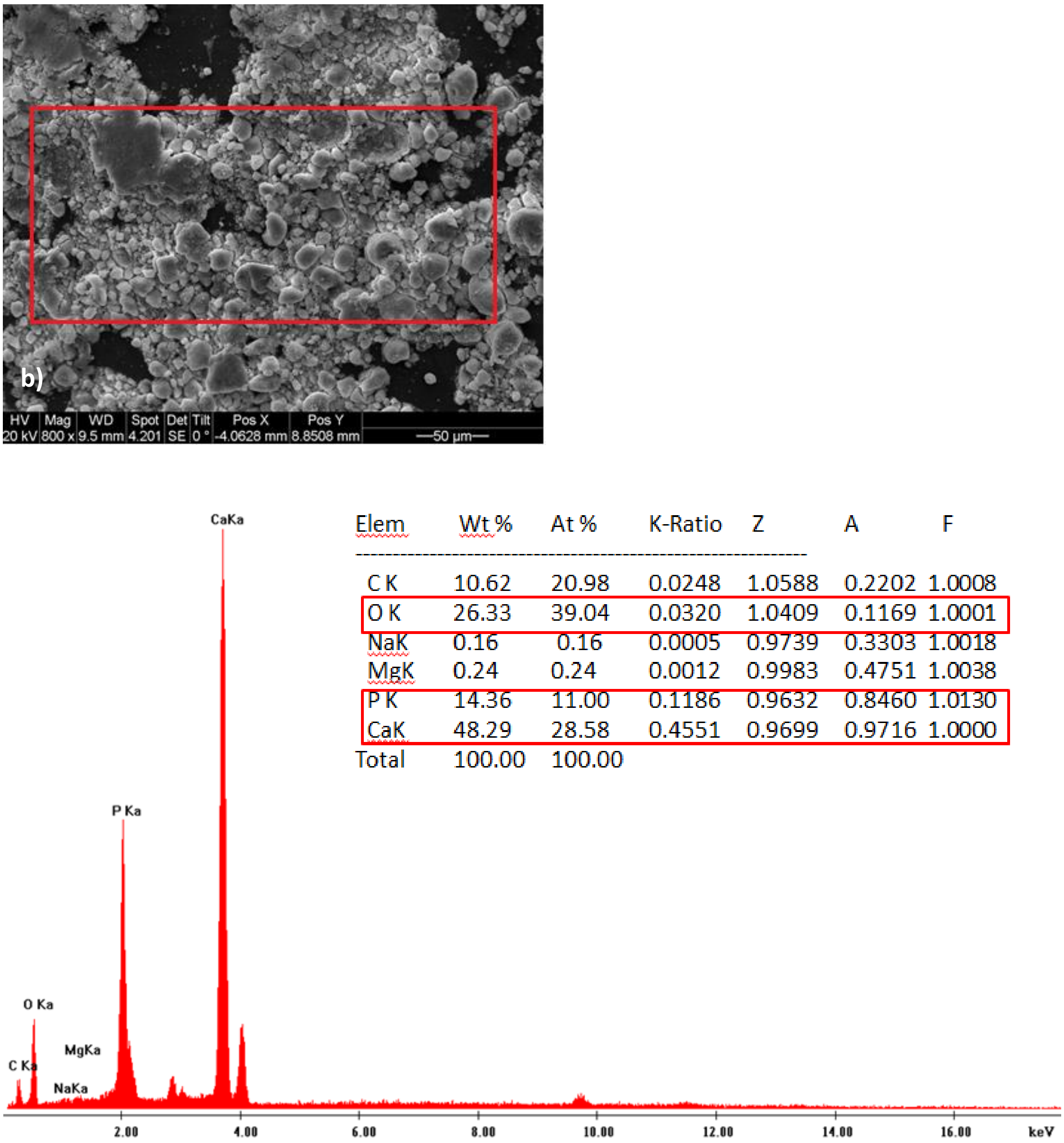

Elem	Wt %	At %	K-Ratio	Z	A	F
C K	10.62	20.98	0.0248	1.0588	0.2202	1.0008
O K	26.33	39.04	0.0320	1.0409	0.1169	1.0001
NaK	0.16	0.16	0.0005	0.9739	0.3303	1.0018
MgK	0.24	0.24	0.0012	0.9983	0.4751	1.0038
P K	14.36	11.00	0.1186	0.9632	0.8460	1.0130
CaK	48.29	28.58	0.4551	0.9699	0.9716	1.0000
Total	100.00	100.00				

b)

Figure 38: a) SEM image of HA coated peg exposed to biogenic SeNPs with reference to chosen area for EDS analysis
b) EDS spectrum and data quantification

As previously discussed considering SEM results, analysis of EDS spectrum and data quantification do not highlight presence of biogenic SeNPs bound to HA coating of pegs. Effectively, EDS results underline presence of higher amount of Calcium (48,29% in weight), Phosphorous (14,36% in weight) and Oxygen (26,33% in weight), typical chemical composition of HA clusters already observed with EDS analysis of negative control sample (HA coated peg). Absence of Selenium signal in EDS analysis permits to suppose that biogenic SeNPs are not able to have strong chemical interaction with HA clusters. In this sense, it's important to consider different size and partial charge of chemical species present in the sample: HA is almost composed of Ca^{2+}, OH^- and PO_4^{2-}, while in biogenic SeNPs are made principally of Se^0 and other elements such as Carbone, Oxygen, Sulfur and Phosphorus able to link together arising in several biological compounds. Since biogenic SeNPs are coated by a strong and organic cap, it's difficult to have chemical interaction with HA. In so doing, HA is normally exposed to exchange of ions with same charge and size of ions composing itself. Normally, this chemical process gives rise to completely different HA structure, with different chemical-physical properties. However, biogenic SeNPs seems to be not able to exchange ions with HA, probably because cap surrounding SeNPs is not organized in chemical groups able to substitute HA cations (Ca^{2+}) and anions (PO_4^{2-} and OH^-). Furthermore, as previously reported in scientific literature, elemental Selenium included in SeNPs has not same size and partial charge of Phosphate or Hydroxide ions of HA polymer and it's very difficult to have a structural exchange between Se^0 and PO_4^{2-} or OH^-. EDS results show that SeNPs are not able to strongly interact with HA, remaining in media solution and avoiding important change in HA structure.[55] Usually it's possible to introduce Selenium in HA structures using SeO_3^{2-} ions as coating. [55] However, even if SeO_3^{2-} ions have antimicrobial properties, SeNPs show stronger antimicrobial ability and normally their use is preferred than use of Selenite ions. [55] Recently, the possibility of obtaining chemical modified HA with SeNPs using HA nanocrystals has been evaluated[54]: in so doing, size and partial charge of groups allow chemical interaction between two nanomaterials. However, there's no published work yet about biogenic SeNPs used in order to coat HA polymer structures to obtain strong antimicrobial properties.

P. aeruginosa NCTC 12934 biofilm growth onto HA coated peg

In order to have a positive control of biofilm growth, I decided to evaluate *P. aeruginosa* NCTC 12934 ability to grow as biofilm onto HA coated peg using EDS analysis.

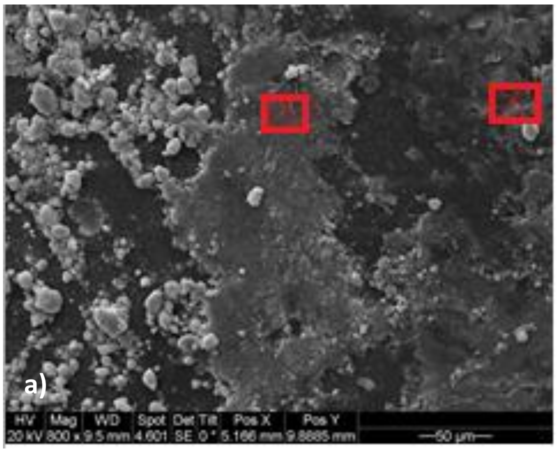

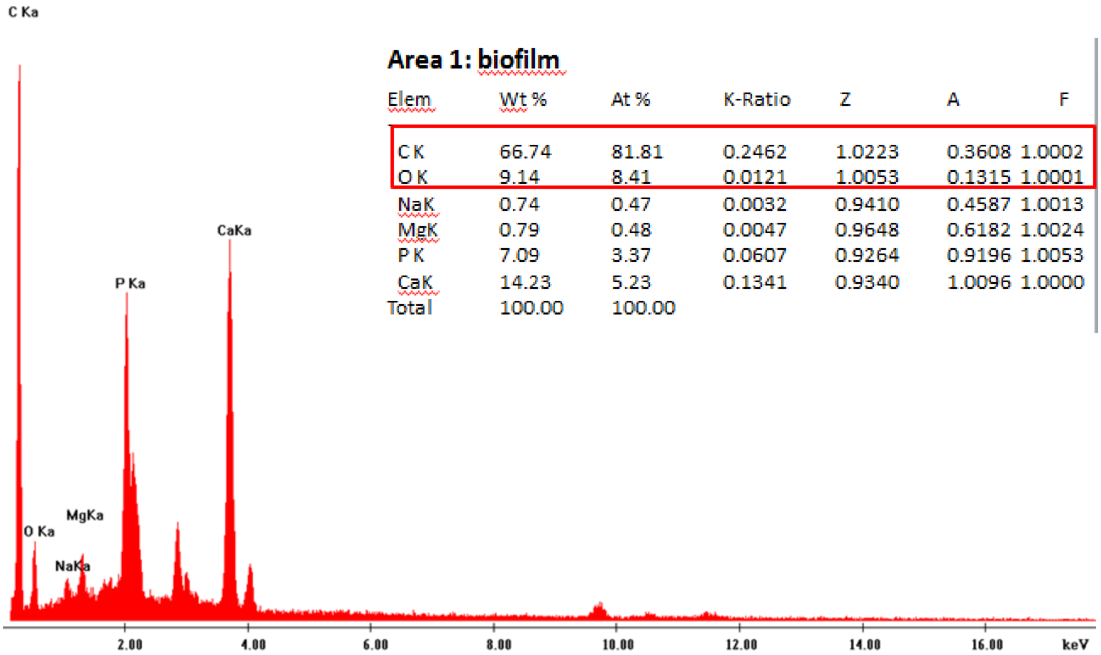

Area 1: biofilm

Elem	Wt %	At %	K-Ratio	Z	A	F
C K	66.74	81.81	0.2462	1.0223	0.3608	1.0002
O K	9.14	8.41	0.0121	1.0053	0.1315	1.0001
NaK	0.74	0.47	0.0032	0.9410	0.4587	1.0013
MgK	0.79	0.48	0.0047	0.9648	0.6182	1.0024
P K	7.09	3.37	0.0607	0.9264	0.9196	1.0053
CaK	14.23	5.23	0.1341	0.9340	1.0096	1.0000
Total	100.00	100.00				

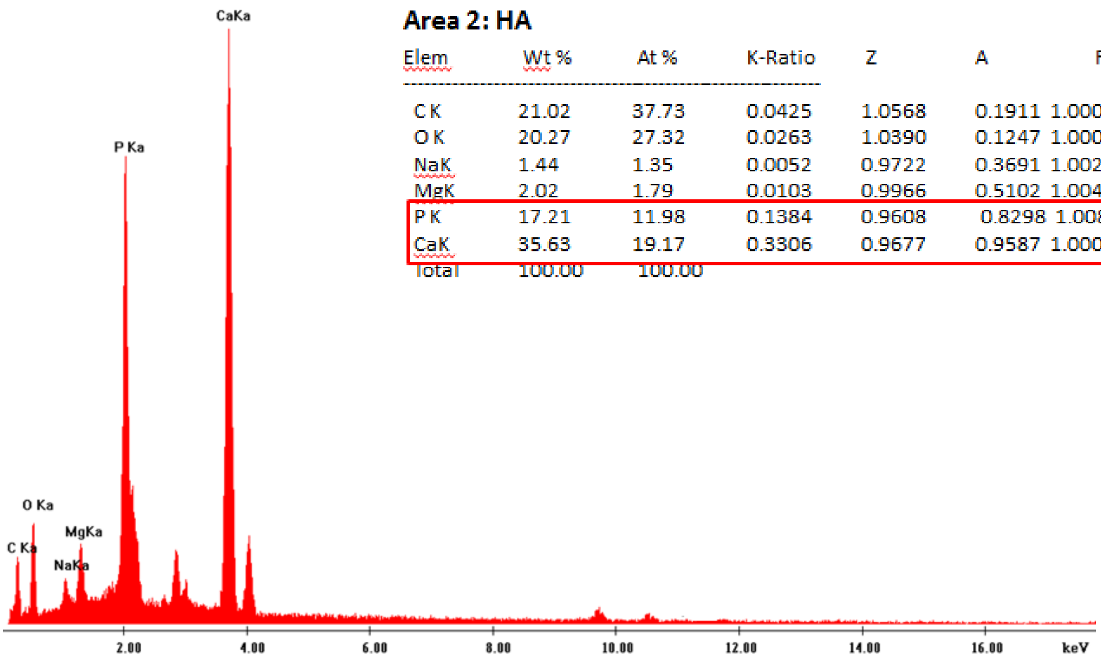

Area 2: HA

Elem	Wt %	At %	K-Ratio	Z	A	F
C K	21.02	37.73	0.0425	1.0568	0.1911	1.0005
O K	20.27	27.32	0.0263	1.0390	0.1247	1.0002
NaK	1.44	1.35	0.0052	0.9722	0.3691	1.0024
MgK	2.02	1.79	0.0103	0.9966	0.5102	1.0044
P K	17.21	11.98	0.1384	0.9608	0.8298	1.0089
CaK	35.63	19.17	0.3306	0.9677	0.9587	1.0000
Total	100.00	100.00				

b)

Figure 39: a) SEM image of HA coated peg inoculated with *P. aeruginosa* NCTC 12934 with reference to chosen area for EDS analysis
b) EDS spectra and data quantification

As shown in SEM image, 2 different sections of this sample have been analyzed, in order to confirm presence of both HA and *P. aeuginosa* NCTC 12934 biofilm. In so doing, considering both EDS spectra and data quantification, it's possible to recognize analyzed area number 1 as mature biofilm as previously supposed with SEM analysis discussion, in which there's high presence of Carbon (66,74% in weight) and Oxygen (9,14% in weight), typical elements composing bacteria cells and EPS biofilm matrix. Furthermore, analysis of area number 2 confirms HA coating presence with Calcium (35,63% in weight), Phosphorous (17,21% in weight) and Oxygen (20,27% in weight). Effectively, chemical composition of this area is similar of the one analyzed in negative control (HA coated peg alone).

P. aeruginosa NCTC 12934 biofilm HA coated peg exposed to biogenic SeNPs

Once established *P. aeruginosa* NCTC 12934 ability to growth onto HA peg, its mature biofilm growth onto HA peg and exposed to SeNPs produced by *Bacillus mycoides* SelTE01 after 6 h of Na_2SeO_3 exposure has been analyzed.

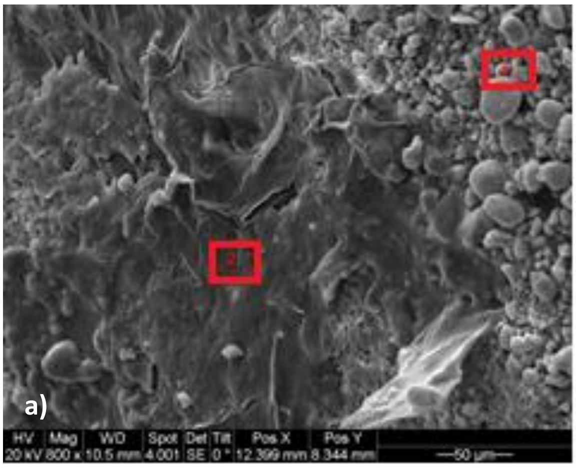

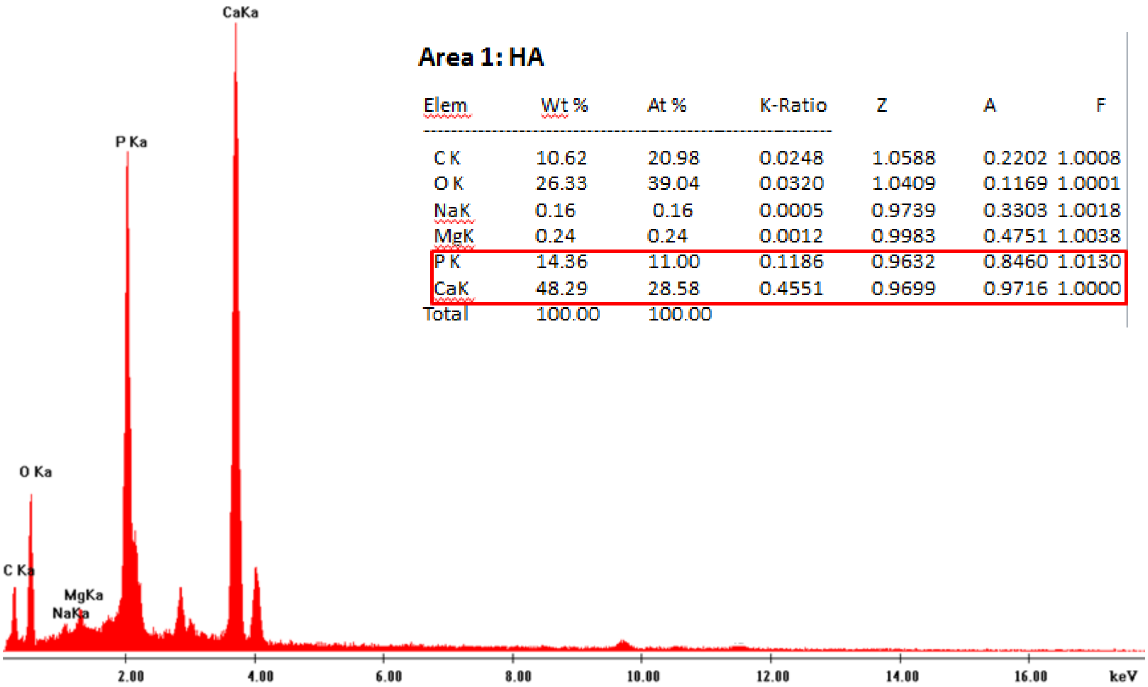

Area 1: HA

Elem	Wt %	At %	K-Ratio	Z	A	F
C K	10.62	20.98	0.0248	1.0588	0.2202	1.0008
O K	26.33	39.04	0.0320	1.0409	0.1169	1.0001
NaK	0.16	0.16	0.0005	0.9739	0.3303	1.0018
MgK	0.24	0.24	0.0012	0.9983	0.4751	1.0038
P K	14.36	11.00	0.1186	0.9632	0.8460	1.0130
CaK	48.29	28.58	0.4551	0.9699	0.9716	1.0000
Total	100.00	100.00				

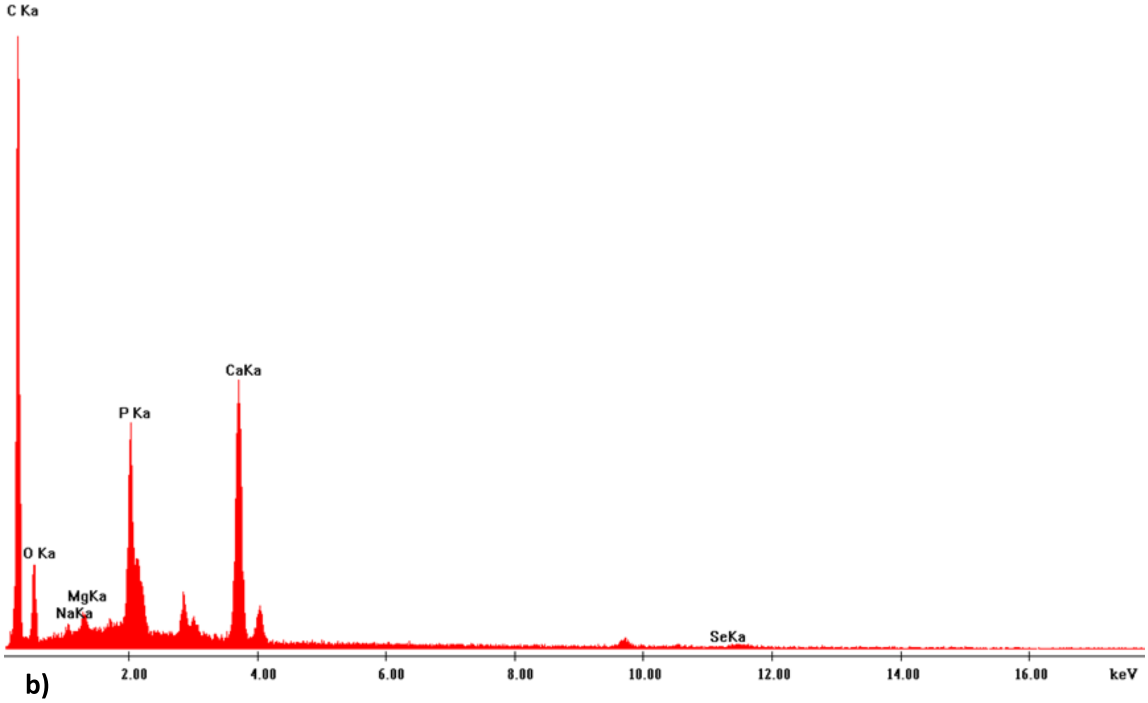

b)

Figure 40: a) SEM image of *P. aeruginosa* NCTC 12934 HA peg exposed to biogenic SeNPs with reference to chosen area for EDS analysis
b) EDS spectra and data quantification

2 different areas of peg section have been analyzed, in order to determine both presence of HA coating and to analyze biofilm composition. In so doing, EDS results of area number 1 show typical chemical composition of HA structure previously determined in negative control analysis: 48,29% in weight of Calcium, 14,33% in weight of Phosphorous and 26,33% in weight of Oxygen. Analyzing EDS results of area number 2 permits to highlight mature biofilm presence, thanks to its chemical composition: 69,91% in weight of Carbone and 11,13% in weight of Oxygen.

Furthermore, it's important to notice existence of little amount of Selenium (1,33% in weight), probably due to bacteria cells ability to hold some SeNPs inside themselves and biofilm structure.

As in the sample of HA coated peg exposed to biogenic SeNPs, there's no evidence of chemical interaction between HA and SeNPs, because little amount of present Selenium in the section is recognizable in biofilm area.

P. aeruginosa NCTC 12934 biofilm HA coated peg exposed to L-cysteine SeNPs

In order to make a comparison between biogenic and chemical SeNPs ability as antimicrobial agents, EDS analysis of *P. aeruginosa* NCTC 12934 mature biofilm grown onto HA coated peg in presence of SeNPs made with L-cysteine has been evaluated.

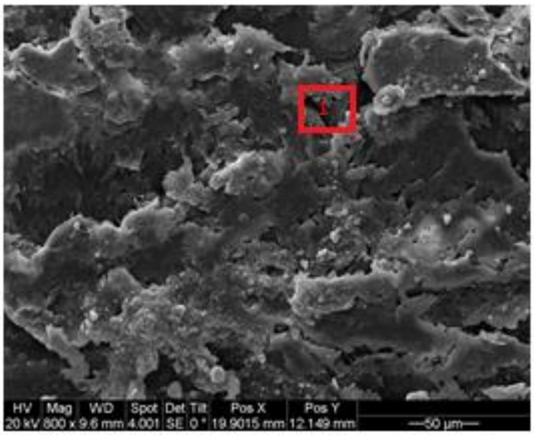

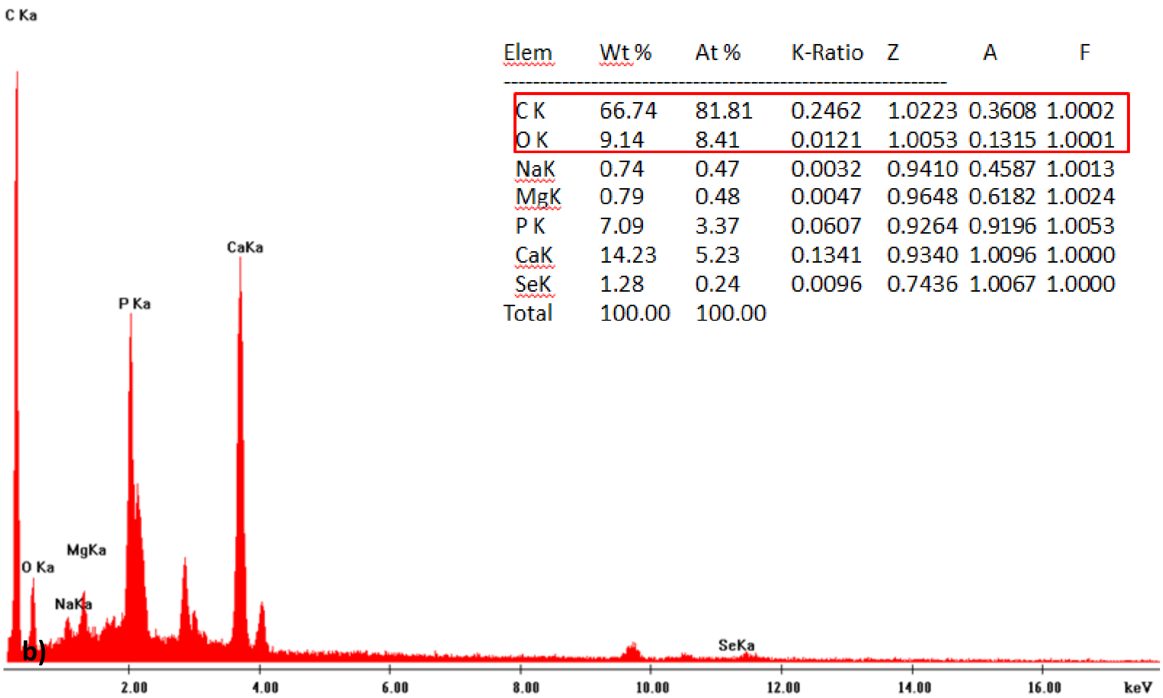

Elem	Wt %	At %	K-Ratio	Z	A	F
C K	66.74	81.81	0.2462	1.0223	0.3608	1.0002
O K	9.14	8.41	0.0121	1.0053	0.1315	1.0001
NaK	0.74	0.47	0.0032	0.9410	0.4587	1.0013
MgK	0.79	0.48	0.0047	0.9648	0.6182	1.0024
P K	7.09	3.37	0.0607	0.9264	0.9196	1.0053
CaK	14.23	5.23	0.1341	0.9340	1.0096	1.0000
SeK	1.28	0.24	0.0096	0.7436	1.0067	1.0000
Total	100.00	100.00				

Figure 41: a) SEM image of *P. aeruginosa* NCTC 12934 HA peg exposed to biogenic SeNPs with reference to chosen area for EDS analysis
b) EDS spectra and data quantification

As shown in figure 41.b, EDS analysis of this sample determines presence of *P. aeruginosa* NCTC 12934 mature biofilm onto HA coated peg. Effectively, chemical composition of analyzed section highlights presence of high amount of Carbone (66,74% in weight) and Oxygen (9,14% in weight), typical components of bacteria cells, together with high amount of Calcium (14,23% in weight), due to HA presence. Furthermore, it's important to underline presence of low amount of Selenium (1,28% in weight), comparable with Selenium present in sample exposed to biogenic SeNPs.

Summary

EDS images of HA coated peg and HA coated peg exposed to biogenic SeNPs show same results of SEM analysis: HA is effectively present as coating onto CBDs peg and there's no evidence of chemical interaction between HA and SeNPs.

Comparison between biogenic and chemical SeNPs EDS results shows many similarities: in both sample there's Selenium signal in almost same amount and there's no evidence of chemical interaction between HA and SeNPs. Furthermore, Selenium in samples is present in biofilm analyzed area. This result permits to suppose that bacteria cells inside biofilm and EPS matrix are able to hold some SeNPs in their organized structure, that gives rise to Selenium EDS signal.

CONCLUSIONS AND FUTURE PRESPECTIVES

As previously discussed, physical-chemical characterization of both biogenic and chemical SeNPs shown presence of NPs similar in size and shape (100-150 nm diameter and almost spherical).

Considering Z potential analysis of biogenic SeNPs, it’s possible to notice presence of some peaks different than those normally underline in chemical SeNPs. This result together with EDS analysis, that showed high presence in weight of Carbon, Oxygen, Phosphorous and Sulfur, suggested evidence of cap surrounding biogenic SeNPs probably made of biomolecules (proteins, lipids, phospholipids, etc..).

MBEC and CLSM results showed higher antimicrobial ability of biogenic SeNPs rather than those chemically synthetized in inhibiting biofilm formation. Probably, biogenic SeNPs stronger antimicrobial ability is due to presence of biomolecular cap. Thanks to its composition (presence of proteins and phospholipids), it could be able to penetrate in forming biofilm and to inhibit bacteria cells adhesion together.

Despite these strong antimicrobial results, biogenic SeNPs didn’t show same properties testing against pre-formed and pre-grown biofilms. In this case, as suggested by MBEC curves, both biogenic and chemical SeNPs had same physical-chemical behavior: they were not able to stop pre-formed biofilms eradication.

SEM and EDS analysis permitted to highlight presence of not uniform HA coating onto CBD pegs in form of several HA clusters linked together and some empty zone onto pegs surface. Moreover, using SEM and EDS results it was possible to determine absence of chemical interaction between HA crystals of pegs coating and biogenic SeNPs in solution: there was no evidence of SeNPs trapped onto HA coating. This outcome suggested that:

- biogenic SeNPs efficacy as antimicrobial agent is independent from HA presence
- HA structure is not structurally modified by biogenic SeNPs presence

In order to have completely analysis of biogenic SeNPs structure, it will be important to establish nature of biomolecular cap surrounding them. In so doing, it will be possible to use both proteomic and biochemical analysis, together with improved microscopy techniques. Knowing structure of biogenic SeNPs cap composition could be fundamental in:

- understanding SeNPs mechanism of synthesis
- studying mechanism of action
- controlling their physical-chemical characteristics
- developing of new industrial and biomedical applications using cap chemistry

Finally, all previously obtained results suggested possibility to use biogenic SeNPs produced by *Bacillus mycoides* SelTE01 as antimicrobial agents able to inhibit biofilms formation useable in biomedical application. In so doing, one of the most innovative opportunity consists in using biogenic SeNPs as antimicrobial coating onto HA artificial implants (bones and teeth) in order to prevent pathogenic biofilms formation.

REFERENCES

1. W. M. Haynes, "*CRC Handbook of Chemistry and Physics 95th Edition*", CRC Press/Taylor and Francis, 2014

2. G. Wulfsberg, *"Principles of Descriptive Inorganic Chemistry",* University Science Books, 185-187, 1991

3. A. L. Stroyuk, A.E. Raevskaya, S.Y. Kuchmiy, V. M. Dzhagan, D.R.T. Sahn, S. Schulze, *"Structural and optical characterization of colloidal Se nanoparticles prepared via the acidic decomposition of sodium selenosulfate"*, Colloids and Surfaces: Physicochem. Eng. Aspects 320 169–174, 2008

4. S.S. Zumdhal, "*Chemistry 4th edition",* Houghton Mifflin Boston, p 916, 1997

5. D. R. Lide, "*CRC Handbook of Chemistry and Physics 83rd edition",* CRC Press, p 4:28, 2002

6. W. K. Whitten, E. R. Davis, M.L. Peck, "*General Chemistry 6th edition",* Saunders College Publishing: Orlando, p 927, 2000

7. S. Lampis, E. Zonaro, C. Bertolini, P. Bernardi, C. S. Butler, G. Vallini, *"Delayed formation of zero-valent selenium nanoparticles by Bacillus mycoides SeITE01 as a consequence of selenite reduction under aerobic conditions",* Microbial Cell Factories 13:35, 2014

8. C. Reilly, *"Selenium in food and health"*, Blackie Academic and Professional, p.2, 1996

9. Agency for Toxic Substances and Disease Registry, *"Toxicological profile for selenium"*, p. 6, 2003

10. Z.H. Lin, C. Wang, *"Evidence on the size-dependent absorption spectral evolution of selenium nanoparticles"*, Materials Chemistry and Physics 92, 591-594, 2005

11. Scientific Committee on Emerging and Newly Identified Health Risks, *"The appropriateness of existing methodologies to assess the potential risks associated with engineered and adventitious products of nanotechnologies"*, European Commission Health & Consumer Protection Directorale-General, Directorate C- Public Health and Risk Assessment C7, 2006

12. V. Ramalingam, R. Rajaram, C. PremKumar, P. Santhanam, P. Dhinesh, S. Vinothkumar and K. Kaleshkumar, *"Biosynthesis of silver nanoparticles from deep sea bacterium Pseudomonas aeruginosa JQ989348 for antimicrobial, antibiofilm and cytotoxic activity"*, J. Basic Microbiol., 53, 1–9, 2013

13. N. Law, S. Ansari, F.R. Livens, J.C. Renshaw, J.R. Loyd, *"Formation of Nanoscale Elemental Silver Particles via Enzymatic Reduction by*

Geobacter sulfurreducens", Applied and Enviromental Microbiology, p. 7090-7093, 2008

14. M.J. Hajipour, K.M. Fromm, A.A. Ashkarran, D.J. de Aberasturi, I.R. de Larramendi, T. Rojo, V. Serpooshan, W.J. Parak, M. Mahmoudi, *"Antibacterial properties of nanoparticles"*, Cell Press: Trend In Biotechnology, 30: 499-511, 2012

15. J. Zhang, E. W. Taylor, X. Wan, D. Peng, *"Impact of heat treatment on size, structure, and bioactivity of elemental selenium nanoparticles",* International Journal of Nanomedicine 2012

16. AA VV, *"The American Heritage Science Dictionary"*, Houghton Miffin, 2002

17. M.E. Olson, H. Ceri,D.W. Morck, A.G. Buret, R.R. Read, "Biofilm bacteria: formation and comparative susceptibility to antibiotics", Canadian Journal of Veterinary Research 66, 86-92, 2002

18. J.J. Harrison, H. Ceri, C. Stremick, R.J. Turner, *"Biofilm susceptibility to metal toxicity",* Environmental Microbiology 6, 1220-1227, 2004

19. J. Dobias, E.I. Suvorova, R. Bernier-Latmani, *"Role of proteins in controlling selenium nanoparticles size"*, Nanotechnology 22, 2011

20. A. G. Ingale, A.N. Chaudhari, "Biogenic Synthesis of Nanoparticles and Potential Applications: an EcoFriendly Approach", Journal of Nanomedicine and Nanotechology 4: 165, 2013

21. H. Ceri, M.E. Olson, D.W. Morck, D. Storey, R.R. Read, A.G. Buret, B. Olson, *"The MBEC assay system: Multiple equivalent biofilms for antibiotic and biocide susceptibility testing"*, Methods in Enzymology 337, 377-384, 2001

22. J.J. Harrison, H. Ceri, J. Yerly, C.A. Stremick, Y. Hu, R. Martinuzzi, R.J. Turner, *"The use of microscopy and three-dimensional visualization to evaluate the structure of microbial biofilms cultivated in the Calgary Biofilm Device"*, Biol. Proced. Online, 8(1): 194-215, 2006

23. H. Ceri, M.E. Olson, C. Stremick, R.R. Read, D.W. Morck, A.G. Buret, "*The Calgary Biofilm Device: New technology for rapid determination of antibiotic susceptibilities in bacterial biofilms"*, Journal of Clinical Microbiology 37, 1771-1776, 1999

24. J.J. Harrison, R.J. Turner, H. Ceri, *"High-throughput metal susceptibility testing of microbial biofilms"*, BMC Microbiology 5, 53, 2005

25. Y. Suetsugu, T. Tateishi, *"Chapter 6: Implants and Biomaterials (hydroxyapatite)"*, Basics and Clinical practice of AQB implants vol.1 The Basics, p.70-76, 2013

26. http://www.azom.com/article.aspx?ArticleID=107

27. J. Kolmas, M. Kuras, E. Oledzka, M. Sobczak, *“A Solid-State NMR Study of Selenium Substitution into Nanocrystalline Hydroxyapatite”*, International Journal of Molecular Science 16, 11452-11464, 2015

28. J. Kolmas, E. Groszyk, U. Piotrowsk, *“Nanocrystalline hydroxyapatite enriched in Selenite and Manganese ions: physicochemical and antibacterial properties”*, Nanoscale Research letters, 10:278, 2015

29. T. Hemalatha, G. Krithiga, B.S. Kumar, T. P. Sastry, “*Preparation and Characterization of Hydroxyapatite-coated Selenium Nanoparticles and their interaction with Osteosarcoma (SaOS-2) Cells”*, Acta Metall. Sin, 27 (6), 1152-1158, 2014

30. Q. Li, T. Chen, F. Yang, J. Liu, W. Zheng, *“Facile and controllable one-step fabrication of selenium nanoparticles assisted by L-cysteine”,* Materials Letters 6, p 614–617, 2010

31. S. Zhang, J. Zhang, H. Wang, H. Chen, *“Synthesis of selenium nanoparticles in the presence of polysaccharides”*, Materials Letters 58, p. 2590– 2594, 2004

32. Kessi, J., Ramuz, M., Wehrli, E., Spycher, M., Bachofen, *“Reduction of selenite and detoxification of elemental selenium by the phototrophic bacterium Rhodospirillum rubrum”,* Appl. Environ. Microbiol. 65, 4734-4740, 1999

33. Biswas K.C., Barton, L.L., Tsui, W.L., Shuman, K., Gillespie, J., Eze, *“A novel method for the measurement of elemental selenium produced by bacterial reduction of selenite*” J. Microbiol. Methods 86, 140-144, 2011

34. D.C. Harris, M.D. Bertolucci, “Symmetry and Spectroscopy: An Introduction to Vibrational and Electronic Spectroscopy”, Dover Publications, p. 93-95, 1989

35. S. Dwivedi, A. A. AlKhedhairy, M. Ahamed, J. Musarrat, *“Biomimetic Synthesis of Selenium Nanospheres by Bacterial Strain JS-11 and its role as a Biosensor for nanotoxicity assessment: a novel Se-Bioassay”,* PLOS ONE, Volume 8, p.57404, 2013

36. AA.VV., “*Dynamic Light Scattering: An Introduction in 30 Minutes*”, Technical Note of Malvern Instruments Ltd, England

37. P. Antonioli, S. Lampis, I. Chesini, G. Vallini, S. Rinalducci, L. Zolla, P.G. Righetti, *“Stenotrophomonas maltophila SelTE02, a New Bacterial Strain suitable for Bioremediation of Selenite-contaminated environmental matrices”*, Applied and Enviromental Microbiology, p.6854-6863, 2007

38. E. Zonaro, S. Lampis, R.J. Turner, S.J.S. Qazi, G. Vallini, *“Biogenic selenium and tellurium nanoparticles synthetized by enviromental microbial isolates efficaciously inhibit bacterial planktonic cultures and biofilms”*, Frontiers of Microbiology, Volume 6, articles 584, 2015

39. S.K. Torres, V.L. Campos, C.G. Leon, S.M. Rodriguez-Llamazares, S.M. Rojas, M. Gonzalez, C. Smith, M.A. Mondaca, *"Biosynthesis of selenium nanoparticles by Pantoea agglomerans and their antioxidant activity",* J Nanopart Res 14:1236, 2012

40. AA.VV. *"Z potential: an introduction in 30 minutes"*, Technical Note of Malvern Instruments Ltd, England

41. P. Sonkusre, R. Nanduri, P. Gupta, S.S. Cameotra, *"Improved Extraction of Intracellular Biogenic Selenium Nanoparticles and their specifity for Cancer Chemoprevention",* Journal of Nanomedicine and Nanotechnology vol.5, issue 2, 2014

42. P.C. Hiemenz, R. Rajagopalan, *"Principles of Colloid and Surface, 3rd edition, revised and expanded"*, Marcel Dekker Inc, 1997

43. K. Tam, C. Tu Ho, J. Lee, M. Lai, C. H. Chang, Y. Rheem, W. Chen, H. Hur, N.V. Myung, *"Growth Mechanism of Amorphous Selenium Nanoparticles Synthesized by Shewanella sp. HN-41",* Biosci. Biotechnol. Biochem., 74, p. 696-700, 2010

44. B. Hafner, *"Energy Disperse Spectroscopy on the SEM"*, Characterization Facilities, University of Minnesota

45. Joseph Goldstein,Dale E. Newbury,David C. Joy,Charles E. Lyman,Patrick Echlin,Eric Lifshin,Linda Sawyer,J.R. Michael, *"Scanning*

Electron Microscopy and X-ray Microanalysis: 3rd Edition", Springer, p. 297-308, 2003

46. I. Wiegand, K. Hilpert, R. E. W. Hancock, *"Agar and broth dilution methods to determine the minimal inhibitory concentration (MIC) of antimicrobial substances",* Nature protocols, vol.3, p-163-175, 2008

47. K. Todar, "Todar's Online Textbook of Bacteriology", Winsconsin, 2012

48. K. Ikuma, A.W. Decho, B. L. T. Lau, *"When nanoparticles meet biofilms-interactions guiding the environmental fate and accumulation of nanoparticles"*, Frontiers in Microbiology, Volume 6, Article 591, 2015

49. H. Flemming, T. R. Neu, D.J. Wozniak, *"The EPS matrix: The "House of Biofilm Cells"*, Journal of Bacteriology, vol.189, n.22, p. 7945–7947, 2007

50. M. Alhede, P. Jensen, M. Givskov, T. Bjarnshot, *"Biofilm medical importance"*, EOLSS, Biotechnology vol.12

51. J.B. Pawley, "*Handbook of Biological Confocal Microscopy* 3rd edition", Springer, 2006

52. T.J. Fellers, MW Davidson*, "Introduction to Confocal Microscopy",* Olympus Fluoview Resource Center, National High Magnetic Field Laboratory, 2007

53. AA. VV., *"LIVE/DEAD® BacLight™ Bacterial Viability Kits: product information"*, Molecular Probes, 2014

54. J. Kolmas, E. Oledzka, M. Sobczak, G. Nalecz-Jawecky, *"Nanocrystalline hydroxyapatite doped with selenium oxyanions: A new material for potential biomedical applications"*, Mater. Sci. Eng. C, 39, 134-142, 2014

55. J. Kolmas, E. Groszyk, D. Kwiatkowska-Rozycka, *"Substituted Hydroxyapatites with Antibacterial Properties"*, BioMed Research International, Article ID 178123, 2014